Two photon study of environmental effects on indole spectra
by Aden Andrew Rehms

A thesis submitted in partial fulfillment of the requirements for the degree of Doctor of Philosophy in Chemistry
Montana State University

Abstract:
Polarized two-photon fluorescence excitation spectroscopy has been applied for the first time to the study of indole, the chromophore of the amino acid tryptophan. Investigations of three nine-membered ring systems, benzimidazole, benzimidazole cation, and indole have emphasized the utility of the experimental technique and revealed that the overlapping La and Lb states of indole have very different two-photon polarization ratios. Substituted indoles, with their varying La-Lb energy gaps, were studied in cyclohexane and n-butanol to explore the usefulness of the polarization ratio difference. The results of this study have directly confirmed the previously deduced La-Lb energy gaps in these compounds, the greater sensitivity of La to polar solvation, La-Lb level inversion, the role of La in producing broad red-shifted fluorescence, the existence of ground state complexes, and the importance of hydrogen bonding in the ground state complexes. The La Lb polarization ratio difference was also exploited to investigate the influence of charge on the La and Lb states. Experiments with tryptophan, 5-methoxytryptophan and yohimbine revealed the great sensitivity of the La state to a positive charge in the vicinity of the 5-ring of indole. The results with tryptophan also hint at a role of the Lb state in the dual exponential decay of tryptophan fluorescence. Two-photon spectra of all the aromatic amino acids and a comparison of the strength of their signals show tyrosine to be comparable to phenylalanine for two-photon excitation. Unlike the situation in one-photon spectroscopy, it may be possible to observe phenylalanine residues in proteins with two-photon spectroscopy. Finally, the first ever two-photon excitation spectrun of a small protein, melittin, shows that it is possible to observe a two-photon signal from a protein.

TWO PHOTON STUDY OF ENVIRONMENTAL EFFECTS ON INDOLE SPECTRA

by

Aden Andrew Rehms

A thesis submitted in partial fulfillment
of the requirements for the degree

of

Doctor of Philosophy

in

Chemistry

MONTANA STATE UNIVERSITY
Bozeman, Montana

February 1990

APPROVAL

of a thesis submitted by

Aden Andrew Rehms

This thesis has been read by each member of the thesis committee and has been found to be satisfactory regarding content, English usage, format, citations, bibliographic style, and consistency, and is ready for submission to the College of Graduate Studies.

Feb 16, 1990
Date

Patrick R Callis
Chairperson, Graduate Committee

Approved for the Major Department

January 13, 1990
Date

Edwin H Abbott
Head, Major Department

Approved for the College of Graduate Studies

Feb 26, 1990
Date

Henry L Parsons
Graduate Dean

STATEMENT OF PERMISSION TO USE

In presenting this thesis in partial fulfillment of the requirements for a doctoral degree at Montana State University, I agree that the Library shall make it available to borrowers under rules of the Library. I further agree that copying of this thesis is allowable only for scholarly purposes, consistent with "fair use" as prescribed in the U.S. Copyright Law. Requests for extensive copying or reproduction of this thesis should be referred to University Microfilms International, 300 North Zeeb Road, Ann Arbor, Michigan 48106, to whom I have granted "the exclusive right to reproduce and distribute copies of the dissertation in and from microfilm and the right to reproduce and distribute by abstract in any format."

Signature Adam A. Rehms

Date 1/8/90

TABLE OF CONTENTS

TABLE OF CONTENTS -- Continued

TABLE OF CONTENTS -- Continued

LIST OF TABLES

LIST OF FIGURES

LIST OF FIGURES -- Continued

LIST OF FIGURES -- Continued

LIST OF FIGURES -- Continued

LIST OF FIGURES -- Continued

LIST OF FIGURES -- Continued

LIST OF FIGURES -- Continued

LIST OF FIGURES -- Continued

ABSTRACT

Polarized two-photon fluorescence excitation spectroscopy has been applied for the first time to the study of indole, the chromophore of the amino acid tryptophan. Investigations of three nine-membered ring systems, benzimidazole, benzimidazole cation, and indole have emphasized the utility of the experimental technique and revealed that the overlapping L_a and L_b states of indole have very different two-photon polarization ratios. Substituted indoles, with their varying L_a-L_b energy gaps, were studied in cyclohexane and n-butanol to explore the usefulness of the polarization ratio difference. The results of this study have directly confirmed the previously deduced L_a-L_b energy gaps in these compounds, the greater sensitivity of L_a to polar solvation, L_a-L_b level inversion, the role of L_a in producing broad red-shifted fluorescence, the existence of ground state complexes, and the importance of hydrogen bonding in the ground state complexes. The L_a-L_b polarization ratio difference was also exploited to investigate the influence of charge on the L_a and L_b states. Experiments with tryptophan, 5-methoxytryptophan and yohimbine revealed the great sensitivity of the L_a state to a positive charge in the vicinity of the 5-ring of indole. The results with tryptophan also hint at a role of the L_b state in the dual exponential decay of tryptophan fluorescence. Two-photon spectra of all the aromatic amino acids and a comparison of the strength of their signals show tyrosine to be comparable to phenylalanine for two-photon excitation. Unlike the situation in one-photon spectroscopy, it may be possible to observe phenylalanine residues in proteins with two-photon spectroscopy. Finally, the first ever two-photon excitation spectrun of a small protein, melittin, shows that it is possible to observe a two-photon signal from a protein.

INTRODUCTION

The near ultraviolet absorption and fluorescence of proteins can be ascribed to the aromatic amino acids phenylalanine, tyrosine, and tryptophan (1). Absorption and emission of light by these amino acids have been exploited to study protein structure and dynamics (2,3,4,). The most useful of these is tryptophan, whose indole chromophore is highly sensitive to local solvation and structural environment. The lowest energy UV absorption band of indole consists of two nearly degenerate electronic transitions designated L_a and L_b (5). One photon studies have indicated that solvent(6,7,8,9,10), substitution (7,8,9), and charge (11) can differentially shift the L_a and L_b states and lead to large changes in the fluorescence spectra of indoles. This occurs without great alterations to their absorption spectra (12,13,14,15).

Perhaps the most notable characteristic of indole photophysics is the large stokes shift of the fluorescence in polar media. Red shifts of the fluorescence relative to that seen in hydrocarbon solvents occur for additions of polar solvent insufficient to alter the bulk dielectric properties of the solvent. Accompanying the red shift is a loss of structure in the fluorescence. It appears that polar solvents interact with indoles in a specific manner (12,13,14). Solvents also seem to have more general effects

on the fluorescence (15,16,17,18,19). The hypotheses advanced to explain how the solvent causes the large red shift of indole fluorescence are based upon solvent shift studies of absorption and fluorescence peaks. Unfortunately, the broad nature of the transitions and complications due to dual absorption and emission from the L_a and L_b states make such studies subject to errors. What has been needed to resolve some of these questions is a way of separating the contribution of each state to these processes. Polarized fluorescence excitation has been used to resolve the band shapes of L_a and L_b in polar solvents (20,21) but has failed in hydrocarbon solvents where minute amounts of polar impurities complex with indoles at the low temperatures necessary to perform the experiments (22). Substituent perturbation (9,23) and derivative spectroscopy (24) have also been tried with largely unsatisfactory results.

Polarized two-photon fluorescence excitation offers a direct method of observing the L_a and L_b states separately in absorption. This technique involves the essentially simultaneous absorption of visible photons to reach excited states of ultraviolet energies. The simultaneous nature of the absorption makes it possible to observe a polarization dependence from non-rigid samples. It was discovered as part of this thesis work (25) that the L_a and L_b states of indole are characterized by very different two-photon

polarization ratios. This enabled the author to directly observe regions of L_a and L_b absorption.

The aim of this thesis was to utilize this powerful technique to learn more about the relative response of L_a and L_b to solvent, substitution, and charge. Indole and various of its methyl and methoxy derivatives were examined in hydrocarbon and alcohol solvents. Models for charge interactions, which included the amino acid tryptophan itself, were also examined. These two-photon experiments represent the first time this technique has been used to look at indoles and were designed to answer specific questions about the validity of conclusions drawn from the indirect one photon methods used by others. The results for these models systems combined with two-photon spectra of all the aromatic amino acids and a small protein, melittin, serve to pave the way for two-photon spectroscopy of proteins. INDO/S calculations have been compared to the experimental results to test their predictions so that they might also prove useful for interpretation of indole and protein spectra.

EXPERIMENTAL

Theory of Two-photon absorption

The simultaneous absorption of two non-resonant photons by matter was first postulated to occur by Maria Goeppert-Mayer in 1931 (26). Observation of this phenomenon at optical frequencies had to await the advent of the laser (27) because of the inherently low transition probabilities associated with two-photon processes. Once practical, this new spectroscopy offered many unique possibilities and was quickly utilized to investigate a large number of compounds (28,29). Theoretical advances (30-40) of the period allowed experiments to be designed and gave a deeper insight into the regularities emerging in two-photon spectra of aromatic molecules.

Second order time-dependent perturbation theory predicts that molecules can absorb two photons through two types of interaction with the radiation. The relativistically invariant form of the Hamiltonian for a system in the presence of an electromagnetic field is given by (41)

$$H = \frac{1}{2m} (p - \frac{e}{c} A)^2 + [V(r) + e\varphi]$$

where A is the vector potential of the radiation field given by

$$A(r,t) = A_o \cos(\omega t - k \cdot r)$$

φ is the scalar potential associated with the electromagnetic field, and V(r) is an effective potential for a given electron due to the nuclei and other electrons in the system. Writing all the terms of equation 1 in detail, the Hamiltonian is

$$H = \frac{1}{2m} \left(-\hbar^2 \nabla^2 + i\hbar \frac{e}{c} A \cdot \nabla + \frac{e^2}{c^2}|A|^2\right) + V(r) + e\varphi$$

If the coulomb gauge is chosen, it provides that $\nabla \cdot A = 0$ and $\varphi = 0$. The equation above becomes

$$H = \frac{1}{2m} \left(-\hbar^2 \nabla^2 + 2i\hbar \frac{e}{c} A \cdot \nabla + \frac{e^2}{c^2}|A|^2\right) + V(r)$$

Rewriting this as

$$H = H^o + H' = \left[-\frac{\hbar^2}{2m} \nabla^2 + V(r)\right] + \left[\frac{ie\hbar}{mc} A \cdot \nabla + \frac{e^2}{2mc^2}|A|^2\right]$$

it is clear that the perturbation is

$$H' = \frac{ie\hbar}{mc} A \cdot \nabla + \frac{e^2}{2mc}|A|^2$$

These two terms describe the coupling with the electromagnetic field that lead to changes in the state function of the system. In Figure 1 are the time ordered Feynmann (42) diagrams which correspond to the couplings described by the $A \cdot \nabla$ and $A \cdot A$ terms. The straight upward arrows represent a molecule moving through time and space in state ψ^o and the wiggly arrows are photons which may interact with the molecule and leave the molecule in a state ψ_ε. Since the $A \cdot A$ term involves 2 photons it makes no contribution to ordinary one photon processes. The calculations of McClain and Harris (31), Honig et al.

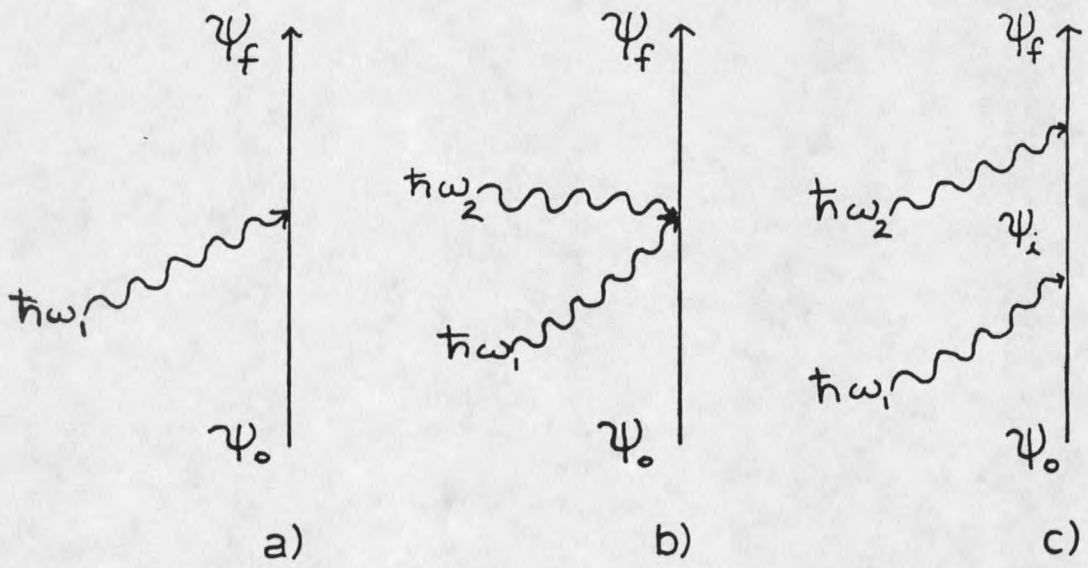

Figure 1: Time-ordered Feynmann diagrams for a) $A\cdot\nabla$ coupling b) $A\cdot A$ coupling and c) two consecutive $A\cdot\nabla$ couplings.

(32,33), and Guccione and Van Kranendonk (43) have indicated that even for two photon absorption, the $A \cdot A$ term gives little contribution. The Hamiltonian can now be taken as

$$H^{o} = H^{o} + H' = \left[\frac{-h^2}{2m}\nabla^2 + V(r)\right] + \frac{ieh}{mc} A \cdot \nabla$$

With the appropriate Hamiltonian it is possible to proceed with a time-dependent perturbation treatment to arrive at the perturbed wavefunction in second order.

$$\psi_o^{(2)}(r,t)=\psi_o^{(1)}(r,t)+\frac{q^2\nabla^2\omega^2}{\hbar^2}\sum_f S_{of}\mu_r^o(r)\left(\frac{1-\exp[-i(\omega_{fo}-2\omega)]}{\omega_{fo}-2\omega}\right)$$

Like one-photon processes, the transition rate for the two-photon process is proportional to the square of the coefficient of the final state μ_r^o. It is (31)

$$W_{gf}^{(2)}=128\pi^3\alpha^2\omega^2F^2|S_{gf}|^2g_m(2\omega)$$

This equation demonstrates the quadratic dependence of the transition rate on the photon flux (F) which distinguishes two-photon from one-photon processes. Dividing out the flux gives a purely molecular quantity, δ_{gf}, the two-photon absorptivity, given by (31)

$$\delta_{gf}=128\pi^3\alpha^2|s_{gf}|^2g_m(2\omega)$$

In both cases above S_{gf} (assuming 2 identical photons) is (31)

$$S_{gf} = \sum_k \frac{(e\cdot\langle f|r|k\rangle)(\langle k|r|g\rangle)\cdot e)}{\omega_{kg}-\omega}$$

S_{gf}, the two-photon tensor, demonstrates the complementary nature of one and two-photon processes. The dipole moment operator appears twice in S_{gf} and both transitions k←g and f←k must be parity allowed (i.e. one-photon allowed) for the two-photon transition to be allowed. For gerade ground states this corresponds to successive u←g and g←u transitions for an overall g←g parity selection rule. The Feynmann diagram, which corresponds to the two successive $A\cdot\nabla$ couplings suggested by the two-photon tensor, is also shown in Figure 1.

The states $|k\rangle$ over which the tensor is summed are termed intermediate states and should include the initial and final states (35,39,40). Inclusion of the ground and final states is especially important in the description of polar molecules, where there are states characterized by

large changes in permanent dipole moment (39). This can be seen by looking only at the two terms in the sum over intermediate states which correspond to the ground and final states as intermediate states. The two terms are:

$$S = \frac{\langle f|r|g\rangle\langle g|r|g\rangle}{\omega_{gg}-\omega} + \frac{\langle f|r|f\rangle\langle f|r|g\rangle}{\omega_{fg}-\omega}$$

If the matrix elements of the dipole operator are denoted in the form R_{xy} this can be written as

$$S_{partial} = \frac{R_{fg}\ R_{gg}}{\omega_{gg}-\omega} + \frac{R_{ff}\ R_{fg}}{\omega_{fg}-\omega}$$

Recognizing that $\omega_{gg} = 0$ and $\omega_{fg} = 2\omega$ for identical photons

$$S_{partial} = \frac{R_{fg}\ R_{gg}}{-\omega} + \frac{R_{ff}\ R_{fg}}{\omega}$$

which leads to

$$S_{partial} = \frac{R_{fg}}{\omega}\ (R_{ff} - R_{gg})$$

R_{fg} is simply the matrix element of a one-photon (dipole induced) transition from the ground state to the final state and $(R_{ff} - R_{gg})$ is the difference in the permanent dipole moment of final and ground states. Thus, for the ground and final states to be important as intermediate states, the transition must be one-photon allowed and there must be a considerable change in permanent dipole moment between the ground and final states. Such an addition to S_{gf} is not important for centrosymmetric molecules, but is for polar molecules like the indoles studied in this thesis. If the transition dipole and the change in dipole moment are collinear, an additional contribution to δ_{gf} proportional to

the oscillator strength of the transition f←g and the square of the change in dipole moment given in debyes is introduced. The contribution of dipole terms for equally polarized photons of the same energy in the case where R_{fg} is parallel to $R_{ff}-R_{gg}$ is in gm given by (39)

$$\delta\uparrow\uparrow = 1.043 \frac{f(\Delta\mu)^2}{\Delta E}$$

where f is the oscillator strength of f←g, $\Delta\mu$ is the change in dipole moment (in debyes), and ΔE is the excitation energy in eV. Excitation energies of 5eV associated with strong one-photon transitions (f=1) and changes of dipole moment on the order of 2 debyes will produce extra two-photon absorptivity contributions as strong as a moderately intense two-photon transition (i.e., 1 Göppert-Mayer, 1gm = 1 X 10^{-50} cm^4sec/photon molecule).

The 3 x 3 cartesian tensorial nature of the two-photon process leads to a polarization dependence of δ upon the light which survives averaging over all molecular orientations. This is not true for one-photon processes where the cross-section has no polarization dependence. The quantities which survive the orientation averaging are denoted ε_f, ε_g, and ε_h are defined as: (28)

$$\delta_f = S_{\alpha\alpha}S_{\beta\beta}^* = \sum_1^3 |\text{diagonal elements}|^2$$

$$\delta_g = S_{\alpha\beta}S_{\alpha\beta} = \sum_1^3 |\text{each element}|^2$$

$$\delta_h = S_{\alpha\beta}S_{\beta\alpha} = \sum_1^3 |\text{hermitian products})$$

Identical photons from the same laser beam make $\delta_g=\delta_h$. Information about the elements of the tensor can still be obtained from the relation for the absorptivity of circularly verses linearly polarized light. This quantity, Ω, the two-photon polarization ratio, is defined as (37)

$$\Omega = \frac{\delta cir}{\delta lin} = \frac{\delta_f+3\delta_g}{\delta_f+2\delta_g}$$

Upper and lower limits on the value of Ω are exhibited by tensors with the following patterns of elements.

$$\begin{pmatrix} 0 & 1 & 1 \\ 1 & 0 & 1 \\ 1 & 1 & 0 \end{pmatrix} \qquad \begin{pmatrix} 1 & 0 & 0 \\ 0 & 1 & 0 \\ 0 & 0 & 1 \end{pmatrix}$$

$\Omega = 3/2$ $\qquad$ $\Omega = 0$

The value of Ω will in general be different for every transition. Molecules which are symmetric will exhibit characteristic tensor patterns for each symmetry species. In order to assign a polarization ratio to a given state for molecules which lack symmetry it is necessary to rely upon approximate molecular orbital calculations such as CNDO/S and INDO/S (35,36,38).

Instrumentation and Procedures

The two-photon fluorescence excitation spectra recorded in this study were obtained using the apparatus drawn schematically in Figure 2. The spectra of benzimidazole,

benzimidazole cation, and indole in cyclohexane were taken with an NRG 0.5 MW (peak) nitrogen pump laser and an NRG single stage scanning dye laser as the light source. Early work on the methylindoles (44) also utilized this laser system. Subsequent spectra of the methylindoles and the spectra of all other molecules were obtained using a Lumonics HD 300 dye laser (8ns, <13mJ/pulse) pumped by the 2nd or 3rd Harmonic of a JK HY200 Nd:YAG laser. A Gallilean telescope expanded and collimated the dye laser beam. It was then routed through a shutter to the glan polarizer which polarized it vertically. A double fresnel rhombahedron on a rotating mount served to rotate the plane of polarization 45° before the beam passed through a stationary fresnel rhombahedron. Linearly and circularly polarized light utilized for measuring Ω were produced here. The shutter and the double rhomb were both rotated by stepping motors under computer control. The beam was either left unfocused or focused slightly from 8 mm in diameter to 4-6 mm in diameter, depending upon the dye being utilized and the sample characteristics. In all cases the peak power density at the sample was below 1.25×10^{10} Wm^{-2}. The signal from the sample was also checked for quadratic behavior by attenuating the beam with crossed polarizers. If the quadratic condition was met, a reduction of the laser energy by 50% led to a two-photon excited fluorescence signal of

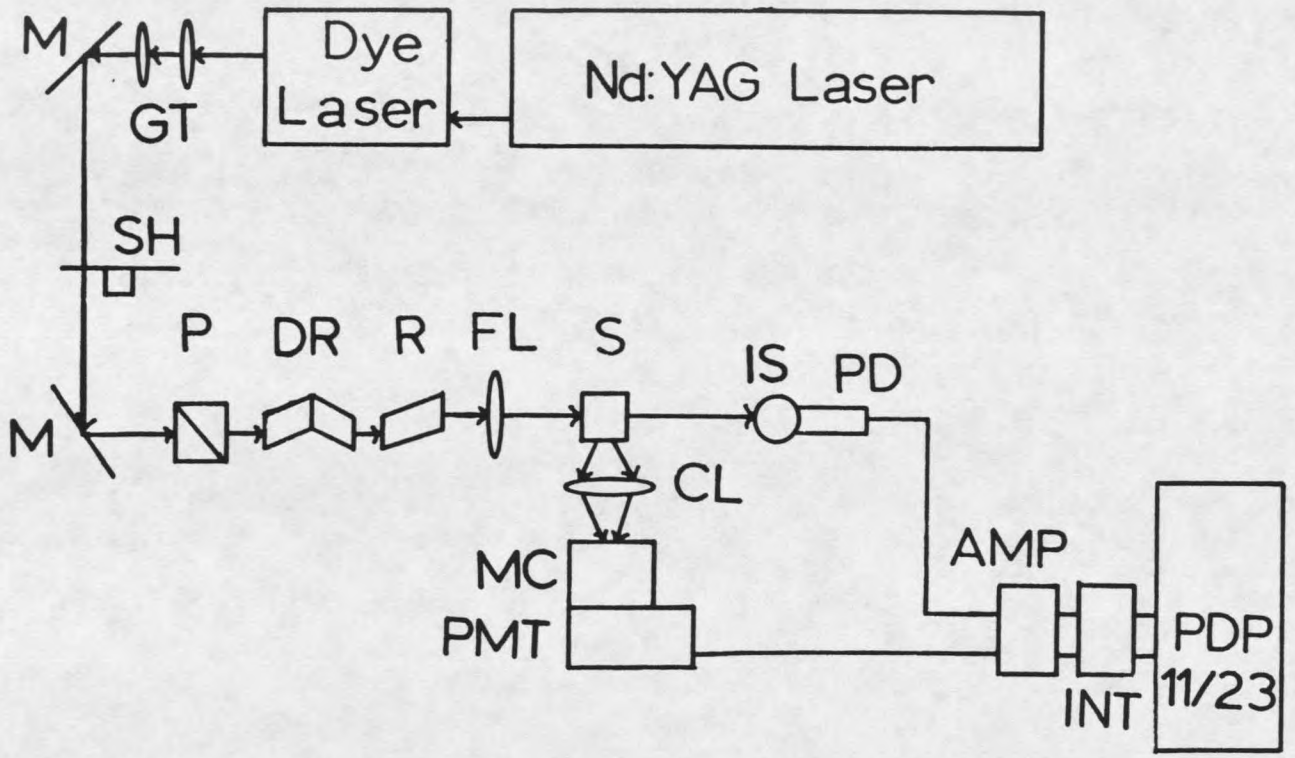

Figure 2: Laser apparatus utilized by the author to obtain the two-photon spectra in this study. GT (gallilean telescope), M (mirror), SH (shutter), P (glan polarizer), DR (double fresnel rhomb), R (fresnel rhomb), FL (focussing lens), S (sample), IS (integrating sphere), PD (photodiode), CL (cylindrical lens), MC (monochromator), PMT (photomultiplier tube), AMP (amplifier), INT (integrator).

25% of the original. These checks were performed at both ends of the dye ranges, the maxima of the dye gain curves, and at peaks due to molecular transitions. Defocusing was performed if necessary. The fluorescence of the sample was collected at right angles by an f3.0 quartz cylindrical lens, which focused it through 2 UV-pass filters (Schott UG-11) and onto the slit of an f/3.3 holographic grating monochromator (Instruments SA, 50 nm bandpass, 16 nm for early work where polarizer was rotated). No slits were used because slight changes in beam height due to the rotation of the double rhomb moved the beam off of the slit, giving a low reading for the circular signal. The laser beam was passed through the sample and into an integrating sphere where a quantum counting solution and a photodiode generated a signal proportional to the average photon flux. Below 600 nm Rhodamine (3g/l) was used as the quantum counter and above 600 nm, Nile Blue (1g/l). The fluorescence signal and the reference signal were amplified and integrated (200 μs) using printed circuit boards purchased from Evans Associates. Integrated signals were stored and processed by a PDP 11/23 computer which also controls the stepping motors and the laser scan control unit. In a typical experiment the signals from the sample fluorescence and the laser reference detectors were averaged for 400 shots. The average of the sample signal was then divided by the square of the reference signal to obtain the normalized two-photon

signal. This was done at each wavelength using linearly polarized light to measure the two-photon fluorescence excitation spectrum. Determinations of the two-photon polarization ratio (Ω) were made at each wavelength using circularly polarized light for excitation and dividing the resulting two-photon signal by that just obtained for linarly polarized excitation.

Nine organic dyes and mixtures thereof covering a wavelength range of 440 nm to 650 nm were utilized in the dye laser to obtain the data segments. At least 5 nm of overlap was maintained between dye segments and they were joined to create the two-photon spectra. A more exact method of joining these segments to create a complete two-photon excitation spectrum has been developed recently by Jones and Callis (45). Within the range of 600 nm to 650 nm, this SHG technique was used as published. It involves second harmonic generation (SHG) from a powder sample of potassium di-hydrogen phosphate (KDP) to obtain a reference signal proportional to the instantaneous photon flux squared. The signal is used to compensate for changes in the temporal and spatial profiles of the laser beam to which the one photon reference is insensitive. In an attempt to extend the technique to shorter wavelengths, suspensions of urea crystals (75-150 μm) in decalin were tried. A quantum counting solution of 1g/l skatole in n-butanol was also added to remove the strong wavelength dependence below

600 nm of the UV pass filters used to separate the second harmonic from the fundamental. These efforts were successful in extending the technique with reasonable confidence to 530 nm where absorption by the decalin and possible scattering due to the mismatch of the refractive indices of decalin and urea caused the corrected two-photon signal to increase. Where reliable SHG data was obtained the procedure was utilized. All segments, corrected or not, were joined at the middle of the overlap and truncated so as to maintain the shape indicated by the midsection of each segment.

All solutes and solvents were of the highest quality available and used as received. Solutions were checked with 1-photon fluorescence excitation (Spex Fluorolog) and revealed no interfering fluorescent impurities. All solutions were approximately 0.01M except as indicated. Absorption spectra of dilute (10^{-5} M) solutions were obtained with a Cary 14 spectrophotometer. Fluorescence spectra were taken with the Spex Fluorolog.

Relative two-photon absorptivities (δ) for the benzimidazoles, toluene, and indole were determined by measuring the relative fluorescence signal excited by one and two-photon absorption. A 150 W Xenon arc lamp and a 0.5M grating monochromator were used for UV excitation. The detection geometry for both one and two-photon excitation

was kept constant. The relative two-photon absorptivity was then calculated from the relation

$$S_A^{(2)}/S_B^{(2)} = \varepsilon_A C_A \varphi_A(\lambda_A)/\varepsilon_B C_B \varphi_B(\lambda_B)$$

where $S^{(2)}A$ is the photon flux normalized two-photon signal for sample A, C_A its concentration, and $\varphi_A(\lambda_A)$ its differential fluorescence quantum yield. φ represents the probability an absorbed photon will be emitted between wavelength λ and $\lambda+d\lambda$. The assumption of $S_A^{(2)} = G\varphi_A(\lambda_A)$ where G is the combined instrumental response function allowed calculation of δ_B. Underlying the whole procedure is the assumption that the quantum yield per excitation is the same for one and two-photon excitation.

Molecular orbital calculations of one and two-photon properties were performed using a spectroscopically calibrated INDO/S program originally obtained from Dr. Michael Zerner, University of Florida(46), coupled to programs for calculating transition densities and two-photon properties.(47,48) Mataga-Nishimoto and Ohno-Klopman electron repulsion integrals were used for singly and doubly excited configuration calculations respectively.

NINE-MEMBERED RING SYSTEMS: INDOLE AND BENZIMIDAZOLE

Background

Nine-membered heterocyclic aromatic ring systems are important in nature. They are found as the side chain of the amino acid tryptophan and are the basis for the nucleic acids adenine and guanine. These systems are non-alternate and lack symmetry, making it necessary to rely mostly upon semi-empirical molecular orbital calculations for theoretical insight. (48,49,50) The two lowest singlet $\pi^* \leftarrow \pi$ states for indole have been assigned (1) L_b (S_1) and L_a (S_2) where the operational difference between the two states is that L_b is structured while L_a is broad and unstructured. This assignment appears to have followed the perimeter model classification scheme introduced by Platt. (5) While the L_a and L_b labels are meaningless for the odd-atom perimeter, a similarity exists between the transition density pattern (48) of the nine-ring states and the L_a and L_b states of benzene. Evleth (49) has also noted a similarity in the configuration wave functions.

The parent molecule for the nine-membered 10 pi electron series is the cyclononatetraenide anion. In this molecule the L_a and L_b states are degenerate. Callis (48) has discussed how cross-linking to form the 5-6 fused ring system of the indenyl anion ($C_9H_7^{1-}$) removes this degeneracy. The L_a state appears to be mixed with the Ba state due to a

large L_a-Ba transition density between the atoms that are cross-linked. The result is that the L_a state is greatly shifted to the red of the L_b state. Introduction of the nitrogen to form indole results in a cancellation of the effect of the cross-link and shifts the L_a state to the blue so that the two states are nearly degenerate again but with the L_b state now lowest. Introduction of another nitrogen at the 3 position to make benzimindole further shifts the L_a to the blue, separating them again. The inductive effect of the nitrogen has been discussed by Feitelson(50) as arising mainly from differences in the electrical charge distribution between the ground and excited states at the site of the nitrogen atom and he stressed the importance of including the interaction between the ground and excited states in the description of heteroatomic indene derivatives. He reasoned that since the inductive effect shifted the L_a and L_b states in different directions to leave L_b lowest for indole, electron donating groups at the 1 or 3 positions would lessen the inductive effect and lead to less of a blue shift for the L_a state. Indeed, the broad L_a state has been shown to move closer to the L_b state for tryptophan (3-substitution) (6) The importance of the charge density of the nitrogen can also be seen in Evleth's(49) work where moderate changes in the nitrogen parameters, leading to less of an inductive effect actually caused the L_a state to again become lowest for indole.

Since two-photon spectroscopy offers information complementary to that obtained with conventional one-photon spectroscopies, two-photon fluorescence excitation spectra of indole, benzimidazole, and benzimidazole cation were obtained. These experimental results have been used to judge the validity of INDO/S calculations. In order to further test the theory, measurements of relative two-photon absorptivities were made.

Two-photon Spectra

Shown in Figure 3 are the two-photon fluorescence excitation for linearly polarized light (solid line), one-photon absorption (dashed lines), and two-photon polarization ratio (dotted lines) spectra for indole (0.2M). As is done throughout this thesis, the one-photon absorption is shifted from its one-photon wavelengths to correspond to wavelengths for two-photon absorption of the same total energy. The 0-0 of the absorption spectrum is also normalized to follow the 0-0 peak of the two-photon spectrum. The polarization spectrum shown is that obtained for a 0.05M solution. Ω is seen to be near the theoretical maximum for the 0-0 L_b. It then drops steeply, presumably due to the onset of L_a absorption, and levels off at ~0.7. The slight drop of the polarization ratio on the red edge is

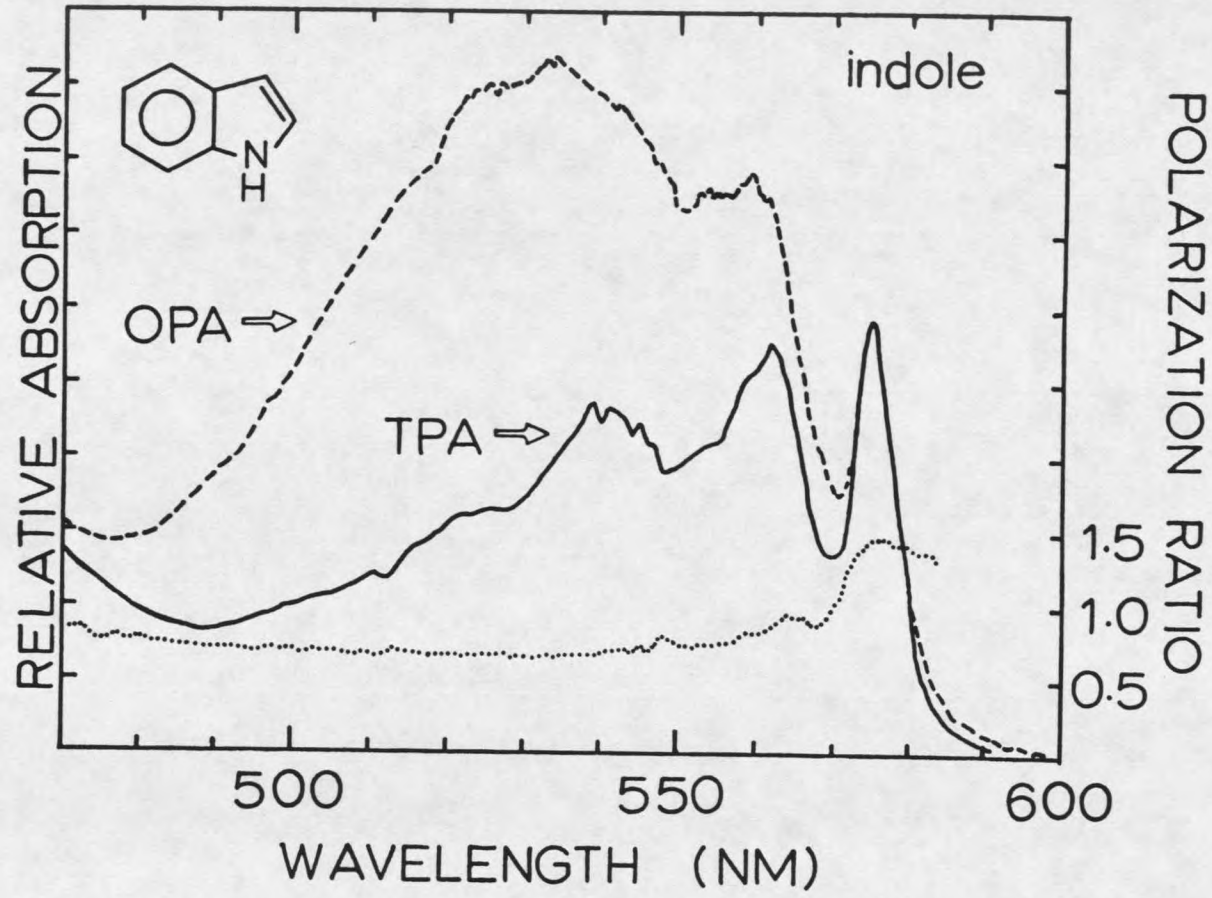

Figure 3: Two-photon fluorescence excitation (solid line), one photon absorption (dashed line), and two-photon polarization (dotted line) spectra for indole dissolved in cyclohexane. (0.2M excitation, 0.05M polarization)

concentration dependent and may be due to intermolecular hydrogen bonding. NMR experiments of concentrated solutions support this contention.(51) Little change is seen once the concentration is below 0.10 M. The two-photon excitation spectrum shows that the broad L_a band is less pronounced in two-photon than in one-photon excitation, but still outweighs the L_b band by a factor of four.

At this point some comment should be made about the apparent profile of the two-photon excitation spectra. The spectra presented in this section were obtained using the N_2 laser described previously. $L_a$ter two-photon spectra utilizing the Nd:YAG system appear to follow the one-photon spectra more closely and then deviate above them at higher energies. The effect seems to be due to the laser and not the detection system. This uncertainty precludes detailed discussion of relative L_a and L_b strengths in these molecules, but the wealth of information contained in the two-photon polarization ratio still makes this a very powerful technique.

In Figure 4 are shown spectra for benzimidazole (0.2 M Isopropanol). The two-photon excitation spectrum follows the one-photon absorption through both the 0-0 and the 0-1 of the L_b band. At approximately 0+1550cm^{-1} there appears a peak which does not appear at all in the one-photon spectrum. With a spacing similar to that of the 0-0 and 0-1 a second peak, also missing in the one-photon absorption,

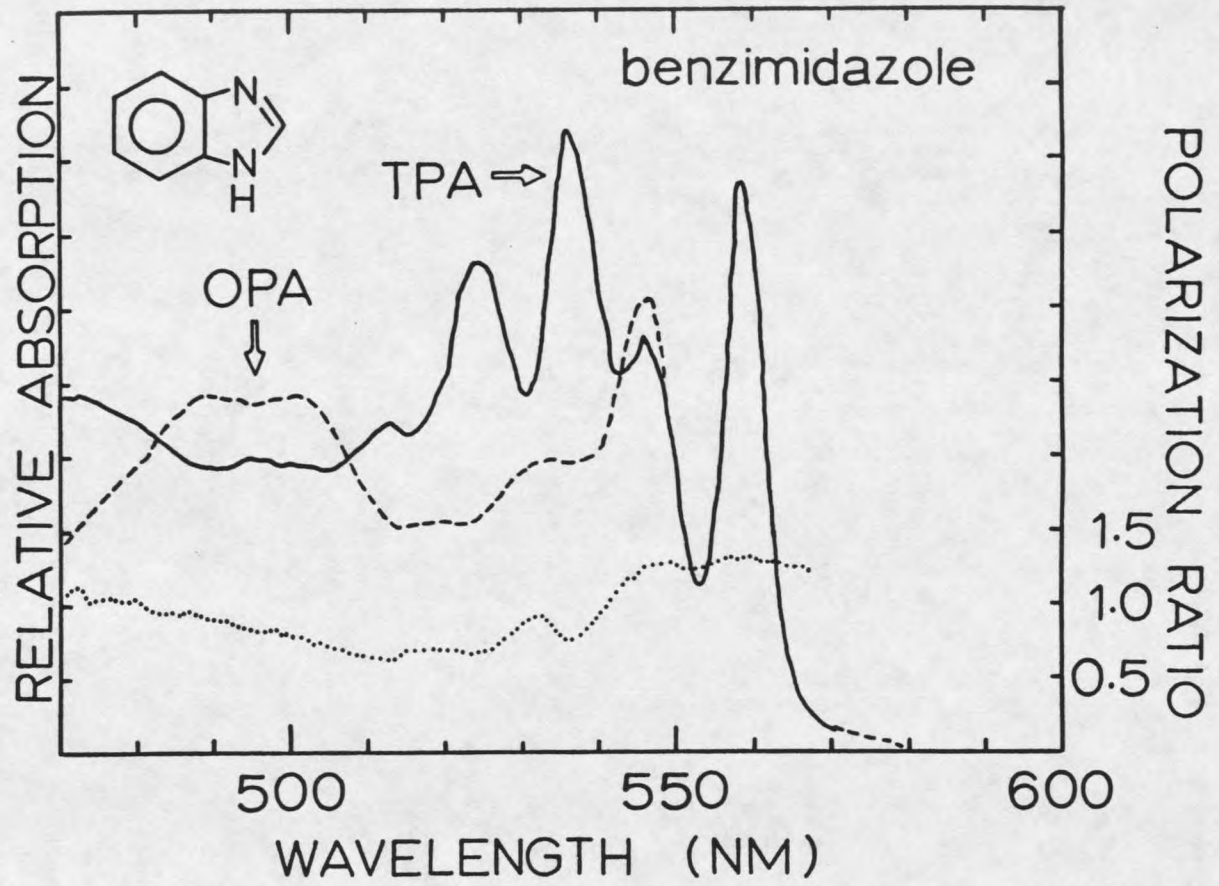

Figure 4: Two-photon fluorescence excitation (solid line), one photon absorption (dashed line), and two-photon polarization (dotted line) spectra for benzimidazole dissolved in isopropanol (0.2M).

appears. The polarization spectrum shows Ω high for the 0-0 and 0-1 of L_b but a much lower polarization is exhibited by the new peaks. The behavior of these peaks indicates a vibronic origin. A smaller dip in the polarization spectrum between the 0-0 and 0-1 may also be due to a two-photon active vibrational mode. The L_a state appears to be reduced also for benzimidazole, and shows an Ω slightly less than 1.0 while the L_b state shows Ω = 1.3.

The data for the cation of benzimidazole (0.2m in methanol-H_2SO_4) is shown in Figure 5. Two peaks which do not appear in the one-photon absorption again appear at about 0+1550 cm^{-1} with a spacing similar to that of the 0-0 and 0-1. The polarization spectrum shows a high Ω value for the 0-0 and 0-1 peaks with dips corresponding to the two vibronic peaks. Interestingly, the polarization ratio falls on either side of the 0-0.

Figure 6 presents the two-photon spectra of each molecule such that the two-photon absorptivity scale is the same for each molecule. This graph was constructed using measurements of the relative δ's as outlined in the experimental section. The units are such that δ = 1 for toluene in cyclohexane excited at 513 nm ($^*\nu_{14}$). Indole shows a two-photon absorptivity approximately five times that for toluene. The benzimidazoles are only slightly stronger than toluene.

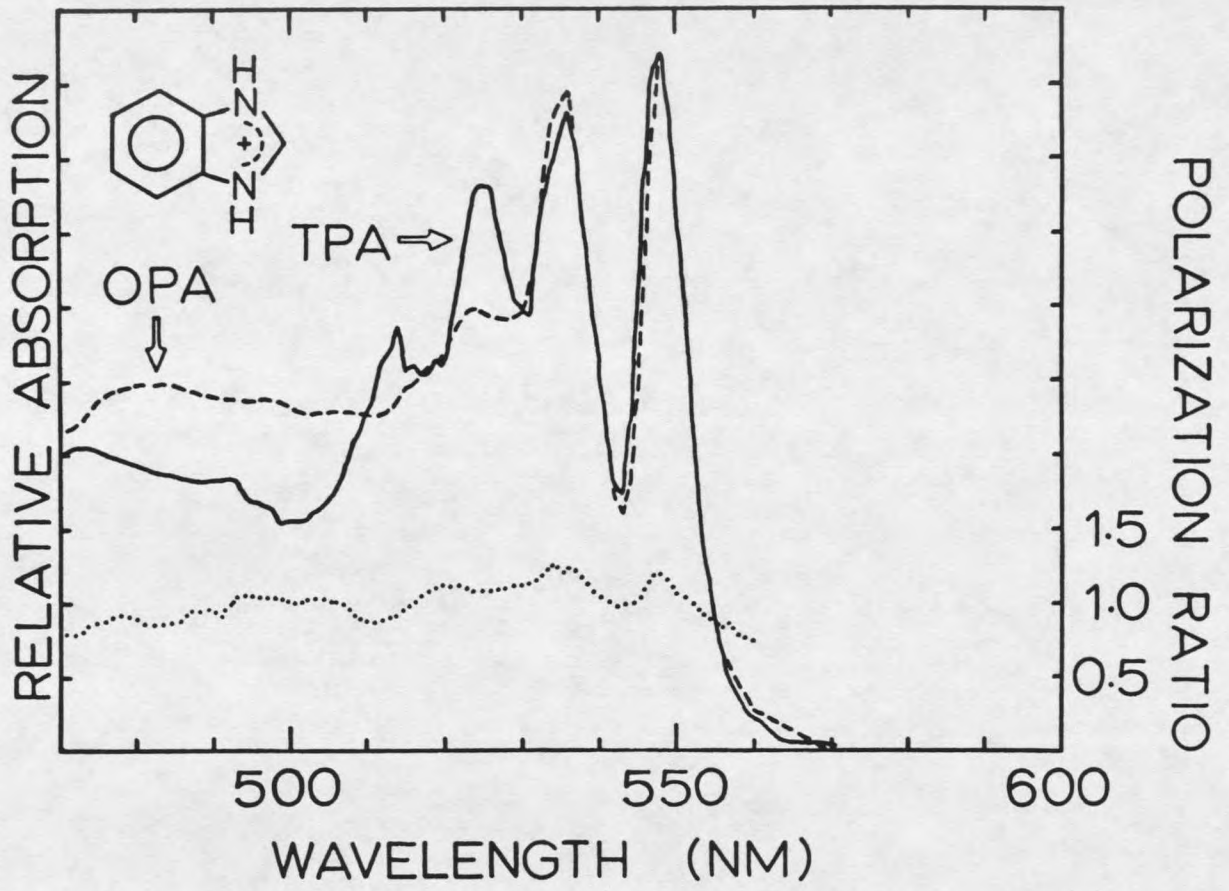

Figure 5: Two-photon fluorescence excitation (solid line), one photon absorption (dashed line), and two-photon polarization (dotted line) spectra for benzimidazole dissolved in methanol + H_2SO_4(0.2M).

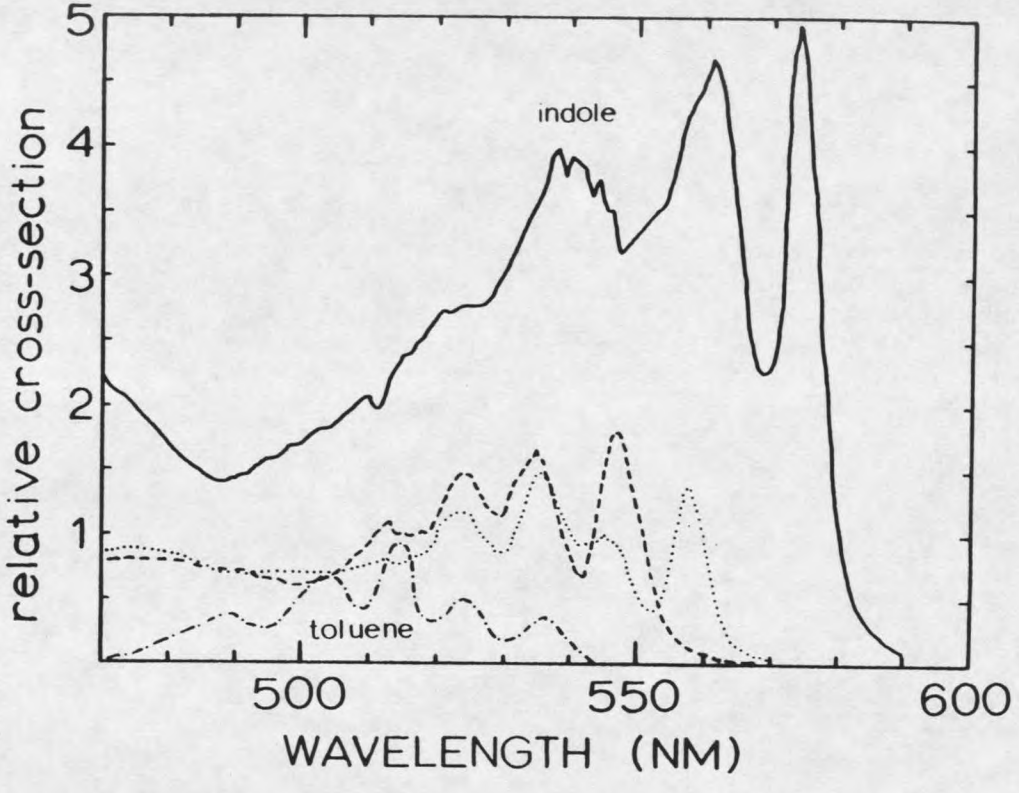

Figure 6: Relative two-photon absorptivities for indole, benzimidazole, benzimidazole cation, and toluene.

Discussion

Indole

The degenerate L_a and L_b bands of indole have been the subject of intensive study (4,53), yet much remains unknown because they do overlap so extensively. A greater sensitivity to solvent environment for the L_a state, believed due to its larger dipole (16,17,54,55), has been the basis for assigning peaks to L_a or L_b in absorption. (7,8,22) The solvent shift technique utilized by Strickland and co-workers has led them to assign a peak at about 1000 cm^{-1} above the L_b 0-0 to the L_a 0-0 for indole in methylcyclohexane. The two-photon results are largely consistent with this assignment. Assuming a 500 cm-1 fwhm for this peak the polarization ratio should begin dropping at 567 nm but it is seen to be dropping already at 572 nm. It may be that the L_a 0-0 is much broader than assumed or is somewhat closer to the L_b 0-0 than previously believed. Nonetheless, L_a absorption begins very close to the L_b 0-0. The structured fluorescence of indole in cyclohexane (Figure 7) is consistent with assigning L_b as the lowest state as indicated by the polarization spectrum.

The computed two-photon properties of indole are in good agreement with the experiment (see Table 1). The L_b state is predicted to show $\Omega = 1.5$, close to that observed. The low Ω observed for the L_a state is also predicted

Table 1. INDO/s results for indoles studied. a) 10 x 20 singles only, Mataga-Nishimoto δ's; b) 14 x 14 singles only Mataga-Nishimoto δ's; c) 9 x 7 singles and doubles Ohno-Klopman δ's.

Derivative		ΩL_a	ΩL_b	$\delta_g+\delta_b$ (L_b.gm)	$\delta_g+\delta_b$ (L_a,gm)	$E_{La}-E_b$ (cm^{-1})
5MI	a)	1.498	0.578	125.573	163.883	4478.6
	b)	1.499	0.583	117.187	169.828	4680.28
	c)	1.497	0.372	24.939	31.889	6255.34
Indole	a)	1.494	0.479	89.846	131.537	3367.90
	b)	1.496	0.468	92.139	164.805	3905.01
	c)	1.497	0.324	12.230	27.693	6584.31
1MI	a)	1.471	0.342	86.437	122.675	3178.50
	b)	1.471	0.350	82.600	138.356	3521.53
	c)	1.378	0.256	15.884	21.326	4734.45
2,3MI	a)	1.480	0.666	137.680	574.880	2946.6
	b)	1.480	0.664	131.630	583.676	2909.50
	c)	1.470	0.500	21.724	81.104	4594.01
3MI	a)	1.480	0.515	116.772	278.827	3021.90
	b)	1.474	0.526	108.867	301.672	3233.66
	c)	1.409	0.411	21.2269	33.700	5062.89
4MTI	a)	1.499	0.834	210.723	120.717	3794.30
	b)	1.498	0.809	205.696	123.411	3942.25
	c)	1.499	1.456	32.320	10.499	6067.99
5MTI	a)	1.495	0.588	156.411	168.303	4938.60
	b)	1.499	0.588	153.251	164.184	5069.59
	c)	1.497	0.429	33.337	55.458	6858.83
6MTI	a)	1.417	0.265	92.654	73.062	4217.50
	b)	1.413	0.266	85.594	76.229	4320.20
	c)	1.433	1.099	17.966	90.040	6233.78
7MTI	a)	1.500	0.449	43.341	115.672	4137.21
	b)	1.499	0.464	40.471	121.477	4305.43
	c)	1.468	0.369	12.131	40.816	5844.24

successfully. It should be noted that unless the ground and final states are included in the sum over intermediate

states, the L_a polarization ratio is predicted to be near 1.5. The charge transfer character and associated dipole moment change for the L_a state contribute to the xx and xy terms of the two-photon tensor and lead to the low Ω value. The ground and final states of this polar molecule contribute because the L_a transition moment and the dipole moment change are largely in the x direction. Such a contribution has been predicted theoretically (39) and this may represent the first experimental observation. INDO/S predicts the two-photon absorptivity of indole to be about 10 times that for benzene, also in good agreement with the results.

Benzimidazole

Perhaps the most interesting feature of the two-photon spectrum of benzimidazole is the appearance of two vibronic peaks without analog in the one-photon spectrum. These peaks are assigned to a vibration similar to the ν_{14} vibration of benzene and the ν_{21} vibration of naphthalene (56) that is so effective in inducing two-photon intensity. A vibration that distorts the six-membered ring of benzimidazole toward a kekule structure is predicted by a normal mode calculation, FORCE, based on an MNDO generated force field (57). The ground state frequency is calculated to be 1302 cm^{-1} and agrees with the analysis by Cordes and Walter (58) who find 1316 cm^{-1} and assign the IR band observed at 1280 cm^{-1} to this vibration. An increase

similar to the 300 cm^{-1} increase in the ν_{14} frequency for the excited L_b state of benzene would bring the frequency to about 1580 cm^{-1}, in close agreement with that observed.

The INDO/S calculations are somewhat less successful for benzimidazole in that the calculated δg+δh values are about three times higher than observed. Also, the L_b of benzimidazole is predicted to be of the same absorptivity as indole's L_b and appears not to be the case. The calculations predict $\Omega_b = 1.33$ and $\Omega_{La} = 1.23$ which is consistent with what is observed since the L_a state is overlapped by states with low polarization on both sides.

Benzimidazole Cation

In addition to the interesting vibronic peaks shown for this molecule, benzimidazole cation shows a very interesting polarization spectrum. Ω is high only at the first two L_b peaks and low elsewhere. The drop in polarization seen on the red edge of the excitation spectrum is interesting in light of the large red shift in fluorescence maximum seen for the benzimidazole cation (59,60). Protonation of benzimidazole shifts the fluorescence maximum from 299 nm to 360 nm. Associated with this large stokes shift is a loss of structure much like that observed for indole dissolved in water (6). The two lowest states of the cation are predicted to have charge transfer character like the L_a state of indole. In the cation, the L_b state appears to have moved closer (blue shift) to the L_a state and may

actually allow L_a to become lowest. It is however possible that another state not predicted by the theory underlies the structured ^1L_b. Tway and Love (60) have proposed that prototropic equilibria in the excited state explain the charge transfer type fluorescence seen in certain benzimidazole and thiabendazole homologues. INDO/s certainly fails in regard to the predicted absorptivity for the cation. It is calculated to be 20 to 40 times that of benzene.

Summary

Two-photon spectroscopy of three nine-membered ring systems has provided a mechanism by which to further test the semi-empirical methods relied upon for insight in these systems. INDO/S does a good job predicting the two-photon properties of indole but fails for the benzimidazoles, especially the cation. The large difference in Ω of the L_a and L_b states of indole offers a method of resolving these two states in room temperature solvent systems as well as in the gas phase. The data for indole in cyclohexane are consistent with literature assignments of the L_b state as the lowest singlet state with L_a about 1000 cm^{-1} above it in hydrocarbon solvent.

SOLVENT AND SUBSTITUENT EFFECTS ON INDOLE

Background

The effect of environment on the fluorescence characteristics of indoles forms the basis for interpretation of protein fluorescence spectra. Solvation is the most obvious and thoroughly studied perturbation of the indole ring. (4) Substituted indoles (see Figure 7), with their varying L_a-L_b energy gaps, have served as models for the study of solvation effects on the L_a and L_b states. For most methyl derivatives, polar solvation leads to a loss

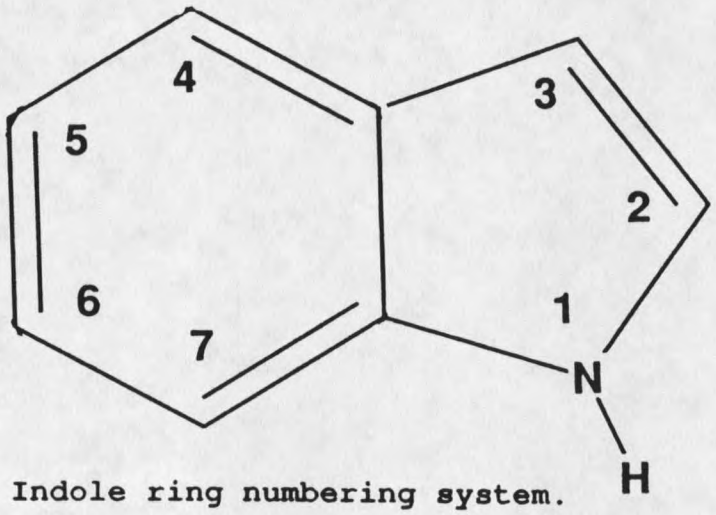

Figure 7: Indole ring numbering system.

of structure and a large red shift of the fluorescence. This drastic change in fluorescence behavior is accompanied by only small changes in absorption. The fluorescence changes, moreover, begin to occur for solutions containing very small amounts of polar solvent in hydrocarbon. Specific interactions between indoles and polar solvents are

implicated by this behavior. As the concentration of polar solvent is increased, the fluorescence slows its broadening and only shifts further to the red. Experiments in viscous polar solvents, where the solvent relaxation time is comparable to the fluorescence lifetime, show that the fluorescence undergoes a red-shift in time due to solute-solvent relaxation (SSR) (68). In rigid polar glasses where SSR cannot occur the fluorescence loses much of its red shift and becomes somewhat structured. These results suggest that a non-specific interaction is responsible for the red shift. Various theories have drawn upon specific and non-specific interactions alike to explain the anomalous fluorescence behavior of indoles in polar solvents.

Van Durren (15) discussed the role of solvent dielectric and hydrogen bonding on indole fluorescence, citing non-specific dielectric properties as more important. Mataga, et al. (16) proposed that a reversal of the L_a and L_b levels during the excited lifetime of indole was responsible for the red shift. In their model, a large increase in dipole moment upon excitation initiates solvent relaxation which preferentially stabilizes the larger dipole moment of the L_a state. Similar models have been proposed by Song & Kurtin (18) and Suzuki et al. (17). Mataga et al. also predicted that the L_a state of indole should have a large contribution from a configuration resembling styrene's lowest charge transfer (CT) state. Furthermore, they stated

that the contribution of this configuration would likely increase as a result of the interactions with the polar solvent during the excited state lifetime.

Based upon the specific nature of the polar interaction, Lumry and co-workers have, in a series of papers (13,61-64), proposed the existence of excited state solute-ground state solvent complexes ("exciplexes") which stabilize charge centers in the excited state by dipole-dipole interactions. These exciplexes were shown to exhibit 1:1 and/or 1:2 stoichiometry and are believed to involve complexation at N-1 and C-3 of the indole ring. 5-methoxyindole was classified as a non-exciplex forming indole since polar solvation produces no greatly red-shifted fluorescence for this molecule. The exciplex model does however neglect the relative L_a-L_b energy gap and the state of origin for the red-shifted fluorescence. Another specific interaction deduced for indoles and used to explain the anomalous fluorescence characteristics is that of ground state complexes. Skalski et al. (14) were able to correlate changes in absorption with the appearance of a red-shifted component in the fluorescence for 1-methylindole.

Virtually all of the work on the nature of the fluorescent state of indoles in polar solvents has based its explanation of experimental results on at least one of the aforementioned proposals; i.e., SSR around the large dipole of L_a, charge transfer, level inversion, exciplex formation,

and ground state complexes. Hydrogen bonding to the indole N-H group has been somewhat ignored as an explanation. This is likely due to the similar photophysics of 1-methylindole. The more recent fluorescence solvent shift studies of $L_a$mi have led to a model which includes ground state complexes and L_a-L_b level inversion as a result of both solvent polarity and solvent reorientation. The growing charge transfer character for L_a due to SSR during the excited state lifetime has been re-emphasized by the time-resolved fluorescence experiments of Meech et al. (19). It is in a synthesis of the above models that a truer picture of indole photophysics has emerged.

Important to interpretation in terms of these models is the relative energy of the L_a and L_b states. This is especially true for derivatives with closely spaced levels where dual emission from L_a and L_b is possible. While the broadening of the L_a and L_b absorption peaks in polar solvents make their assignment difficult, it is even more difficult to discern the onset of L_a absorption which is apparently so important in describing the anomalous fluorescence. Polarized two-photon fluorescence excitation spectroscopy provides a direct method of viewing the L_a and L_b states separately despite their large degree of overlap.

It is the aim of this section to describe efforts in following the movement of the L_a and L_b states under the influence of polar solvation for a series of methyl and

methoxy derivatives of indole. As a reference point, two-photon spectra of the compounds dissolved in cyclohexane were obtained. These are then compared to those observed in n-butanol. The two-photon spectra, especially the Ω spectra, provide a firm basis on which to discuss the proposed models of indole fluorescence. The absorption and fluorescence changes upon polar solvation were recorded as an aid in the discussion. The results of INDO/S calculations for the derivatives are also presented as they lend insight and support.

Two-Photon Spectra

Indoles in Cyclohexane

5-methylindole (5MI). Of all the methylindoles, 5-methylindole (Figure 8, 0.01M cyclohexane) shows the largest L_a-L_b energy gap (9). The structured L_b state is well separated from the broad L_a state in both the one-photon absorption (OPA) (dashed lines) and the two-photon excitation spectra (TPA) (solid line). The polarization spectrum (Ω) (dotted line) shows a high value of ~1.3 for the L_b 0-0 and is still above 1.0 for the L_b 0-1. It then drops to ~0.6 for shorter wavelength excitation and then rises again to the blue as a third transition with a higher polarization ratio is excited below 510 nm.

Indole. Presented again (Figure 9, 0.01M in cyclohexane) but this time at a slightly lower concentration

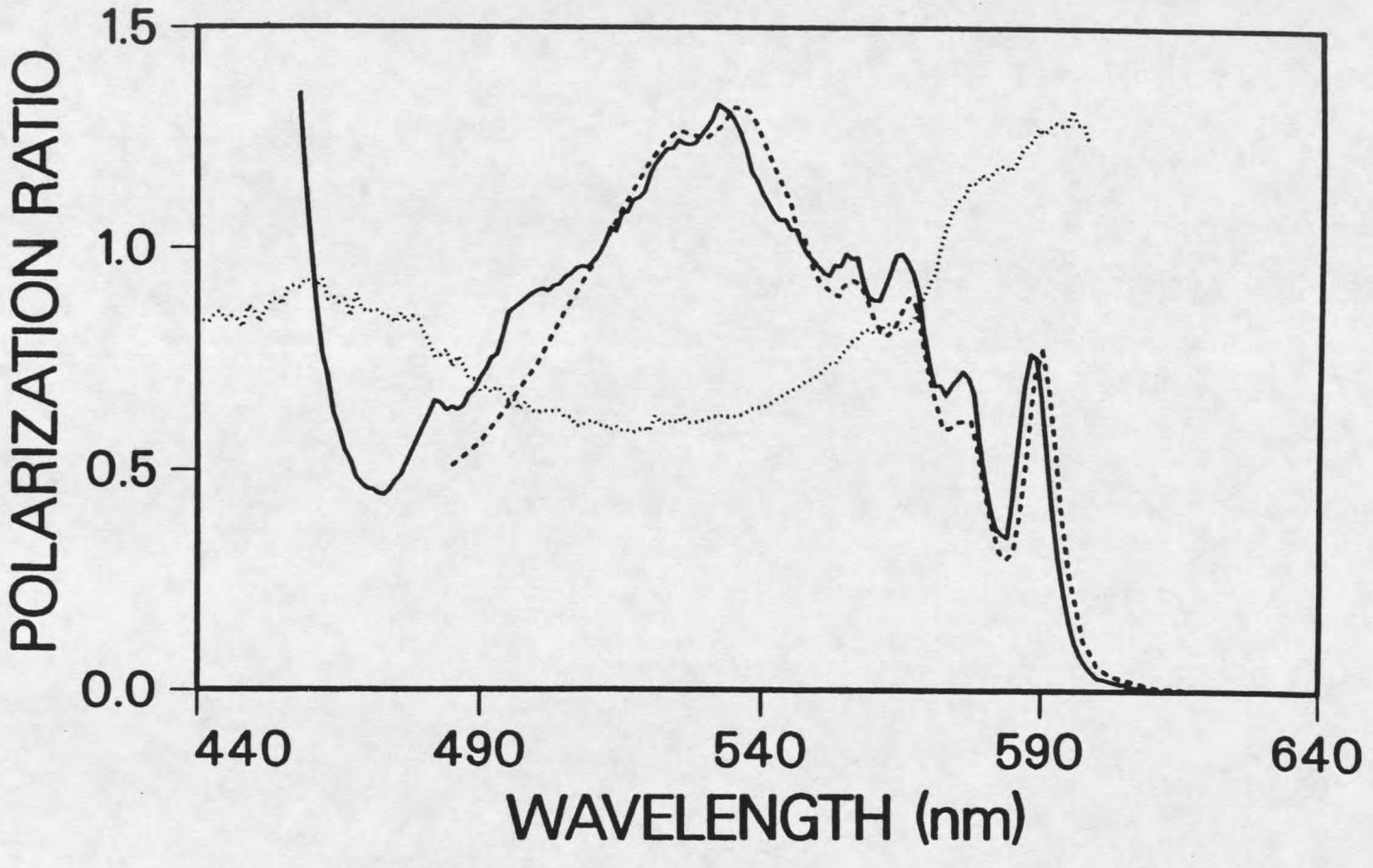

Figure 8: Two-photon fluorescence excitation (solid line), one photon absorption (dashed line), and two-photon polarization (dotted line) spectra for 5-methylindole dissolved in cyclohexane (0.01M).

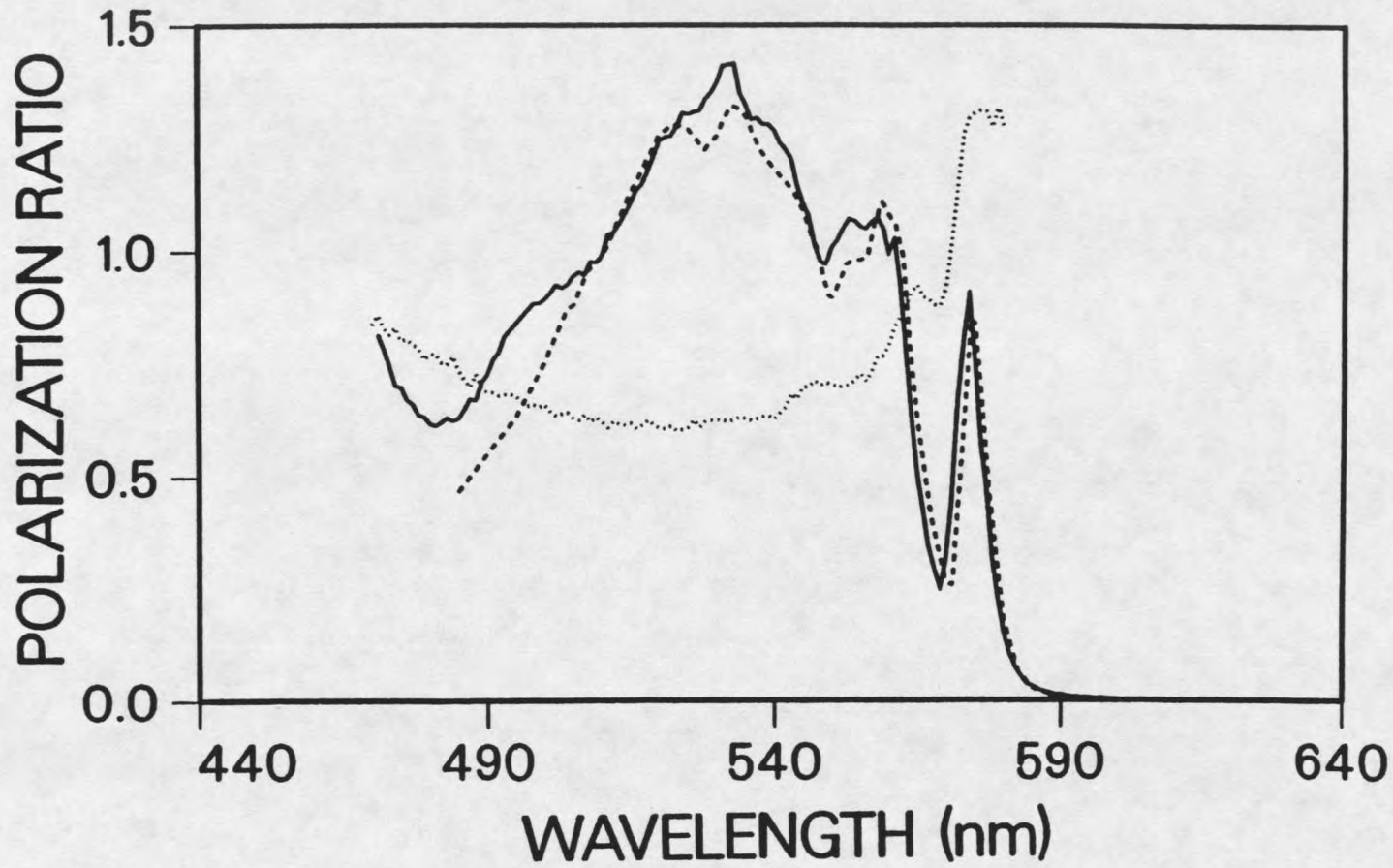

Figure 9: Two-photon fluorescence excitation (solid line), one photon absorption (dashed line), and two-photon polarization (dotted line) spectra for indole dissolved in cyclohexane (0.01M).

the profile seen with the YAG system, the TPA is seen to follow the OPA closely like the TPA of 5-methylindole. The polarization spectrum is identical to that shown before for the 0.05M solution with $\Omega \sim 1.4$ at the origin and dropping steeply to the blue where it levels off at $\Omega \sim 0.65$ for bulk L_a excitation. Again, a third transition with a higher Ω value begins to absorb below 510 nm.

1-methylindole (1MI). Figure 10 shows the results for 1-methylindole (0.01 M cyclohexane). This molecule is believed to have a somewhat smaller L_a-L_b energy gap than indole (12) and the Ω spectrum is consistent with L_a being closer in energy to the L_b 0-0. The Ω value at the origin is just above 1.1 and drops steeply in the region between the L_b 0-0 and 0-1 which are still resolved. The polarization ratio for what should be L_a excitation drops only to about 0.8. The third transition, growing in below 520 nm, shows a polarization ratio above 1.1. The high polarization ratio for L_a excitation may be a reflection of the fact that 2 states with high Ω values straddle it on both sides and seems to indicate that L_a may be somewhat reduced in this molecule despite the apparent TPA.

3-methylindole (3MI). 3-methylindole (Figure 11, 0.01M cyclohexane) is the most closely related to tryptophan (also 3-substituted) and is believed to have the L_b 0-0 and L_a 0-0 superposed in hydrocarbon (7). This would account for the strength of the origin peak relative to the rest of the

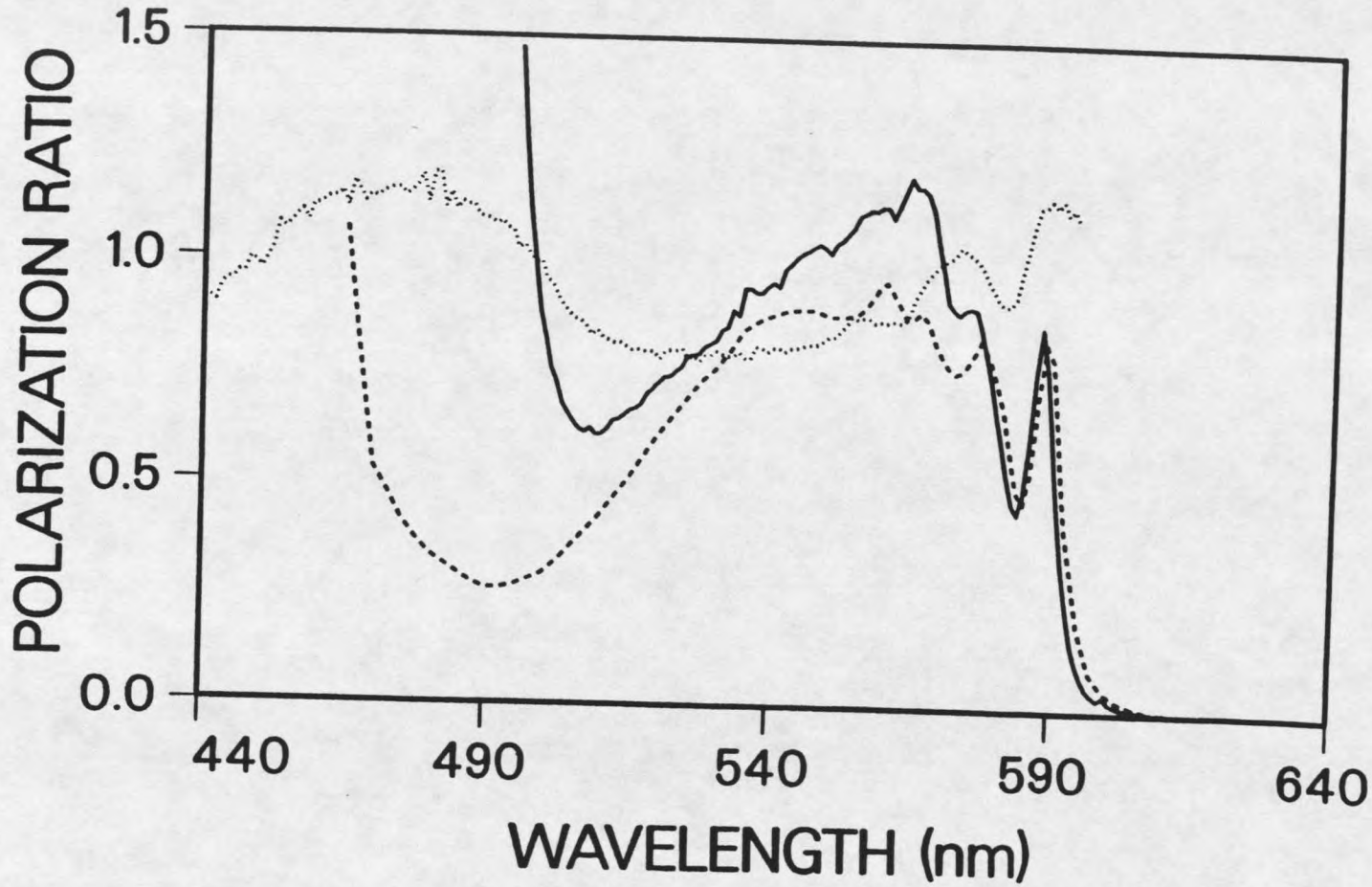

Figure 10: Two-photon fluorescence excitation (solid line), one photon absorption (dashed line), and two-photon polarization (dotted line) spectra for 1-methylindole dissolved in cyclohexane (0.01M).

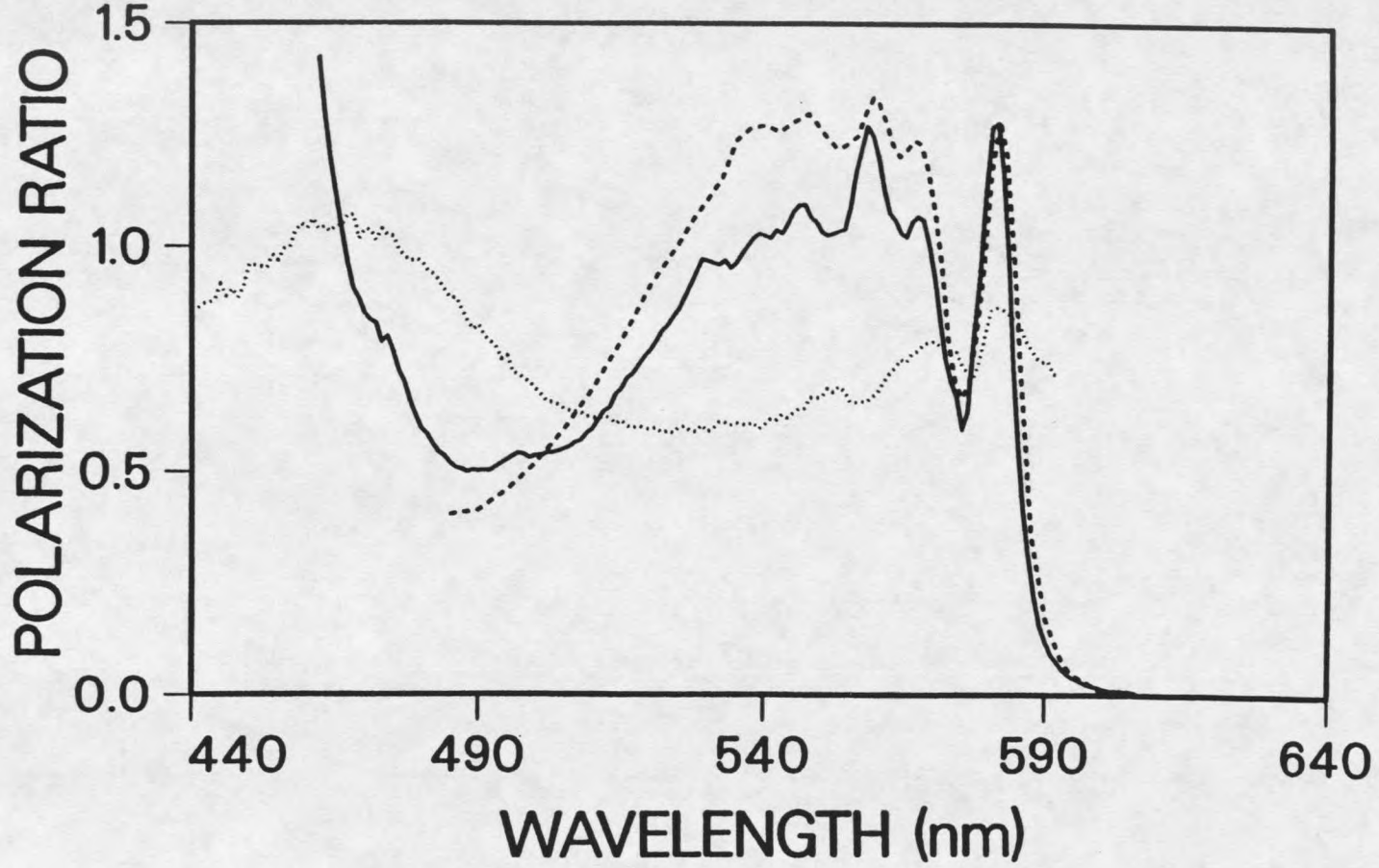

Figure 11: Two-photon fluorescence excitation (solid line), one photon absorption (dashed line), and two-photon polarization (dotted line) spectra for 3-methylindole dissolved in cyclohexane (0.01M).

absorption in both the OPA and TPA. The Ω value of only 0.9 at the origin also hints that this is the case. The polarization ratio drops on the red edge indicating that the L_a 0-0 is somewhat broader than the L_b 0-0. Like 1-methylindole, the rise in Ω for the 0-1 peak of L_b is broader than is seen for indole. This may be a manifestation of the L_b 0+730 cm^{-1} and 0+980 cm-1 peaks seen for indole and 3-methylindole by Strickland (7). L_a may also in fact be reduced for this molecule and the TPA seems to indicate this is true. A prominent peak appearing at 558 nm in the TPA has a dip in the polarization spectrum associated with it and surely is part of the L_a manifold. Strickland tentatively assigned this peak in OPA as L_b 0+1340 cm^{-1}. It appears it may be a superposition of an L_a peak and an L_b peak. L_a excitation gives an Ω value of about 0.6 and again a third transition with high Ω grows in below 510 nm.

2,3 dimethylindole (2,dMI). The 2,3 dimethyl substituted derivative (Figure 12, 0.01M cyclohexane) exhibits the smallest L_a-L_b energy gap (8). In fact, this molecule is believed to have L_a lowest even in the vapor state (65). The polarization ratio is ~0.5 on the red edge and a shoulder is visible in the TPA. Strickland has assigned this shoulder in OPA as the 0-0 L_a. An intrinsic polarization ratio of 0.5 can thus be assigned to the L_a state; very different from the Ω=1.4 found for the L_b

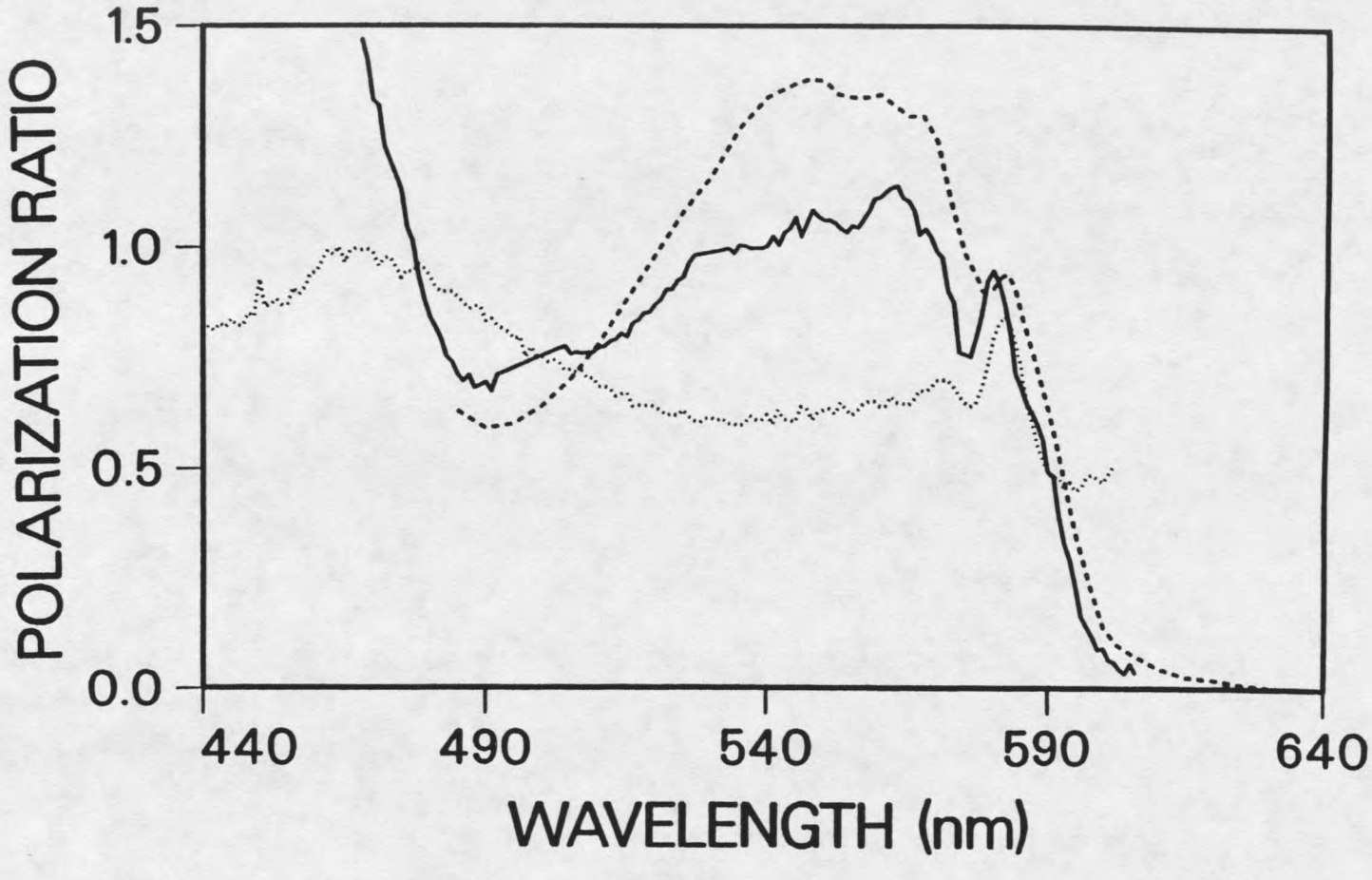

Figure 12: Two-photon fluorescence excitation (solid line), one photon absorption (dashed line), and two-photon polarization (dotted line) spectra for 2,3-dimethyl-indole dissolved in cyclohexane (0.01M).

state. The L_b origin peak shows Ω=0.85 and excitation of L_a gives an Ω of about 0.6. Overlap of L_a with the L_b state and the third transition seen again must contribute to the somewhat higher L_a Ω.

4-Methoxyindole (4MTI). The one and two-photon spectra of 4-methoxyindole in cyclohexane (.004M) are shown in Figure 14. The Ω value of 1.45 for the origin of this molecule is the highest observed and is quite close to the theoretical maximum. The polarization ratio begins to fall after the 0-1 of the L_b to a low value of 0.85. A conspicuous dip at 552 nm probably corresponds to the 0-0 of the L_a state. 4-methoxyindole is predicted to have a much reduced intensity for the L_a state (Table 1). The TPA and the high Ω value for L_a excitation support this picture. The third transition again appears to the blue and may also contribute to the high Ω.

5-methoxyindole (5MTI). The 5-methoxy derivative (0.004M cyclohexane) exhibits the largest separation of the L_a and L_b states seen (Figure 14). The structured L_b state exhibits a high polarization ratio of about 1.25 for the first three peaks visible. Substitution at the 5-position apparently lowers the Ω value of the L_b state. The 5-methyl derivative (Figure 8) also has a somewhat lower value of Ω L_b than is seen for indole. The L_b state of 5-methoxyindole also shows another sign of being quite perturbed relative to indole's L_b. A shoulder appears at

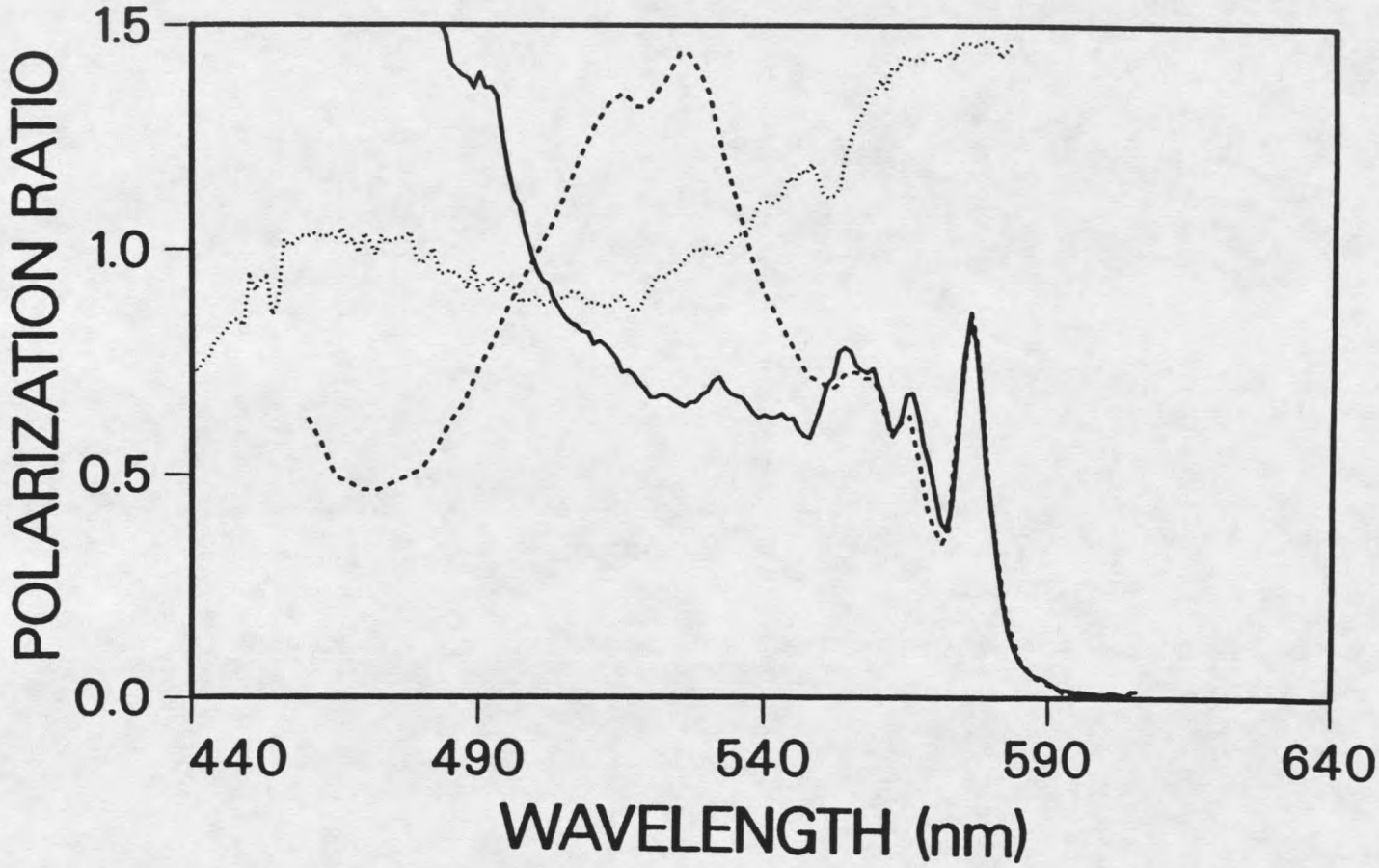

Figure 13: Two-photon fluorescence excitation (solid line), one photon absorption (dashed line), and two-photon polarization (dotted line) spectra for 4-methoxy-indole dissolved in cyclohexane (0.004M).

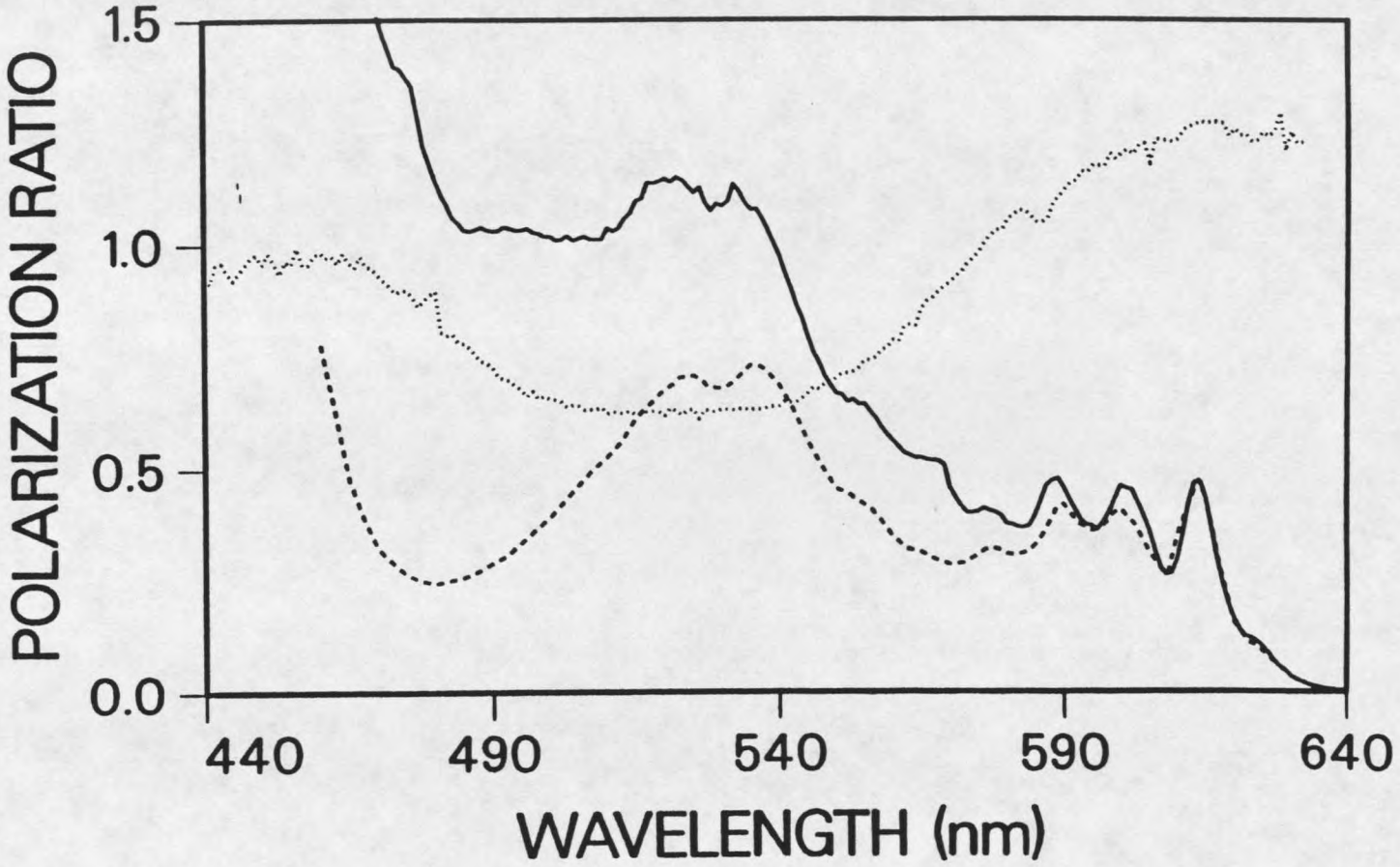

Figure 14: Two-photon fluorescence excitation (solid line), one photon absorption (dashed line), and two-photon polarization (dotted line) spectra for 5-methoxy-indole dissolved in cyclohexane (0.004M).

about 623 nm in TPA and 311nm in OPA which is not observed for the other derivatives. This peak was assigned as a hot band by Strickland (9) but this does not appear to be true. They cooled a sample to 90°K in polar solvent and saw that it had disappeared. The polar solvent has the effect of blurring all the transitions and the room temperature spectrum in n-butanol (see Figure 35) does not show the shoulder resolved either. The new assignment of the shoulder would be L_b 0-0 which results in an L_b band shape much different than for indole. Such an alteration of the L_b band shape might be expected since the transition density pattern of the L_b state is mostly in the six ring (48). Another interesting feature appears in the Ω spectrum at 587 nm where a reproducible dip like that seen in 4-methoxyindole apparently reveals the position of the L_a 0-0 or a vibronic peak of L_b. L_a excitation gives a value of about 0.62 and the third transition grows in below 500 nm.

6-methoxyindole (6MTI). Like 4-methoxyindole, 6-methoxyindole (Figure 15, 0.004M cyclohexane) is predicted to have a much reduced L_a intensity (Table 1). The TPA indicates that this is true. Very little TPA intensity is seen in the wavelength region where L_a should appear. Unlike the other molecules studied, the TPA does not correspond well to the OPA. The TPA is seen to have a maximum at 563nm which does not have an analog in the OPA. Another peak in this new band appears at 573nm, and the

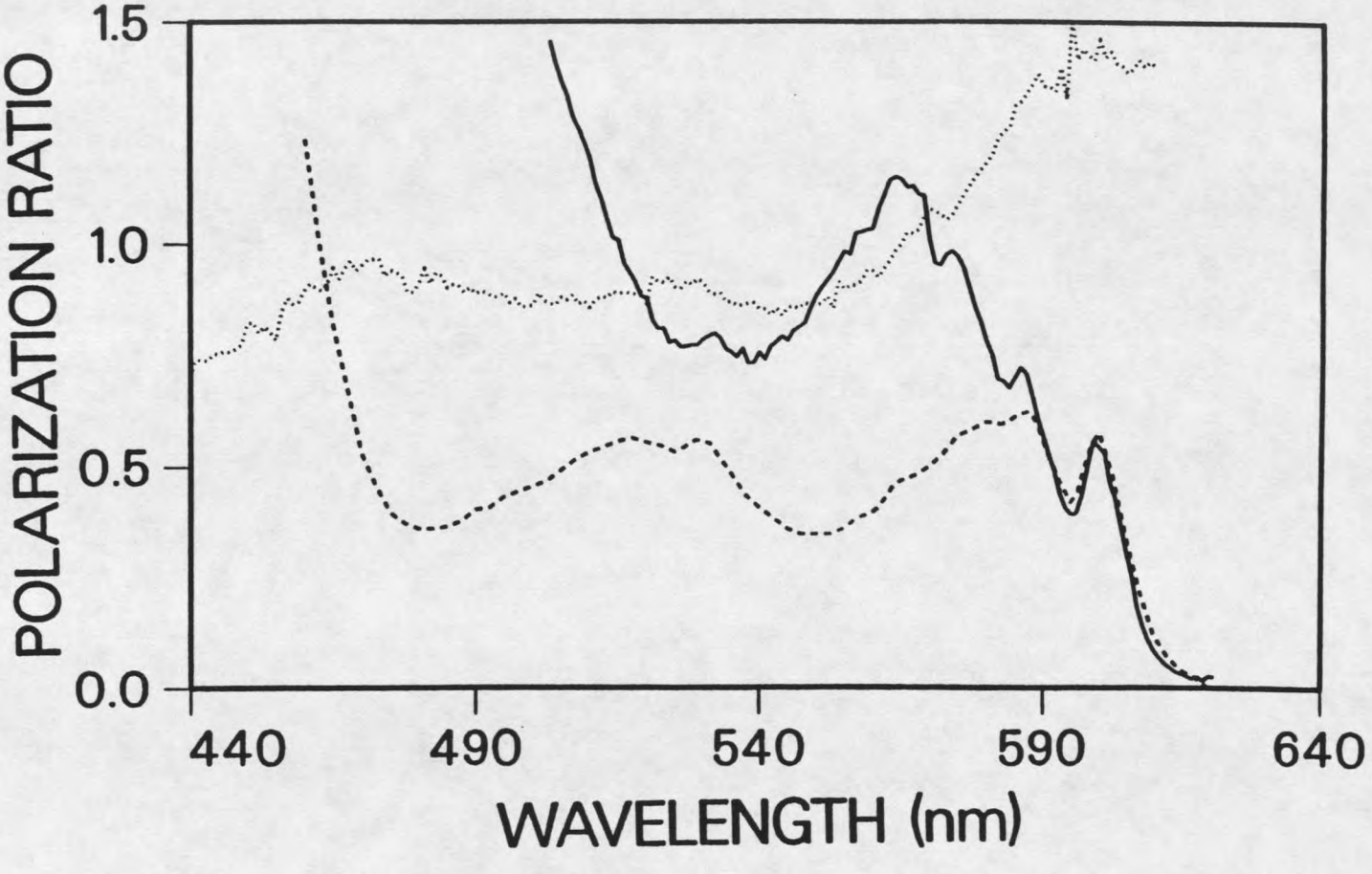

Figure 15: Two-photon fluorescence excitation (solid line), one photon absorption (dashed line), and two-photon polarization (dotted line) spectra for 6-methoxy-indole dissolved in cyclohexane (0.004M).

separation of the 0-0 to this peak is 1572cm-1. In analogy to the benzimidazoles, this suggests a vibronic origin for the anomalous structure seen for this molecule. In the other indoles, the strongly allowed L_a covers up the vibronic structure. The strong third transition seems to cover L_a completely to the blue and L_b covers it to the red giving an L_a Ω value of 0.85. A slight rise in Ω corresponding to the dip seen in the OPA at 525 nm belies L_a's existence in the two-photon spectrum.

7-methoxyindole (7MTI). In contrast to 4 and 6-methoxyindole, for 7-methoxyindole (Figure 16, 0.04M cyclohexane) it is the L_b band which is predicted to be substantially reduced (Table 1). This would appear to be the case. The sharp origin peak is seen to have a polarization ratio that is lower (Ω = 0.8) than 2 peaks in Ω that appear to the blue. The Ω value for L_a excitation is 0.5, the value of Ω L_a in 2,3 dimethylindole where L_a is to the red of L_b and exposed. The low value of Ω around 525 nm does seem to indicate that L_b is quite reduced for 7-methoxyindole but why does the origin have a low polarization? It is possible that like 5-methoxyindole, 7-methoxyindole has a very different L_b band shape and a lower intrinsic polarization ratio. Another possibility is that the L_a 0-0 is superposed with the L_b 0-0 and this leads to the low Ω value.

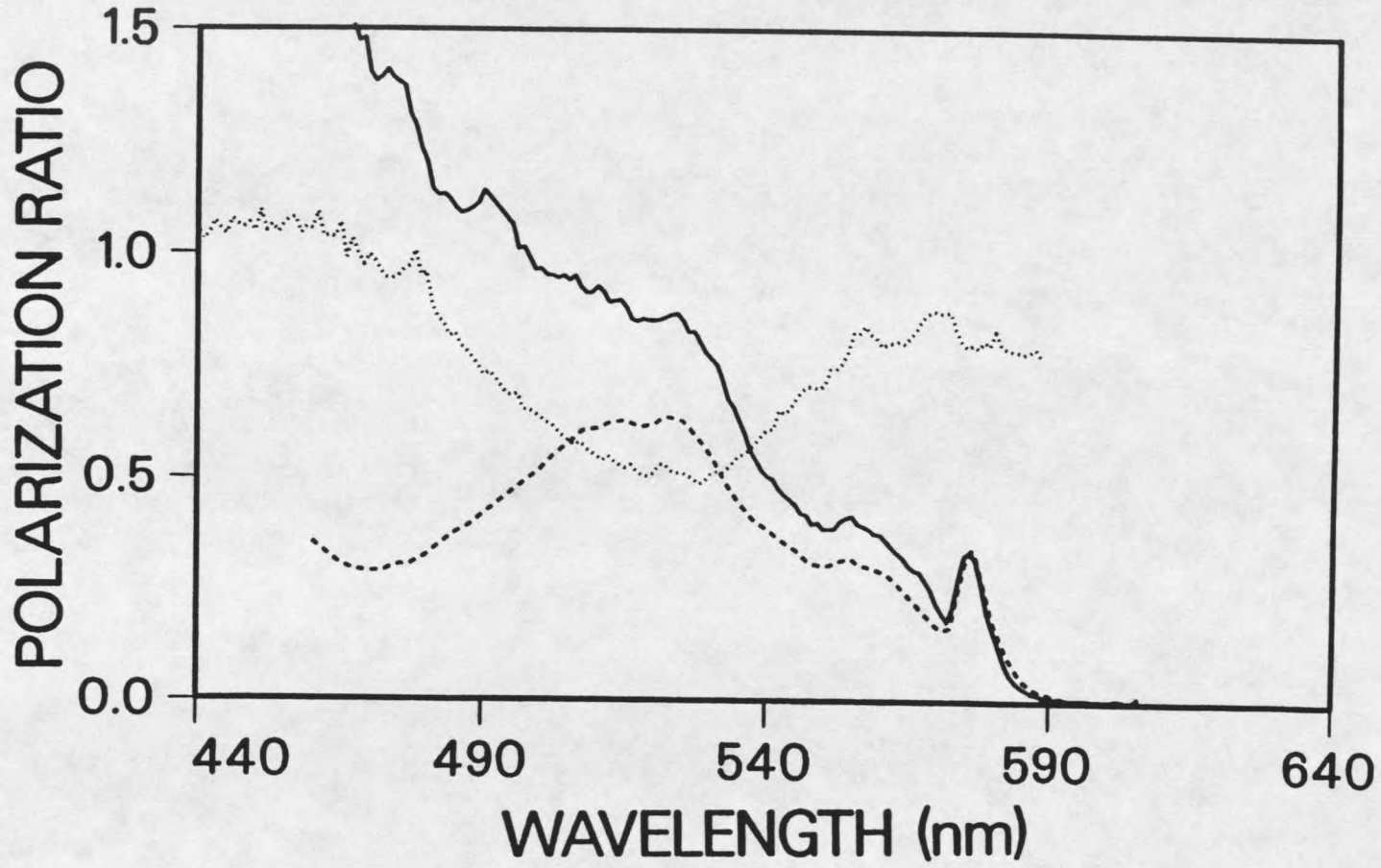

Figure 16: Two-photon fluorescence excitation (solid line), one photon absorption (dashed line), and two-photon polarization (dotted line) spectra for 7-methoxy-indole dissolved in cyclohexane (0.004M).

Indoles in Butanol

5-methylindole. Figure 17 shows the TPA (solid line), the Ω (dotted line), and the OPA (dashed line) for 5-methylindole dissolved in n-butanol at 0.01M. The main effect of polar solvation is to lower the polarization ratio at the origin and cause it to drop on the red edge. The polarization changes seen going from hydrocarbon by n-butanol are shown in Figure 18 and are consistent with a red shift of L_a. The fluorescence changes seen going to the polar solvent are shown in Figure 19 along with the absorption changes. The fluorescence maximum shifts from 310 nm in cyclohexane to 313 nm in butanol and the fluorescence becomes somewhat broader while losing structure in butanol.

Indole. The TPA, Ω, and OPA for indole in butanol (0.01M) are shown in Figure 20. The polarization spectrum now closely resembles that seen for 3-methylindole in cyclohexane. Martinaud and Kadiri (10) have placed the 0-0 L_a and 0-0 L_b on top of one another for indole in polar solvents as a result of their solvent shift studies. The two-photon results suggest this is correct. The changes in the Ω spectra for polar solvation are shown in Figure 21 and the associated absorption and fluorescence charges appear in Figure 22. Loss of structure in the fluorescence is accompanied by a shift in the maximum from 300 nm to 328 nm.

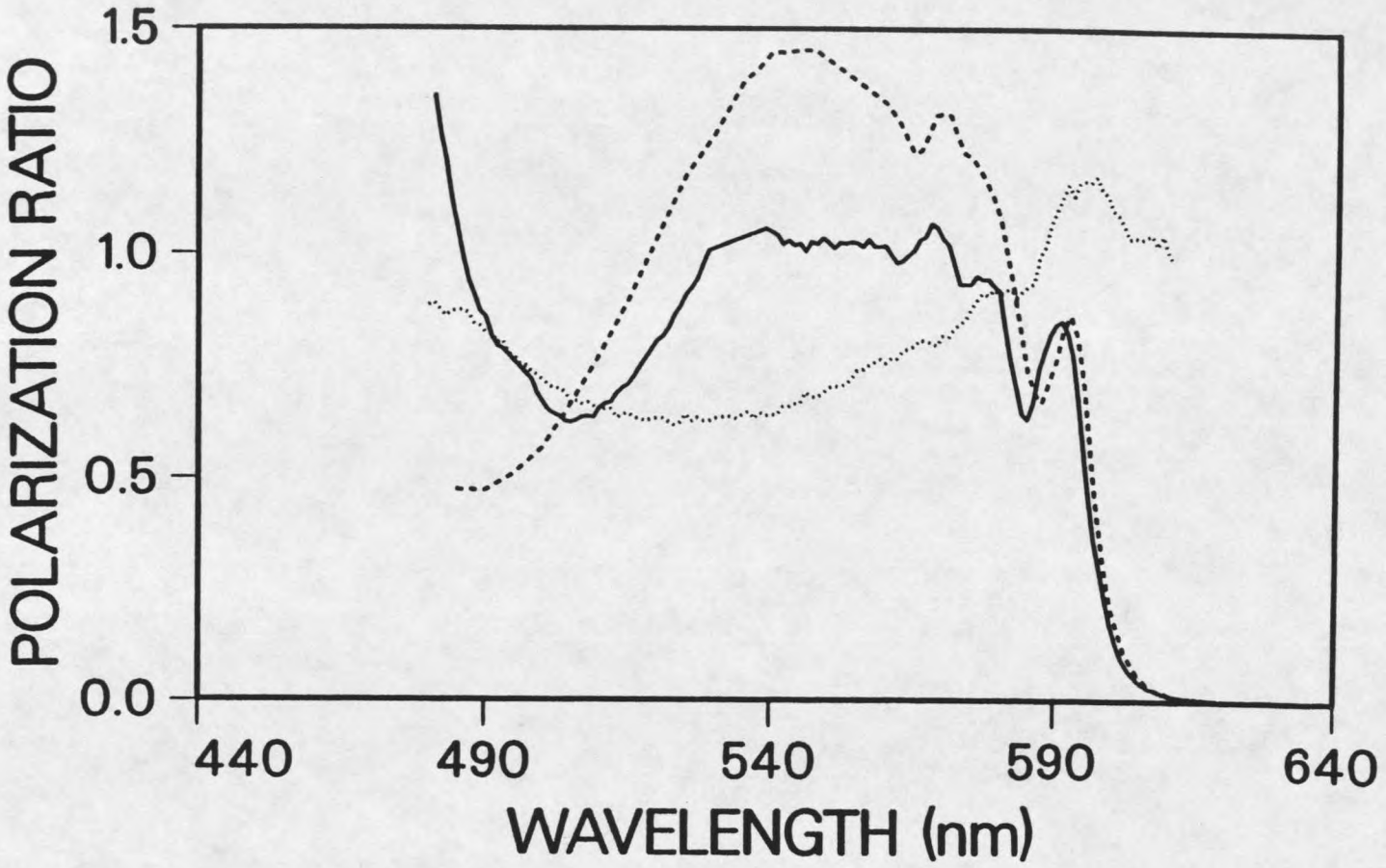

Figure 17: Two-photon fluorescence excitation (solid line), one photon absorption (dashed line), and two-photon polarization (dotted line) spectra for 5-methylindole dissolved in butanol (0.01M).

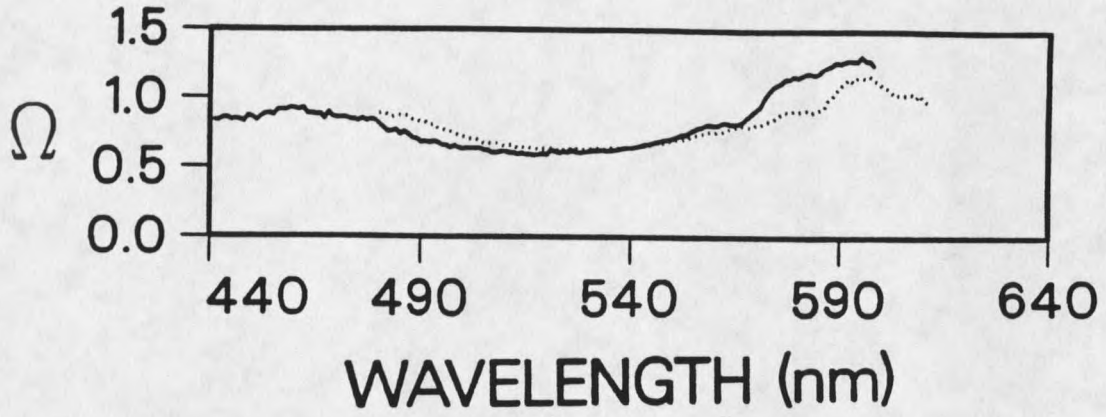

Figure 18: Two-photon polarization spectra of 5-methyl-indole in cyclohexane (solid line) and in butanol (dotted line) (0.01M).

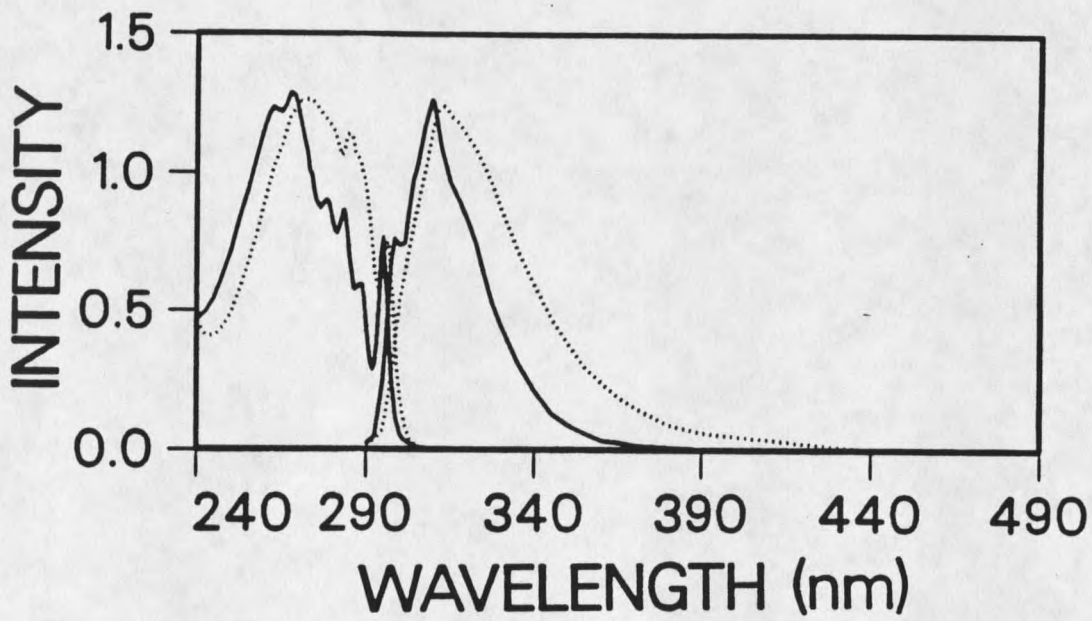

Figure 19: One-photon absorption and fluorescence spectra of 5-methylindole in cyclohexane (solid lines) and in butanol (dotted lines) (~10-5M).

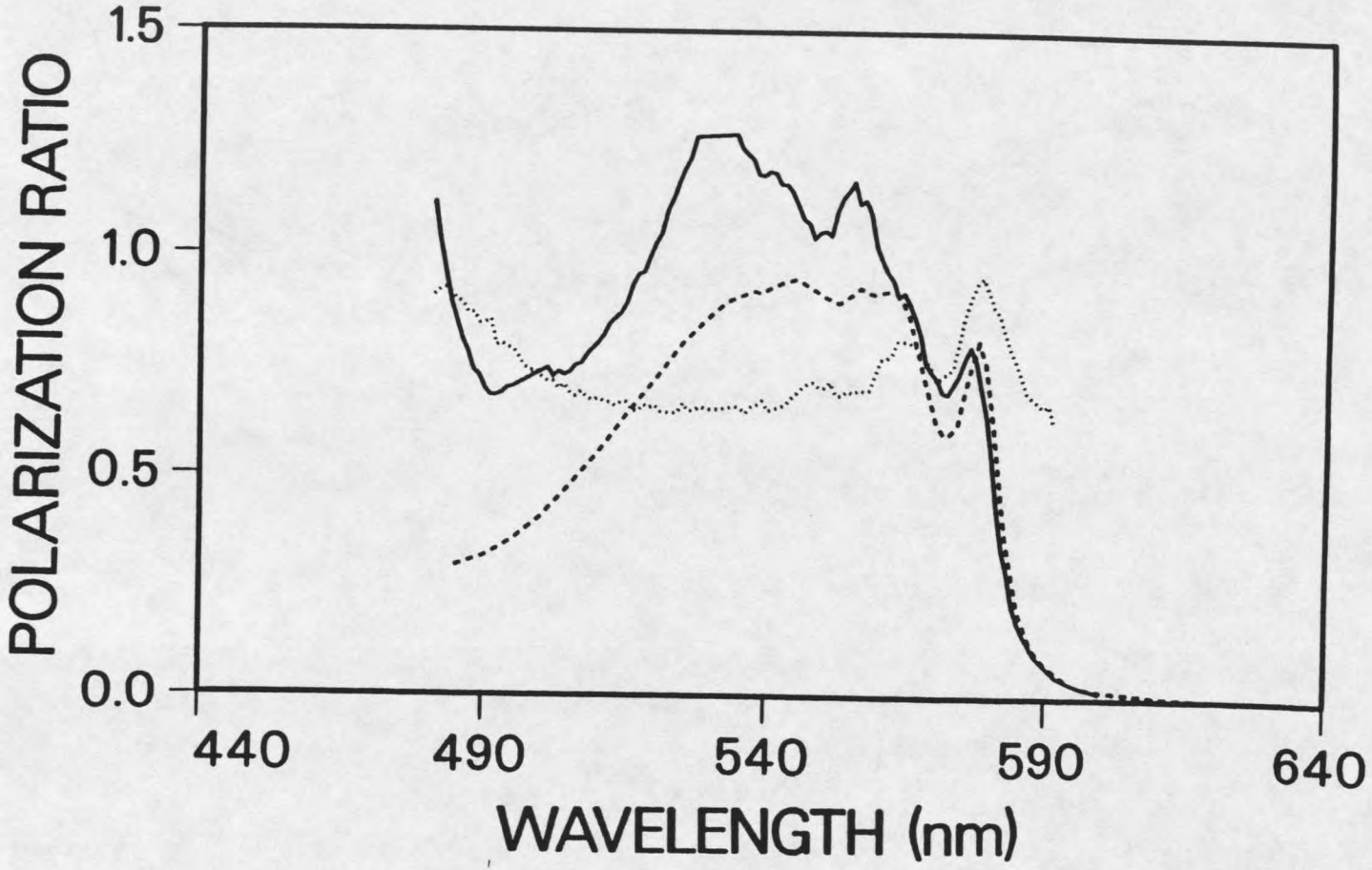

Figure 20: Two-photon fluorescence excitation (solid line), one photon absorption (dashed line), and two-photon polarization (dotted line) spectra for indole dissolved in butanol (0.01M).

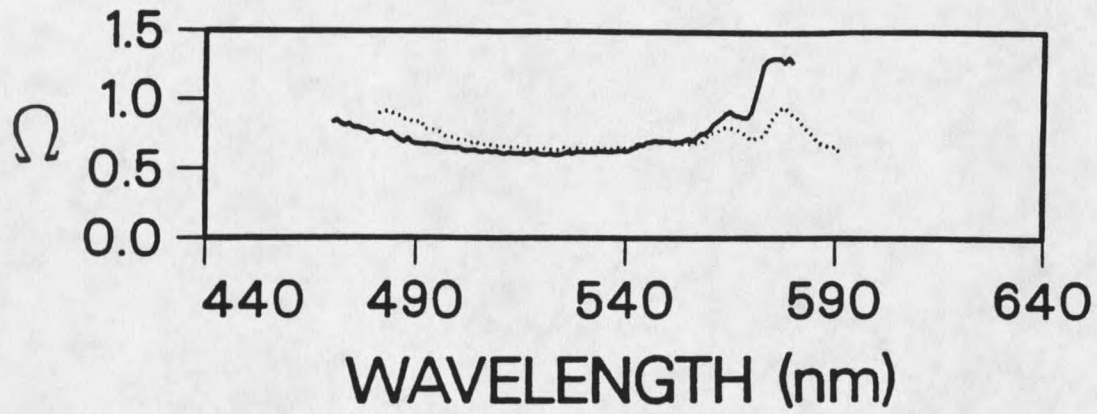

Figure 21: Two-photon polarization spectra of indole in cyclohexane (solid lines) and in butanol (dotted line) (0.01M).

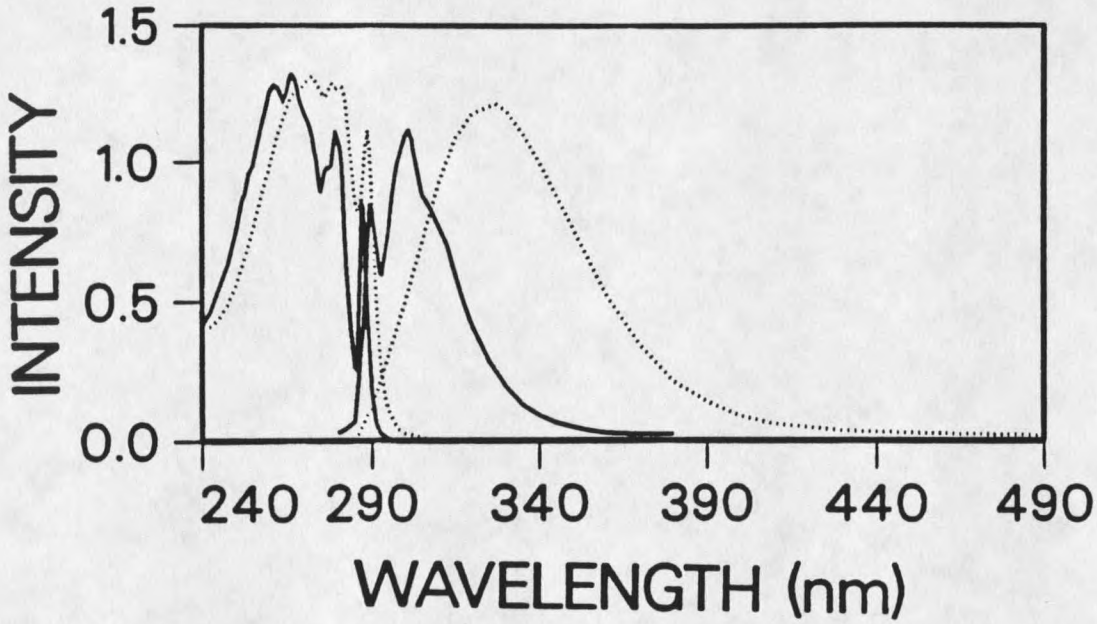

Figure 22: One-photon absorption and fluorescence spectra of indole in cyclohexane (solid lines) and in butanol (dotted line) (0.01M).

1-methylindole. The data for 1-methylindole in butanol (0.01M) are shown in Figs. 23-25. Again the values of Ω are lowered in the origin and the fluorescence loses structure and shifts to the red (310 nm to 326 nm).

3-methylindole. The 3-methyl derivative which had the L_a and L_b 0-0's superposed in cyclohexane now has L_a as the lowest singlet state. The polarization ratio (Figure 26, 0.01M butanol) at the red edge is about 0.5 as was seen for 2,3 dimethylindole in cyclohexane. The TPA and OPA now appear less steep on the red edge. Figures 27 and 28 show the changes in Ω and in the absorption and fluorescence for 3-methylindole.

2,3 dimethylindole. The spectra for 2,3 dimethylindole in butanol (0.01M) are shown in Figure 29 along with the associated changes in Ω (Figure 30) and fluorescence (Figure 31). The fluorescence spectra are of interest because they show what fluorescence from L_a looks like in non-polar and in polar solvents.

4-methoxyindole. This molecule with its reduced L_a absorption in TPA shows a small drop in Ω on the red edge when dissolved in butanol (0.004M) (Figures 32 and 33). The fluorescence maximum shifts from 305 nm to 307 nm (Figure 34) and loses little structure. It appears this molecule emits predominantly from the L_b state and this is consistent with the high Ω value on the red edge.

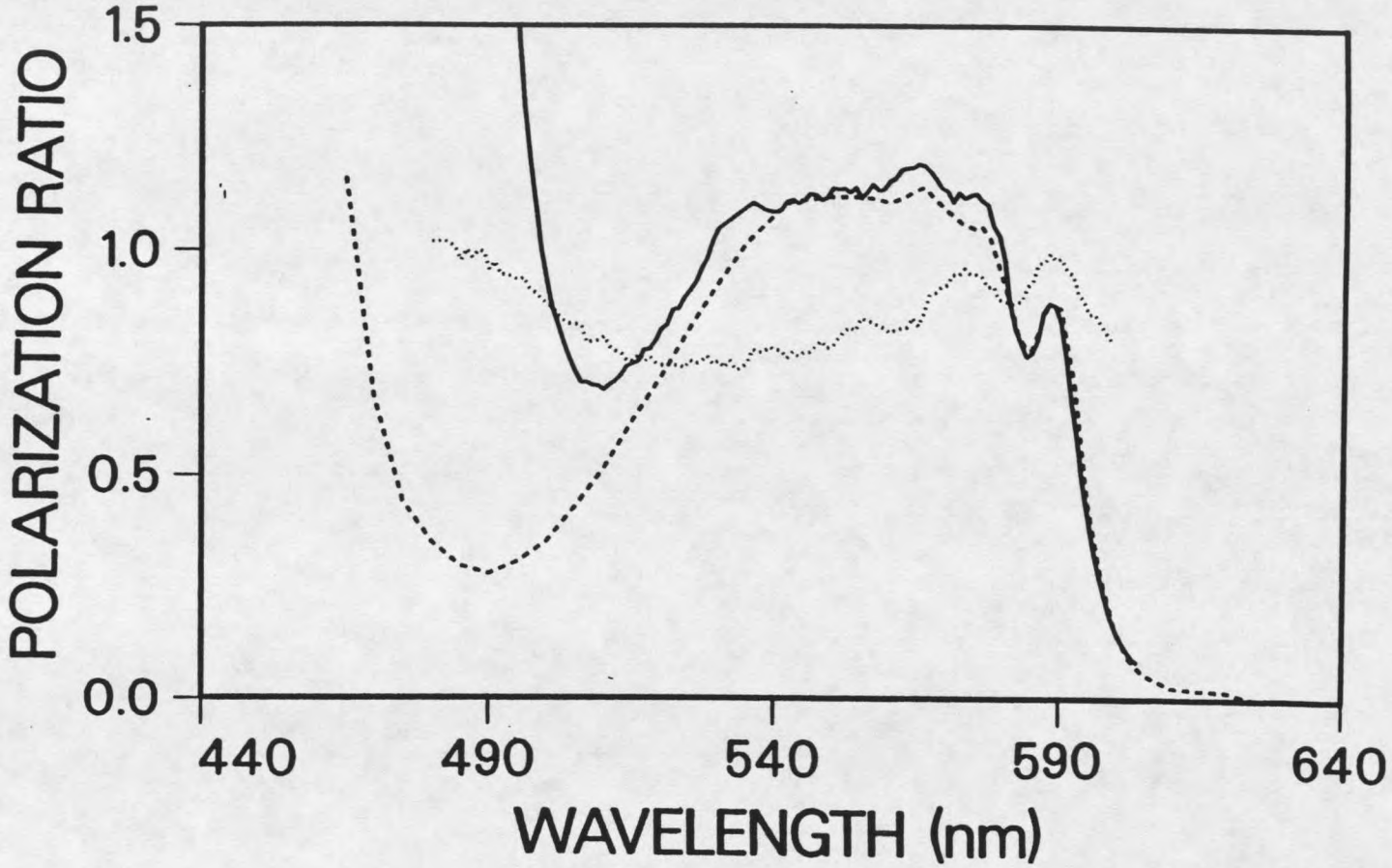

Figure 23: Two-photon fluorescence excitation (solid line), one photon absorption (dashed line), and two-photon polarization (dotted line) spectra for 1-methylindole dissolved in butanol (0.01M).

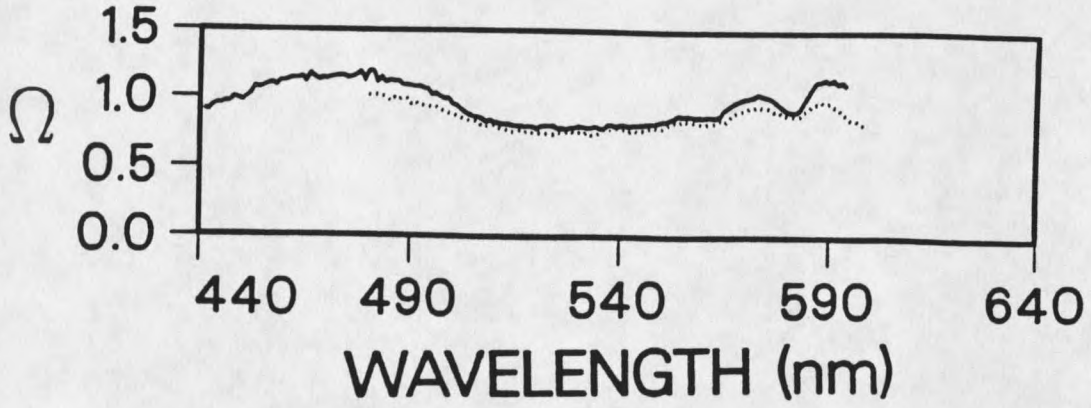

Figure 24: Two-photon polarization spectra of 1-methylindole in cyclohexane (solid line) and in butanol (dotted line) (0.01M)

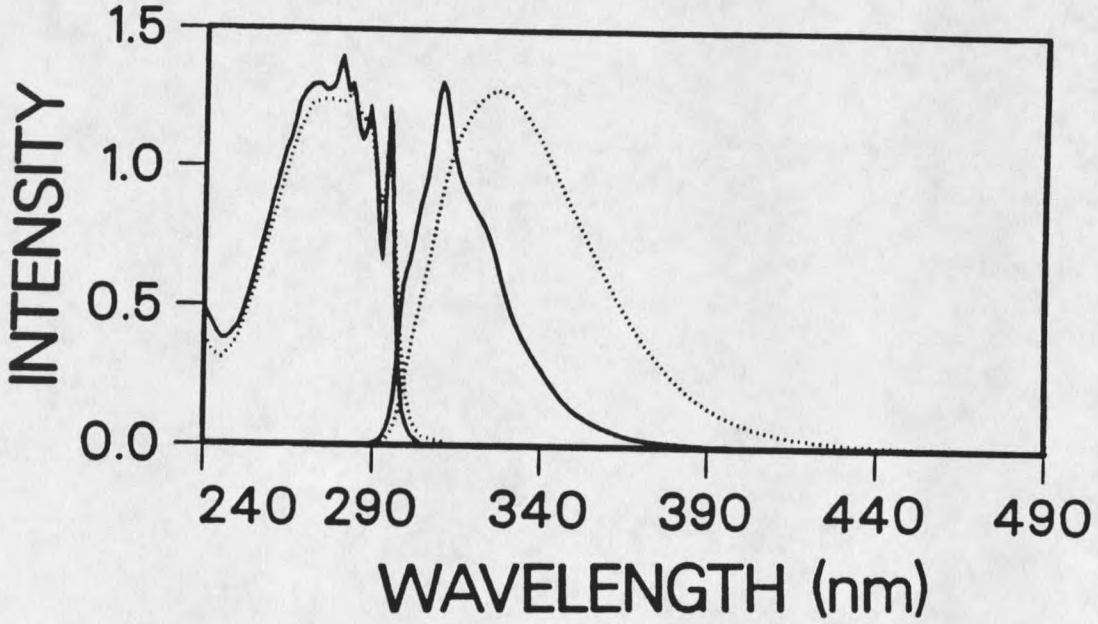

Figure 25: One-photon absorption and fluorescence spectra of 1-methylindole in cyclohexane (solid lines) and in butanol (dotted lines) (~10-5M).

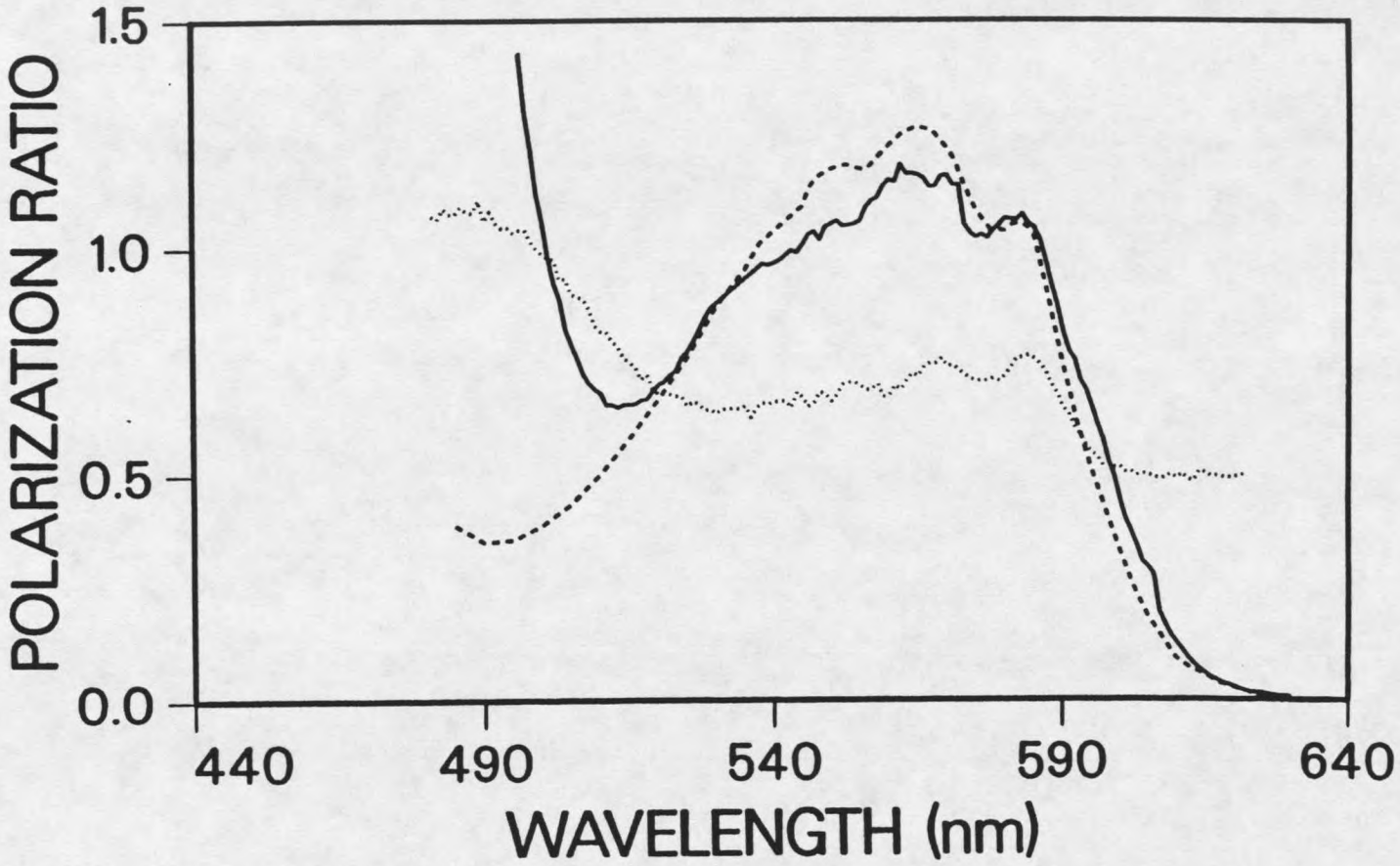

Figure 26: Two-photon fluorescence excitation (solid line), one photon absorption (dashed line), and two-photon polarization (dotted line) spectra for 3-methylindole dissolved in butanol (0.01M).

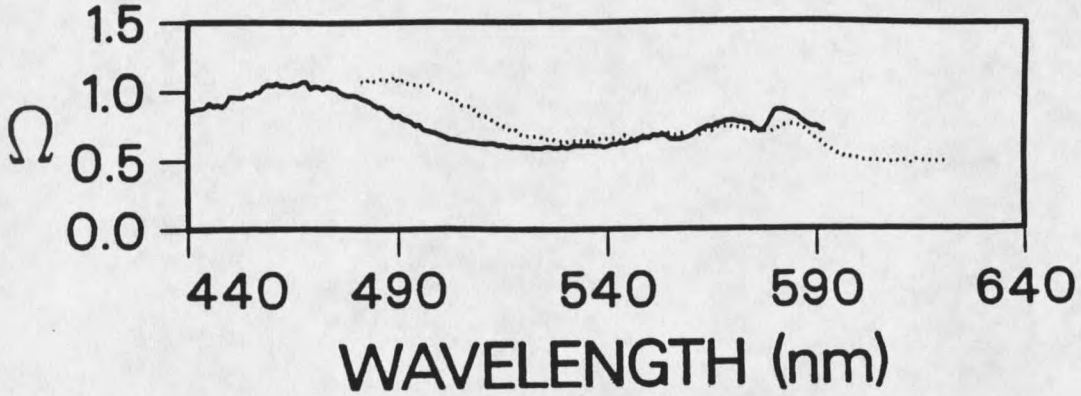

Figure 27: Two-photon polarization spectra of 3-methyl-indole ind cyclohexane (solid line) and in butanol (dotted line) (0.01M).

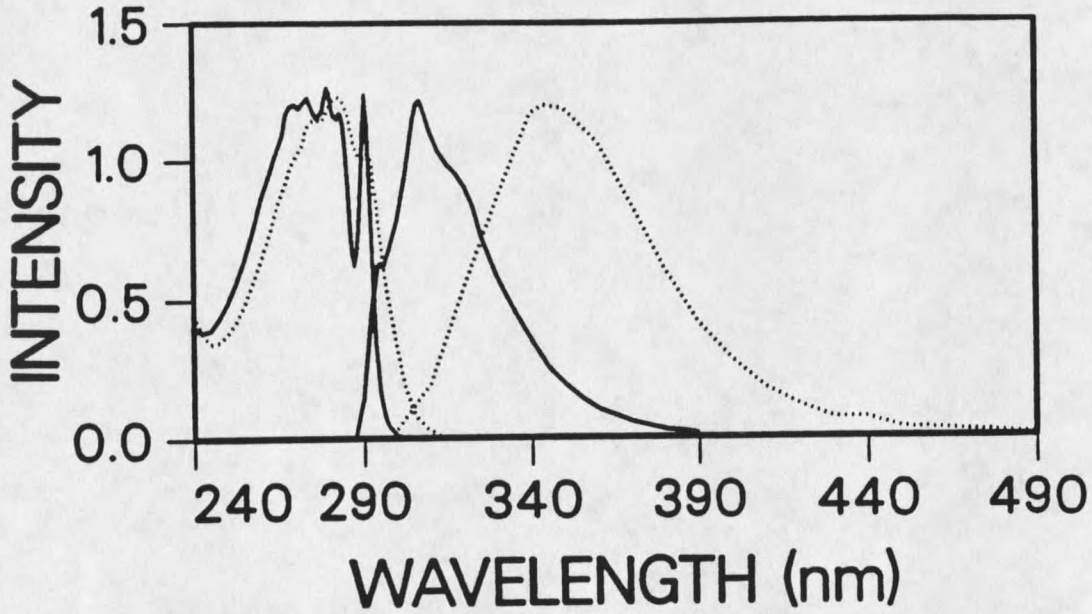

Figure 28: One-photon absorption and fluorescence spectra of 3-methylindole in cyclohexane (solid lines) and in butanol (dotted lines) (~10-5M).

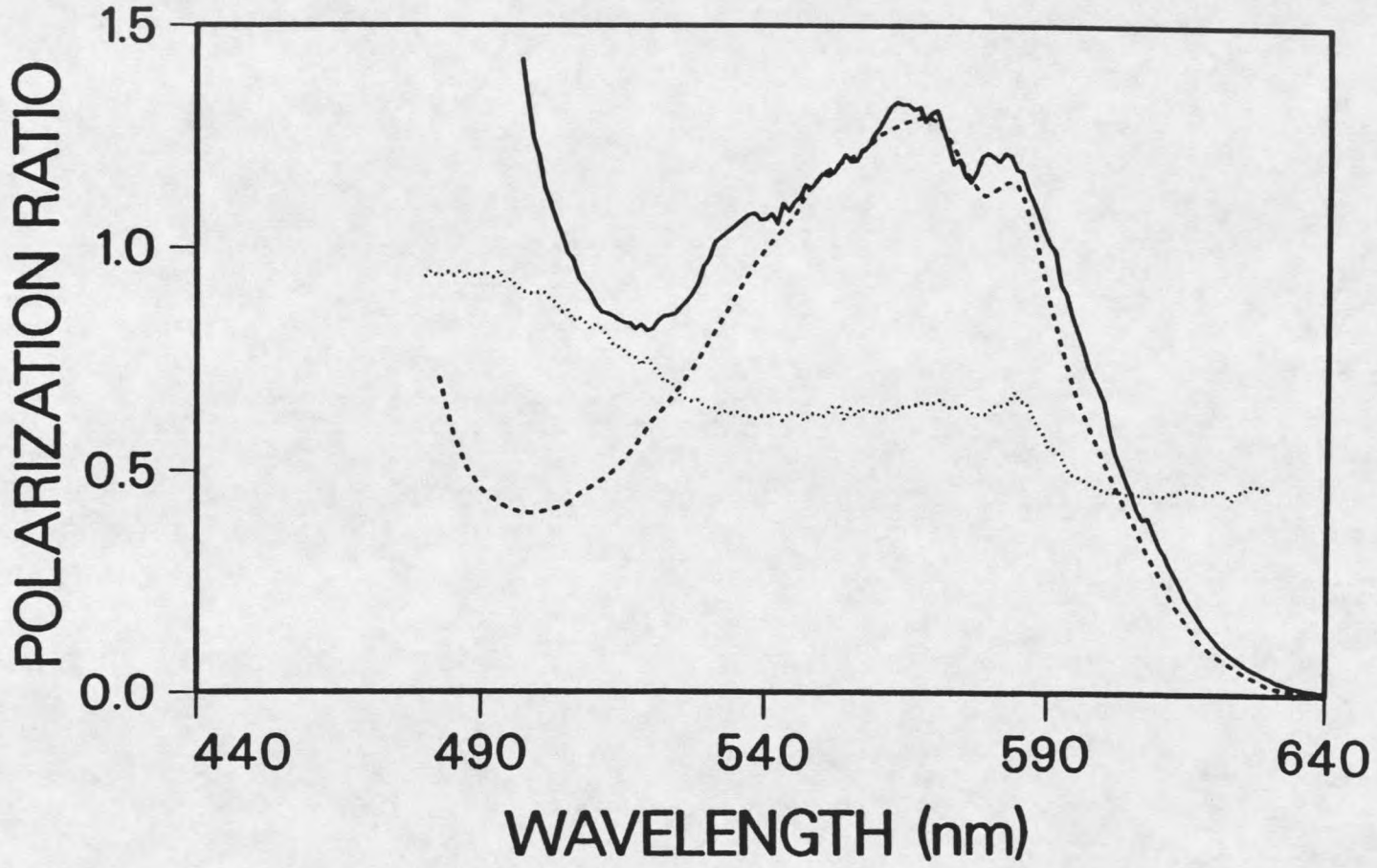

Figure 29: Two-photon fluorescence excitation (solid line), one photon absorption (dashed line), and two-photon polarization (dotted line) spectra for 2,3-dimethyl-indole dissolved in butanol (0.01M).

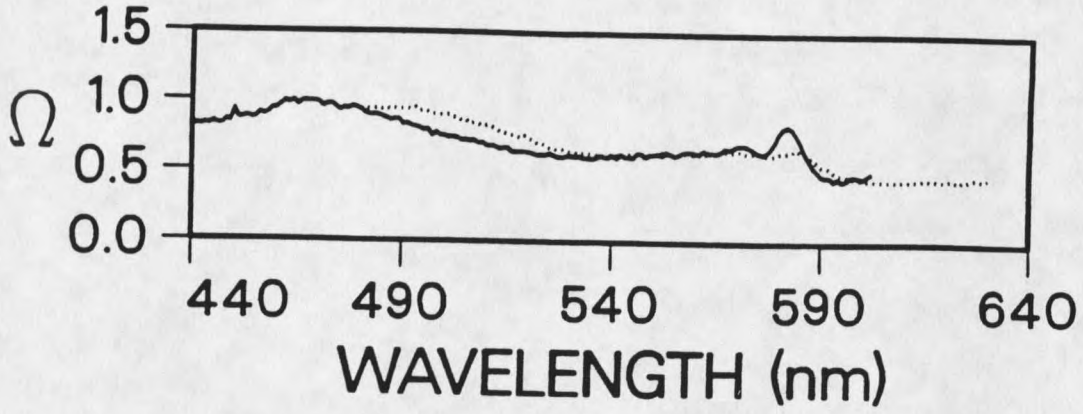

Figure 30: Two-photon polarization spectra of 2,3-dimethylindole in cyclohexane (solid line) and in butanol (dotted line) (0.01M).

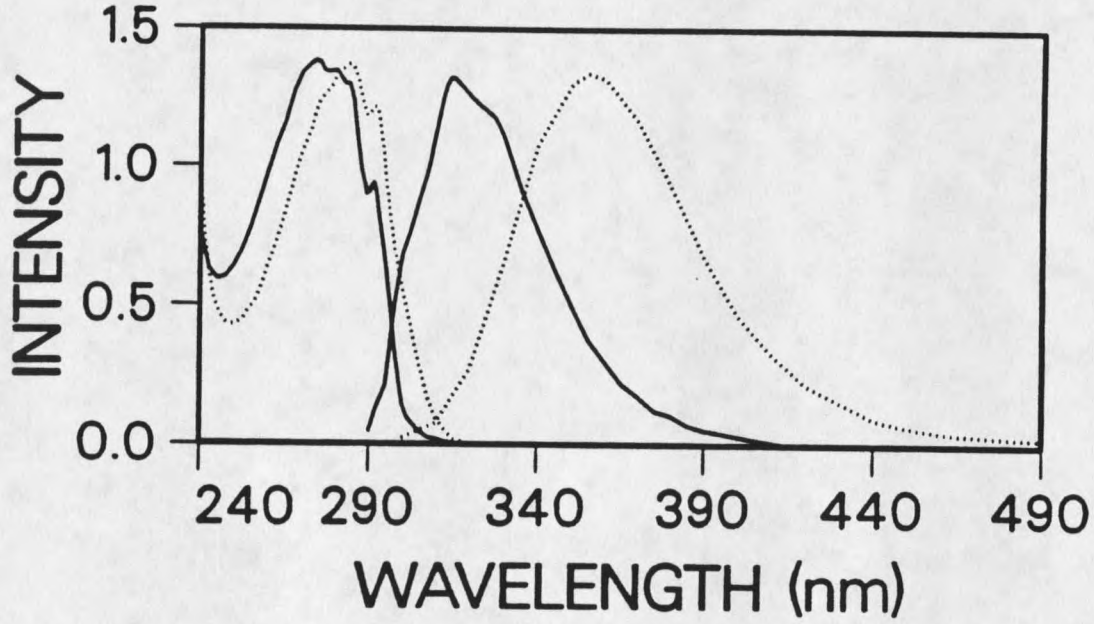

Figure 31: One-photon absorption and fluorescence spectra of 2,3-dimethylindole in cyclohexane (solid lines) and in butanol (dotted lines) (~10-5M).

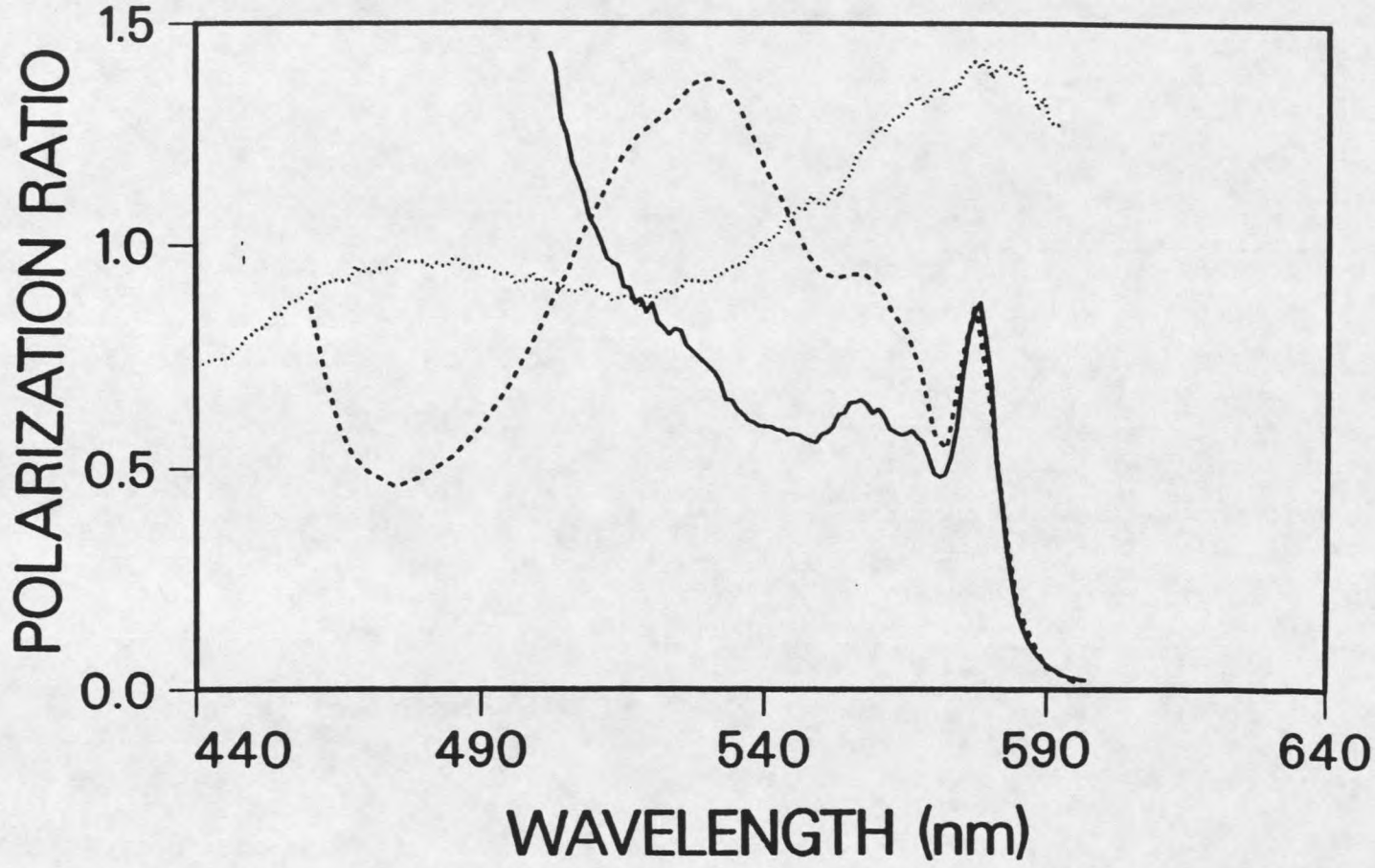

Figure 32: Two-photon fluorescence excitation (solid line), one photon absorption (dashed line), and two-photon polarization (dotted line) spectra for 4-methoxy-indole dissolved in butanol (0.004M).

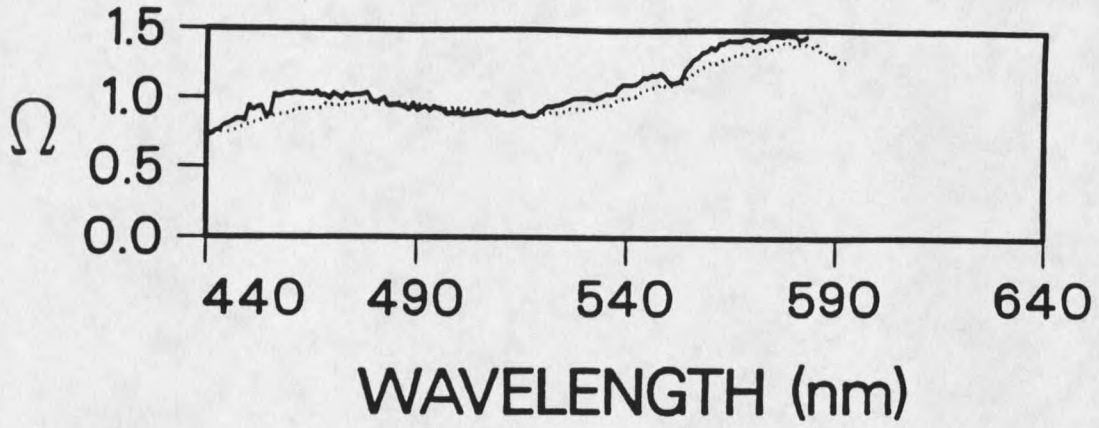

Figure 33: Two-photon polarization spectra of 4-methoxy-indole in cyclohexane (solid line) and in butanol (dotted line) (0.004M).

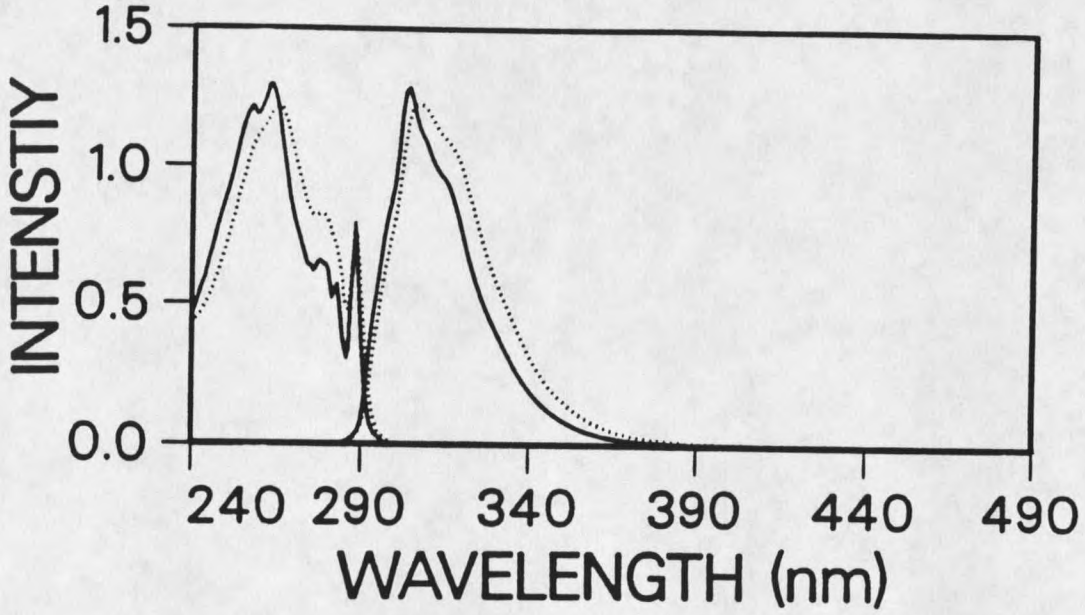

Figure 34: One-photon absorption and fluorescence spectra of 4-methoxyindole in cyclohexane (solid lines) and in butanol (dotted lines) (~10-5M).

5-methoxyindole. The broad L_a state shifts red and covers most of the L_b state for 5-methoxyindole in butanol (0.004M) (Figure 35). The Ω value on the red edge never changes and correspondingly there is only a shift in fluorescence maximum from 327 nm to 330 nm with very little broadening (Figures 36 and 37), indicating L_b fluorescence.

6-methoxyindole. The TPA shows very little L_a intensity (Figure 38) for this molecule (0.004M butanol) and the peak not seen in OPA is also evident in butanol solvent. Ω drops on the red edge and the fluorescence maximum shifts from 318 nm to 334 nm and becomes much broader (Figures 39 and 40). 6-methoxyindole is the only methoxyindole which shows such a large red shift. Perhaps the L_b state is more sensitive to solvation when it is substituted at position 6.

7-methoxyindole. As the broad L_a shifts red in the polar solvent, the Ω value at the origin drops and the 2 peaks associated with the L_b band are somewhat smeared out (Figure 41, 0.004M butanol). However, virtually no change in fluorescence is observed, the maximum staying at 305 nm. (Figures 42,43). It is likely that this molecule emits from L_b.

Discussion

Assigning a high polarization ratio of ~1.4 to the ^1L_b state and a low ratio of ~0.5 to the ^1L_a state gives a general picture in accord with that deduced from one-photon

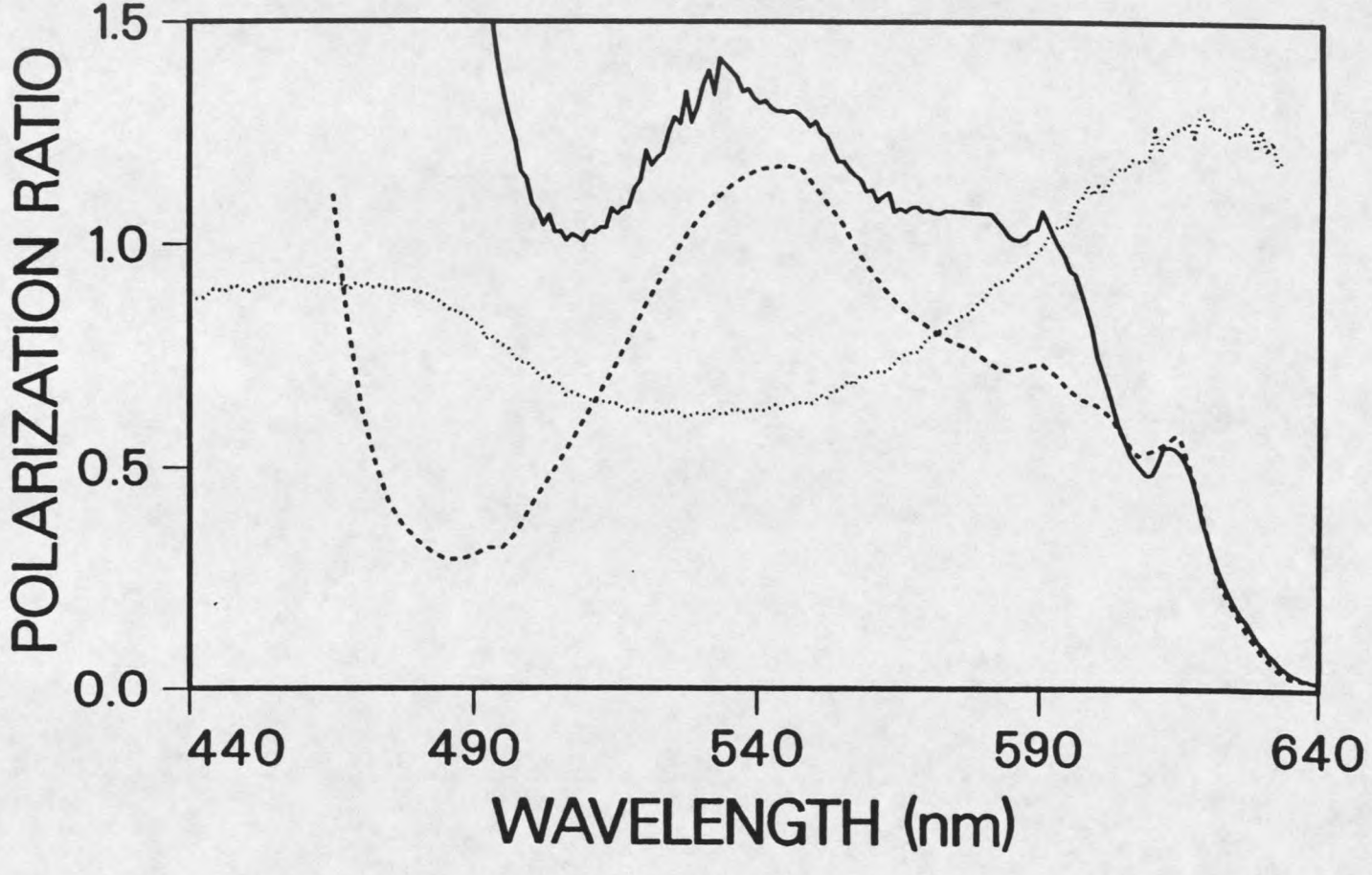

Figure 35: Two-photon fluorescence excitation (solid line), one photon absorption (dashed line), and two-photon polarization (dotted line) spectra for 5-methoxy-indole dissolved in butanol (0.004M).

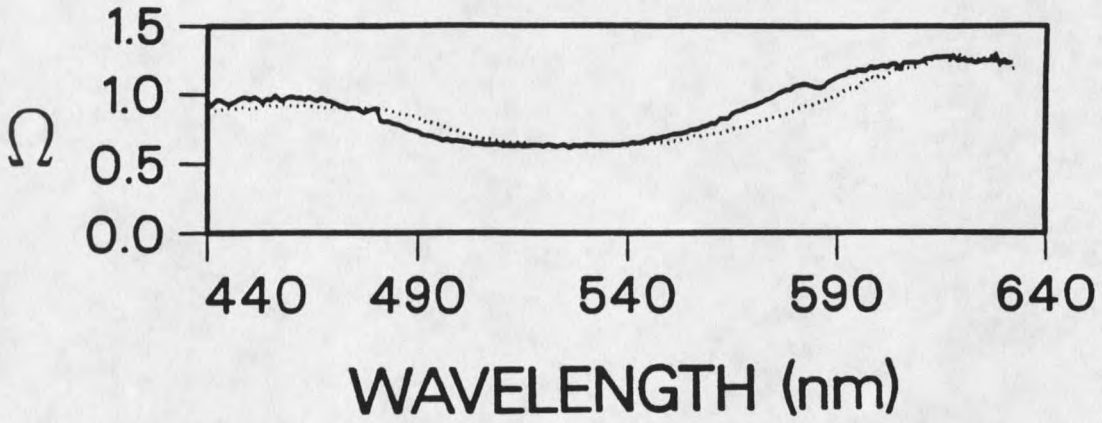

Figure 36: Two-photon polarization spectra of 5-methoxy-indole in cyclohexane (solid line) and in butanol (dotted line) (0.004M).

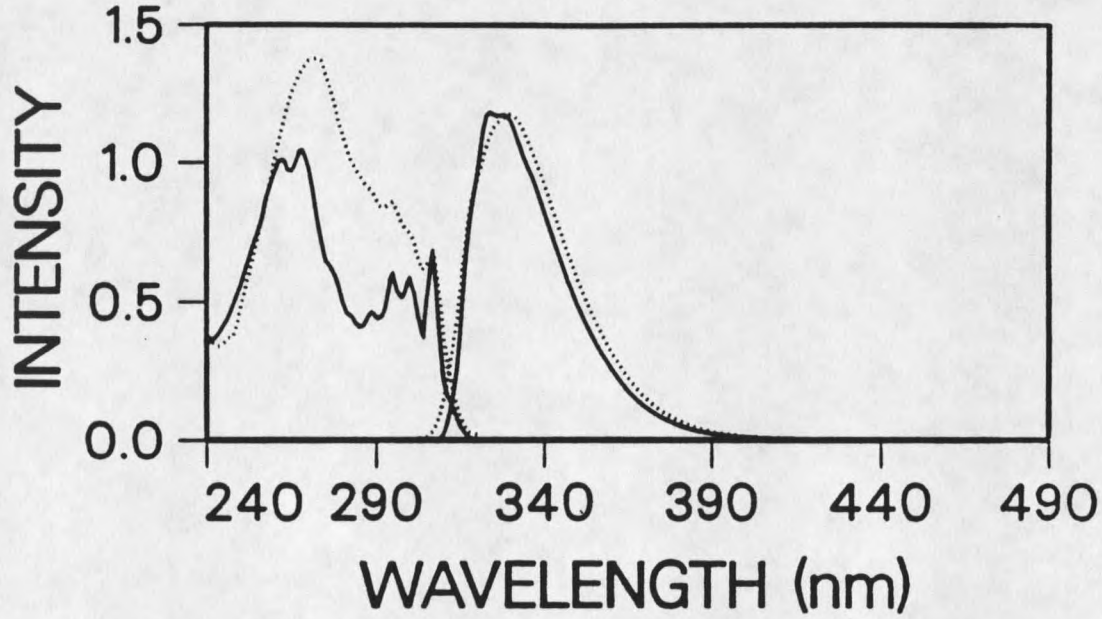

Figure 37: One-photon absorption and fluorescence spectra of 5-methoxyindole in cyclohexane (solid lines) and in butanol (dotted lines) (~10-5M).

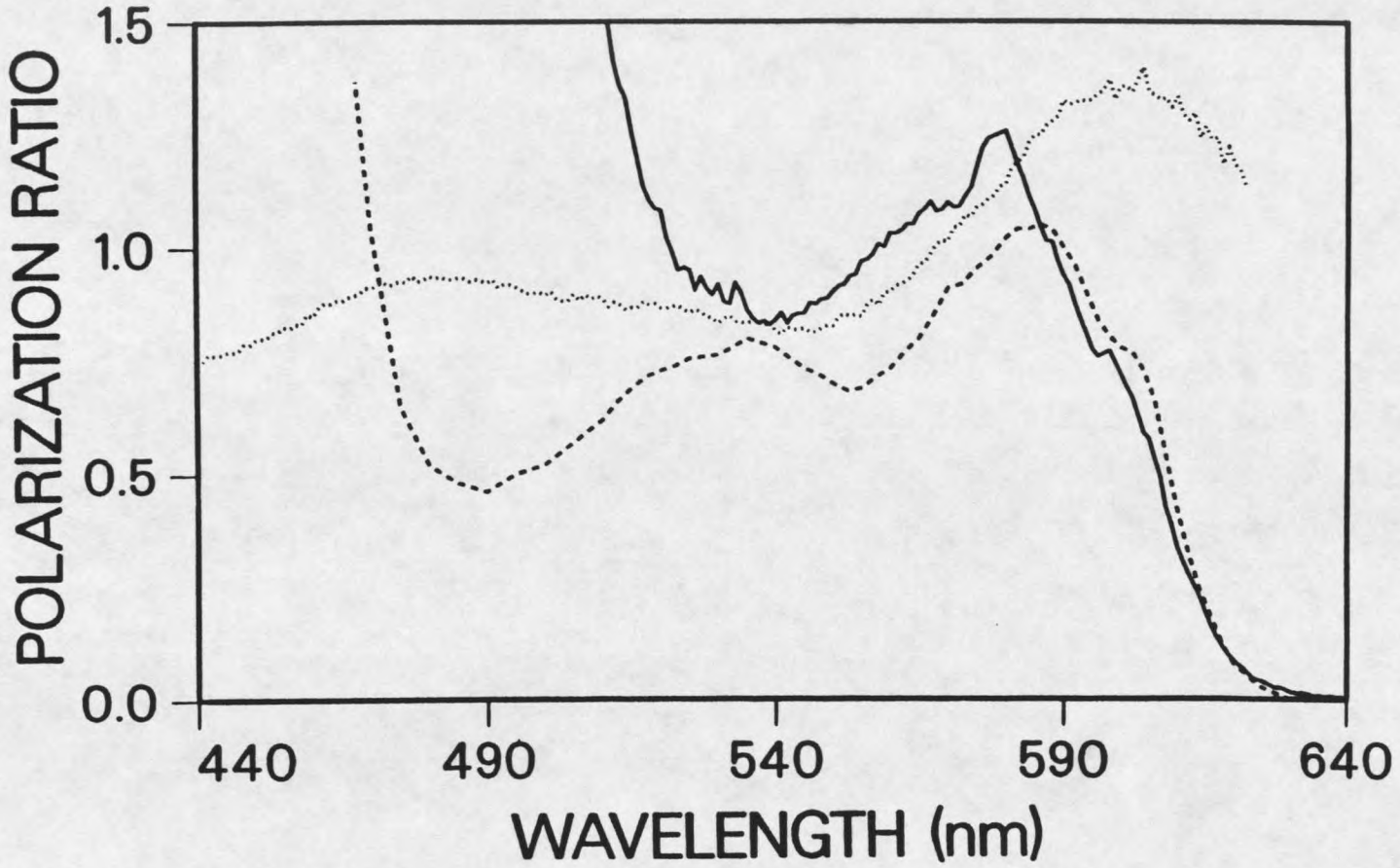

Figure 38: Two-photon fluorescence excitation (solid line), one photon absorption (dashed line), and two-photon polarization (dotted line) spectra for 6-methoxy-indole dissolved in butanol (0.004M).

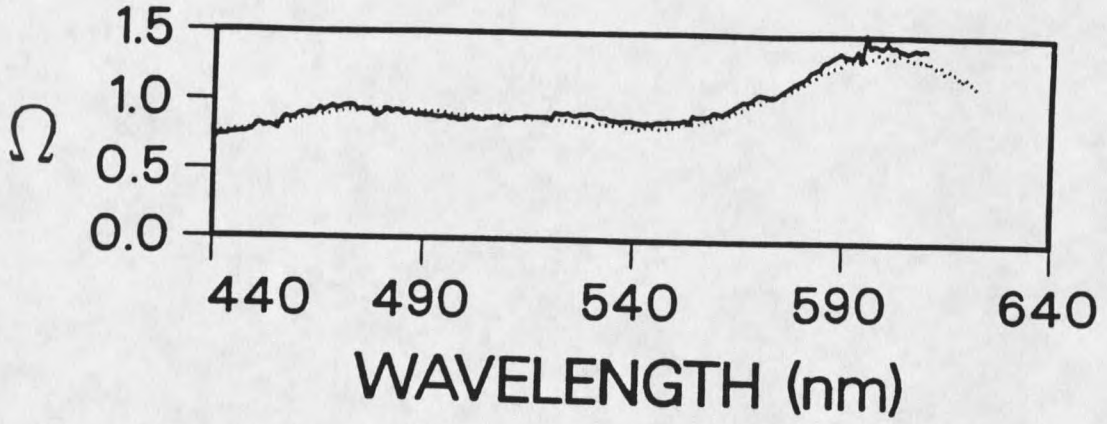

Figure 39: Two-photon polarization spectra of 6-methoxy-indole in cyclohexane (solid line) and in butanol (dotted line) (0.004M).

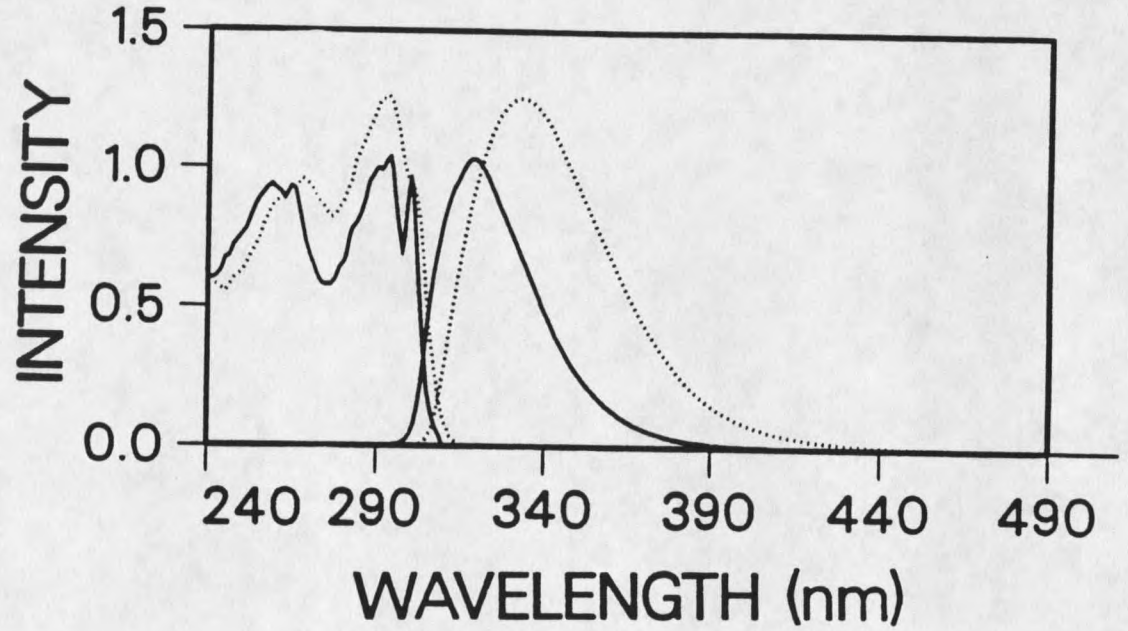

Figure 40: One-photon absorption and fluorescence spectra of 6-methoxyindole in cyclohexane (solid lines) and in butanol (dotted lines) (~10-5M).

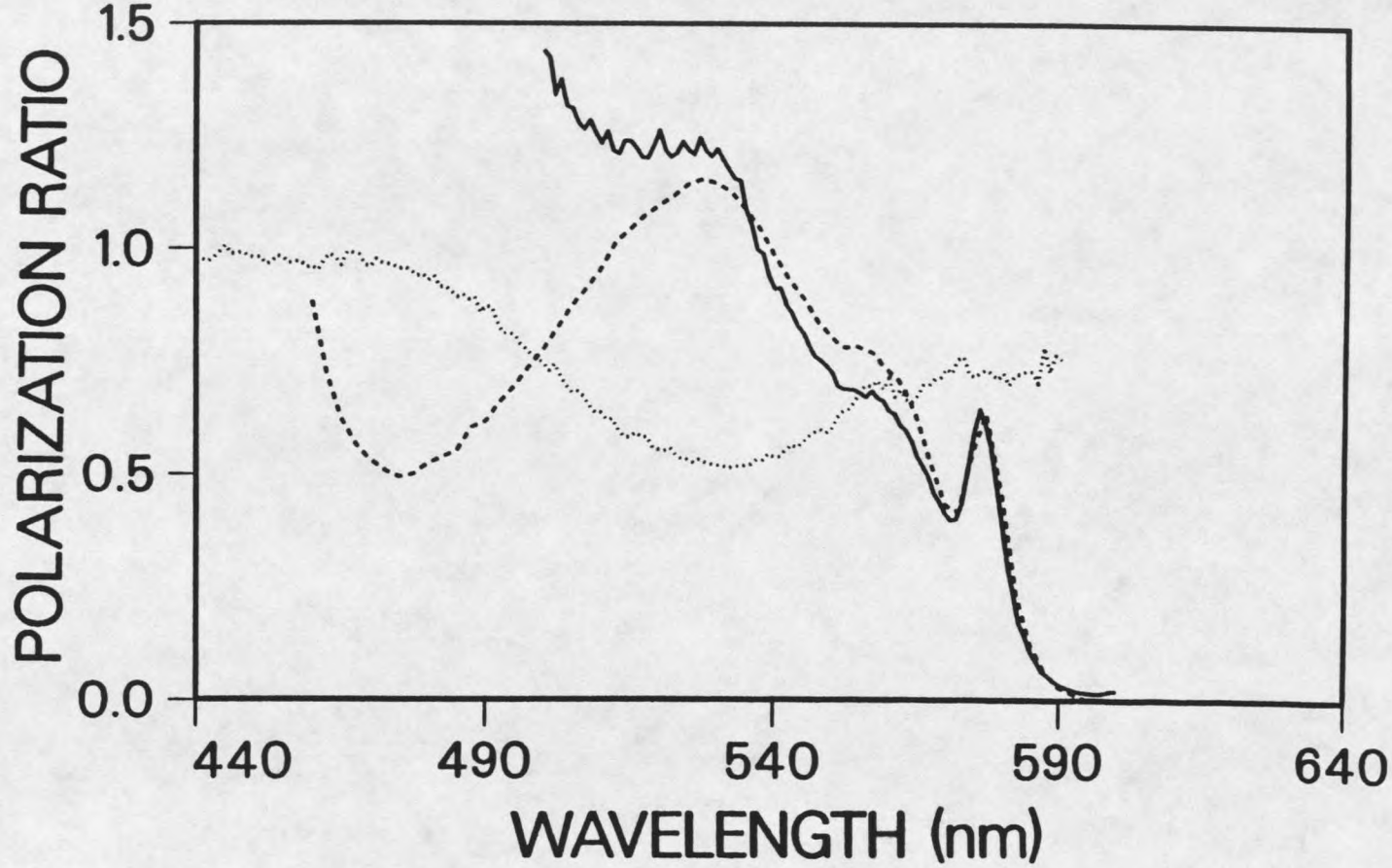

Figure 41: Two-photon fluorescence excitation (solid line), one photon absorption (dashed line), and two-photon polarization (dotted line) spectra for 7-methoxy-indole dissolved in butanol (0.004M).

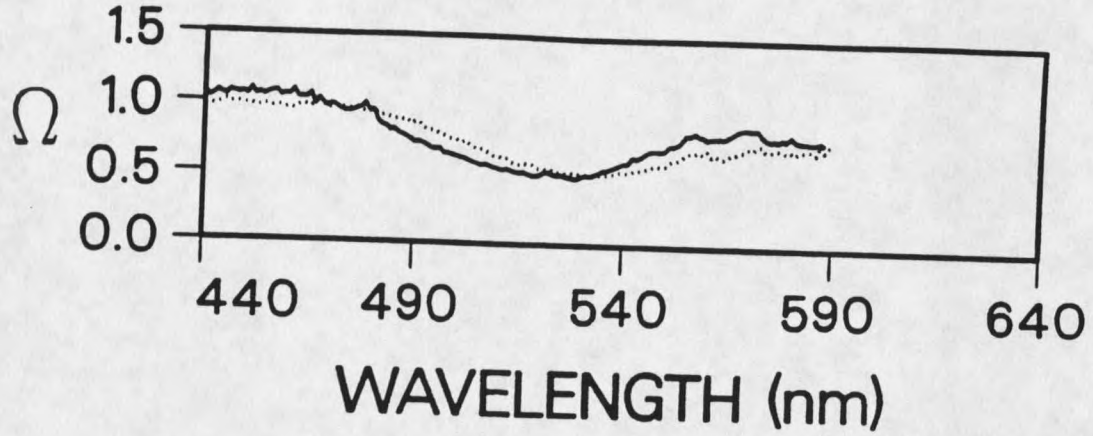

Figure 42: Two-photon polarization spectra of 7-methoxy-indole in cyclohexane (solid line) and in butanol (dotted line) (0.004M).

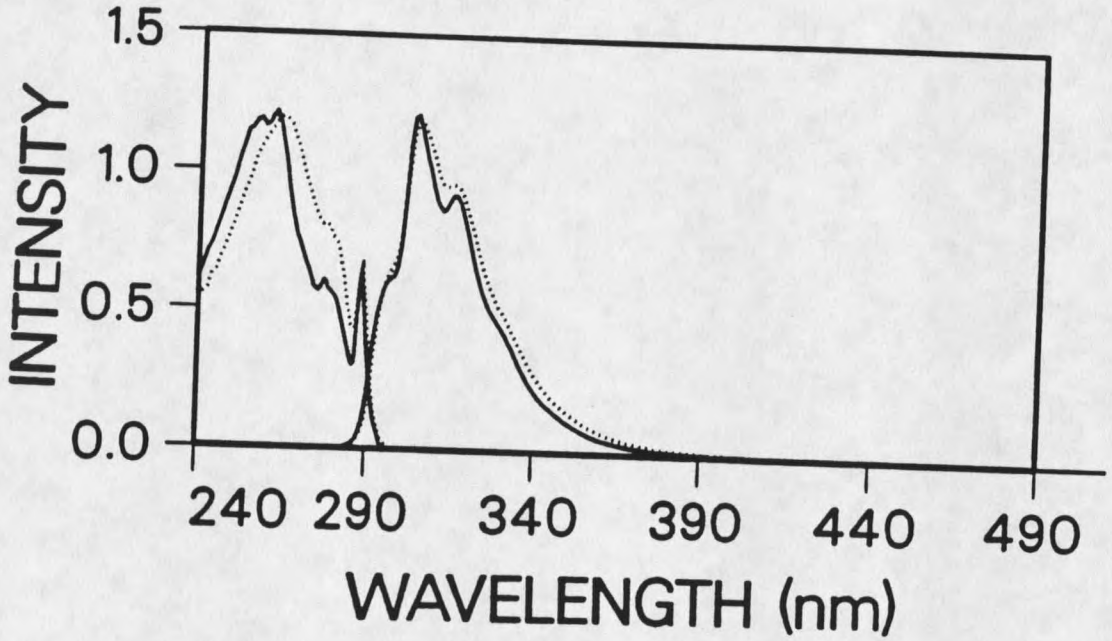

Figure 43: One-photon absorption and fluorescence spectra of 7-methoxyindole in cyclohexane (solid lines) and in butanol (dotted lines) (~10-5M).

experimental results (4). In every case, the ^1L_a state is clearly more sensitive to the solvation environment than ^1L_b and shifts to lower energies due to polar solvation while the ^1L_b state is largely unaffected. The results of polar solvation on the fluorescence characteristics of these molecules, however, are more variable. It is generally recognized that for a large stoke's shift of fluorescence to occur, the more polar ^1L_a state must be lowest in energy and hence the emitting state. Indole derivatives that exhibit these large red shifts of fluorescence in polar media have been assigned small L_a-L_b energy gaps (12). Unless ^1L_a appears to be lowest in hydrocarbon as it does for 2,3 dimethylindole (8), there has been some question as to how the ^1L_a state becomes lowest in polar solvents for these derivatives. Ground state complexes (14,64) and solvent reorientation around the excited state dipole (16,17,18) are the two most often cited mechanisms by which L_a-L_b level inversion occurs.

The polarization dependence of the two-photon absorption process has allowed a direct confirmation of the existence of ground state complexes. Unlike one-photon fluorescence polarization experiments, the two-photon polarization is independent of events subsequent to absorption and therefore is indicative only of the ground state environment. The red shift of the ^1L_a state evidenced in the two-photon polarization spectra is thus a result of

ground state interactions. The net result of this interaction depends intimately upon the L_a-L_b energy gap. In molecules with small gaps like indole, 1-methylindole, and 3-methylindole, the result of the ground state complexation is inversion of the L_a and L_b states. While other studies have suggested that this occurs, this work represents the first direct evidence that it does. It occurs partially for indole and 1-methylindole, but is complete for 3-methylindole which exhibits a pure ^1L_a polarization ratio of 0.5 for long wavelength excitation in butanol. Molecules which exhibit significantly lower Ω for the red edge in butanol do show larger stokes shifts and a loss of structure in their fluorescence confirming that the ^1L_a state is responsible. Intermediate values of Ω are seen for molecules such as 5-methylindole in butanol and are associated with fluorescence spectra exhibiting both a structured component and a broad red shifted component. This is presumably due to dual fluorescence from ^1L_a and ^1L_b combining to form the resultant steady state fluorescence. Dual fluorescence has been suggested for indole in polar solvents (17,18,66), and for 3-methylindole (68) in non-polar solvents. The intermediate values of Ω exhibited for these molecules at their red edge are wholly consistent with this picture. Extending this behavior to other molecules, it is likely that dual emission occurs for 5-methylindole in butanol, 6-methoxyindole in butanol, 1-methylindole in

cyclohexane and 1-methylindole in butanol. The degree to which a broadening of the fluorescence occurs correlates well with the drop in Ω seen at the red edge. 7-methoxyindole is an exception, but the two photon spectrum could be misleading since L_b makes little contribution to the TPA and may in fact be very strong in emission. The two-photon results are summarized in Table 2.

Table 2. Table of Results

Lowest State	cyclohexane			n-butanol		
Compound	L_b	L_a	Dual	L_b	L_a	Dual
indole	X					X
1-methylindole			X			X
3-methylindole			X		X	
2,3-methylindole		X			X	
5-methylindole	X					X
4-methoxyindole	X			X		
5-methoxyindole	X			X		
6-methoxyindole	X					X
7-methoxyindole	X			X		

The nature of the ground state interaction which lowers the ^1L_a state has not been elucidated. Hydrogen bonding is perhaps the most obvious candidate for such an interaction, but has been dismissed due to seemingly identical results for 1-methylindole which cannot form donor hydrogen bonds. In fact Skalski et al. (14) used 1-methylindole to show the existence of a ground state interaction. The two-photon results obtained for indole and 1-methylindole question this

interpretation. Shown in Figure 44 are the polarization spectra of indole and 1-methylindole in both cyclohexane and in butanol. It is apparent that the ground state interaction is stronger for indole than it is for 1-methylindole. Despite a smaller L_a-L_b energy gap in cyclohexane and a lower Ω value at the origin, 1-methylindole has less level inversion and a higher Ω value for the red edge in butanol than does indole.

Theory shows that the indole nitrogen atom is negatively charged in the ground state (55). Hydrogen bond formation would further donate electrons to the negative center. The inductive effect of the nitrogen is very important in cancelling the red shift of L_a due to cross-linking (48) and making the nitrogen more negative would reduce the inductive effect (49) and lead to a red shift of L_a as is seen. The smaller L_a-L_b energy gap for 1-methylindole relative to indole is likely a manifestation of electron donation by the methyl group. Solvation of the negative nitrogen of course can occur by an ion-dipole interaction and is probably the source of the reduced polar ground state effect in 1-methylindole. Experiments with derivatives having more bulky substituents at position one would surely show a further reduction of the effect.

The effect of the hydrogen bonding on indoles' excited states has been dismissed by several authors. (12,13,15) As discussed before, the extent of the red shift in

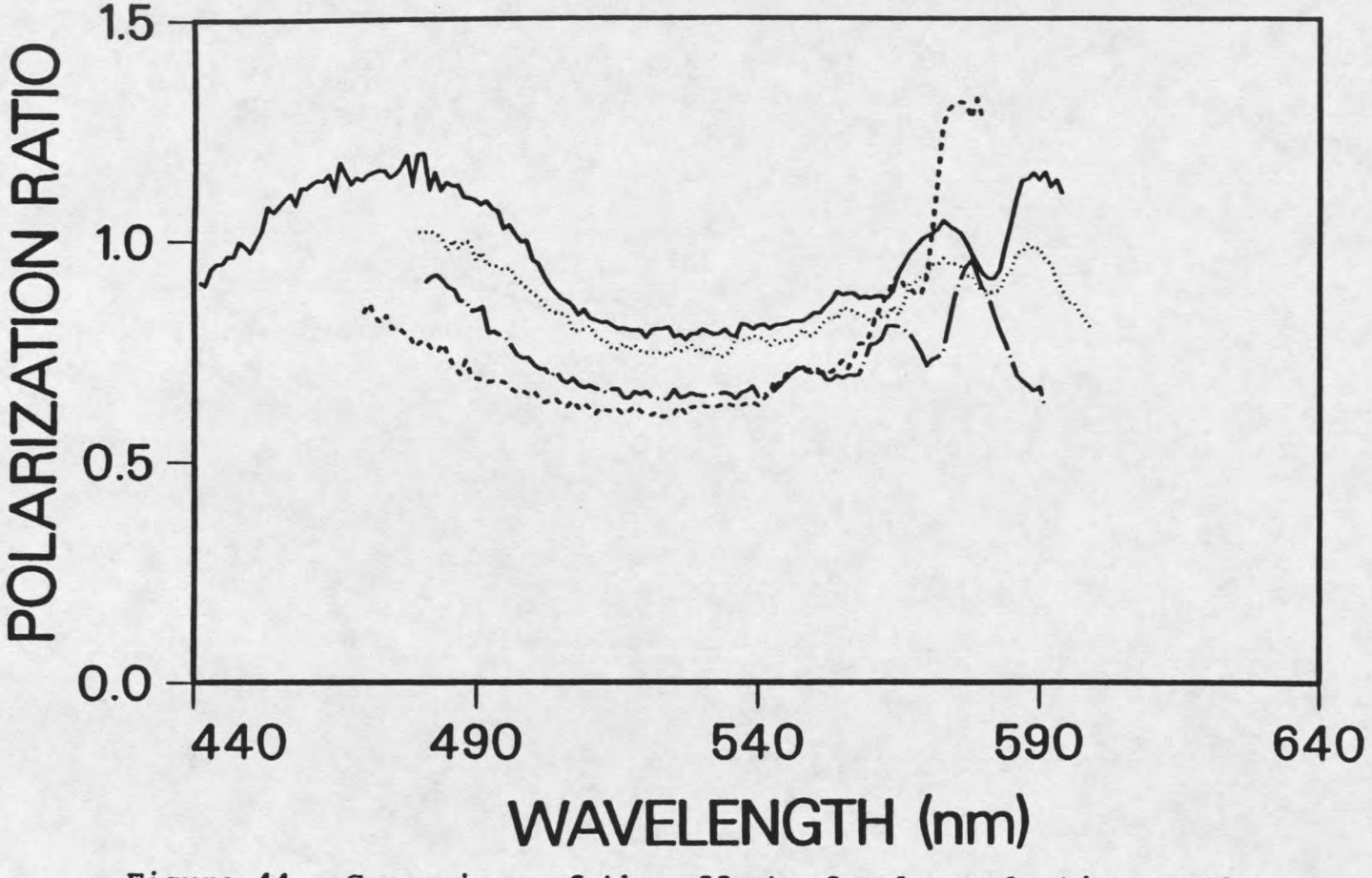

Figure 44: Comparison of the effect of polar solvation on the polarization spectra of indole and 1-methylindole. Indole in cyclohexane (dashed line) and in butanol (dash-dotted line). 1-methylindole in cyclolhexane (solid line) and in butanol (dotted line).

fluorescence depends intimately on which state, ^1L_a or ^1L_b is the lowest excited state. Therefore, if hydrogen bonding shifts these states, it must have an effect. Figure 45 compares the result of polar solvation on the fluorescence of indole and 1-methylindole. Clearly it has a greater effect for indole. Additional effects due to the ability of the solvent to stabilize excited state dipoles could also be related to hydrogen bond formation.

Excitation to the L_a state is computed to result in a large change of permanent dipole moment in the x direction (Figure 46). Associated with this change in dipole is charge transfer from N-1 and C-3 to C-4. This has the effect of making the nitrogen even less negative in the excited ^1L_a state. A solute molecule which is already hydrogen bonded in the ground state would perhaps have a larger charge transfer component upon excitation. Since the charge transfer character grows with time after excitation due to SSR (19), this would give a "head start" to hydrogen bonded molecules and lead to further red shifts. Associated with the increase in CT is a decrease in radiative rate. 3-methylindole fluorescence has been shown to be quenched by ethylacetate with a negative activation energy (63). This implies that if hydrogen bonds are being broken due to thermal fluctuations, the CT component is decreased. It therefore seems that the hydrogen bond should be included in

the analysis of indole (and hence protein) spectra because of its effect on both the ground and excited states.

The two-photon properties of indoles seem to be well represented by the results of INDO/S calculations. (Table 1) The low polarization ratio of L_a is predicted faithfully and general trends in the relative L_a and L_b intensities for the methoxyindoles are well represented. The trends in the L_a-L_b energy gap are also predicted successfully. A recent study involving the author (21) compared one-photon polarized fluorescence excitation spectra of substituted indoles to the predictions of INDO/S and showed a similar reliability in predicting the transition moment directions for L_a and L_b (21). Figure 46 shows the permanent dipole moments of the ground, L_b, and L_a states of indole as predicted by INDO/S. These results suggest an interesting mechanism by which L_a could become the lowest state even if the molecule is excited to L_b and L_b is the lowest state. The change in dipole moment between ground and L_b is in the same direction as the change for excitation to L_a. As the solvent reorients to solvate the L_b state, it is also making the L_a dipole more stable and may lower it below L_b during the excited state lifetime. The larger dipole of L_a has been suggested (16,17) to lead to its preferential stabilization, but the idea that solvation of L_b enhances this effect does not appear in the literature. The same pattern is evident for all of the derivatives. This process

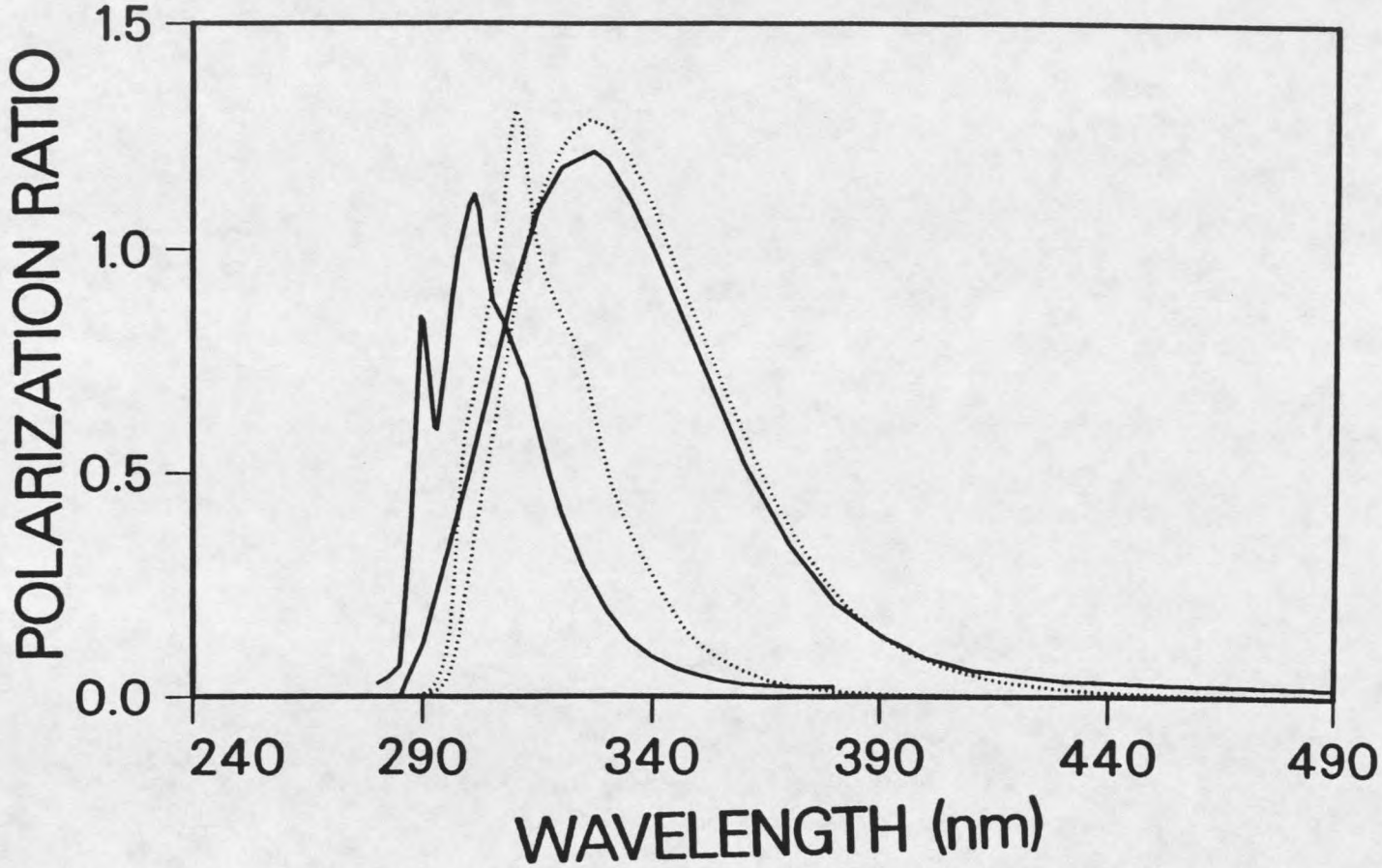

Figure 45: Comparison of the effect of polar solvation on the fluorescence spectra of indole (solid lines) and 1-methylindole (dotted lines). In each case the broad fluorescence is that seen in polar solvents.

would be expected to be important in molecules with a small L_a-L_b energy gap. Level inversion of L_a and L_b due to SSR for 1-methylindole has been shown to occur (68). A comment should be made on the third transition seen for all the derivatives studied. This transition is seen to move to the red along with the L_a state. The INDO/S calculations predict a sizeable state dipole which also is largely in the x direction and it appears that this state is also stabilized by polar solvation.

Summary

The two-photon results demonstrate that the L_a state is more sensitve to solvent environment and is responsible for the events which lead to the broad red-shifted fluorescence of indoles. Level inversion of L_a and L_b in polar solvents is shown to be the result of ground state complexes. These ground state complexes are strengthened by the ability to hydrogen bond and result in a lessening of the inductive effect of the nitrogen. Hydrogen bonding may also predispose CT character and lead to greater red shifts of fluorescence. Mixed L_a-L_b absorption on the red edge evidenced by Ω values intermediate between ~0.5 and ~1.4 seems to be a good indicator of dual emission. INDO/S calculations are faithful in predicting one and two-photon properties of indoles and suggest that solvation of the L_b

state enhances the stabilization of L_a during the excited state lifetime and leads to further level inversion.

CHARGE EFFECTS

Background

In addition to perturbations caused by solvent and possible hydrogen bonding to peptide linkages and other residues, the tryptophan residues of a protein may be subject to perturbations caused by charges. These charges could be the result of nearby glutamic acid or arginine residues for example. The effect of charge on the absorption and fluorescence of tryptophan has received very little attention (11,70,71) and yet is likely a common source of perturbation in proteins.

The most striking example of the effect of charge on the indole ring is contained in the work of Andrews and Forster (11). Yohimbine (Figure 47), a molecule isolated from the bark of the yohimbi tree, has a protonatable nitrogen in proximity to a 2,3 disubstituted indole ring. Protonation of this nitrogen was shown by difference spectrophotometry to cause a 7nm blue shift of L_a and a smaller 1nm blue shift of L_b. Their results for yohimbine and other compounds suggest that while solvation always shifts the two states in the same directions, an appropriately placed charge can shift them in opposite directions. The recent INDO/S CISD results of Ilich et al. (72) are in accord with the results of Andrews and Forster.

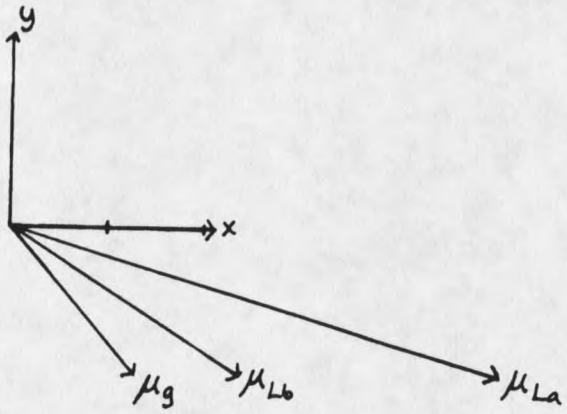

Figure 46: Permanent dipole moments for the ground (μ_g), Lb (μ_{Lb}), and La (μ_{La}) states of indole.

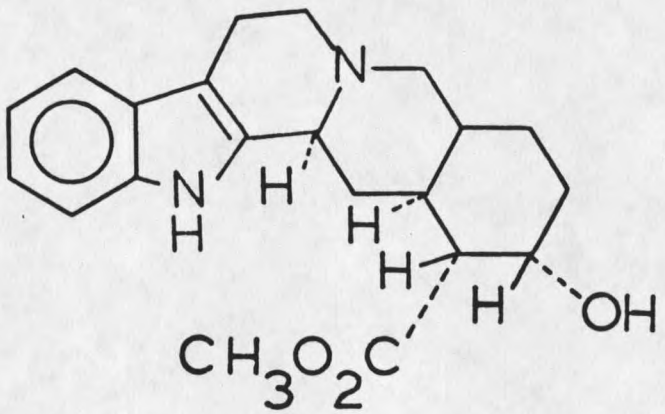

Figure 47: Structure of Yohimbine.

In order to investigate the usefulness of polarized two-photon fluorescence spectroscopy in detecting charge induced shifts of L_a and L_b, spectra were obtained for yohimbine in both its protonated and unprotonated forms. 5-methoxytryp-tophan was also investigated because of the sensitivity of its fluorescence spectrum to the ionization state of its alanyl chain. Gudgin-Templeton and Ware (72) have shown that changing the pH so as to convert the zwitterionic alanyl chain of 5-methoxytryptophan to the anionic form causes a shift in fluorescence maximum from 338nm to 353nm. This molecule seemed to be a likely candidate for charge induced shifts. Tryptophan itself was also investigated to see if shifts of L_a and L_b could be detected as a function of the ionization state of its alanyl chain. The investigation of tryptophan was also designed to shed light on the much studied (3) dual exponential fluorescence decay of zwitterionic tryptophan. Dual exponential decays of tryptophyl residues in proteins are common and it is therefore important to elucidate its mechanism.

Two-photon Spectra

Figure 48 shows the one-photon absorption (dashed lines), two-photon fluorescence excitation (solid lines) and two-photon polarization spectra of unprotonated yohimbine at high pH in isopropanol (5 X 10-3M). Figure 49 shows the same information for yohimbine in its protonated state at

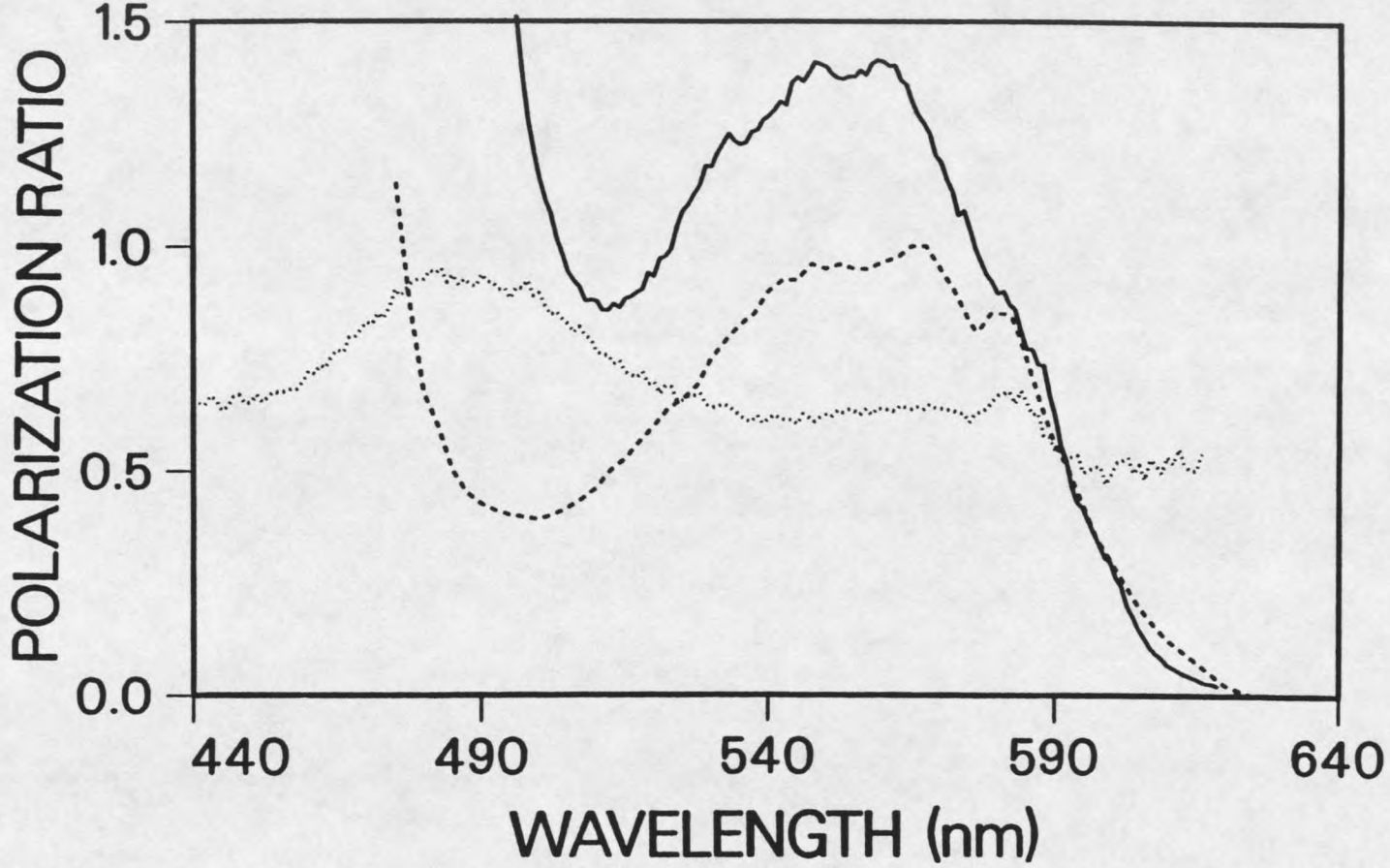

Figure 48: Two-photon fluorescence excitation (solid line), one-photon absorption (dashed line) and two-photon polarization (dotted line) spectra of Yohimbine dissolved in isopropanol at high pH (5x10-3M).

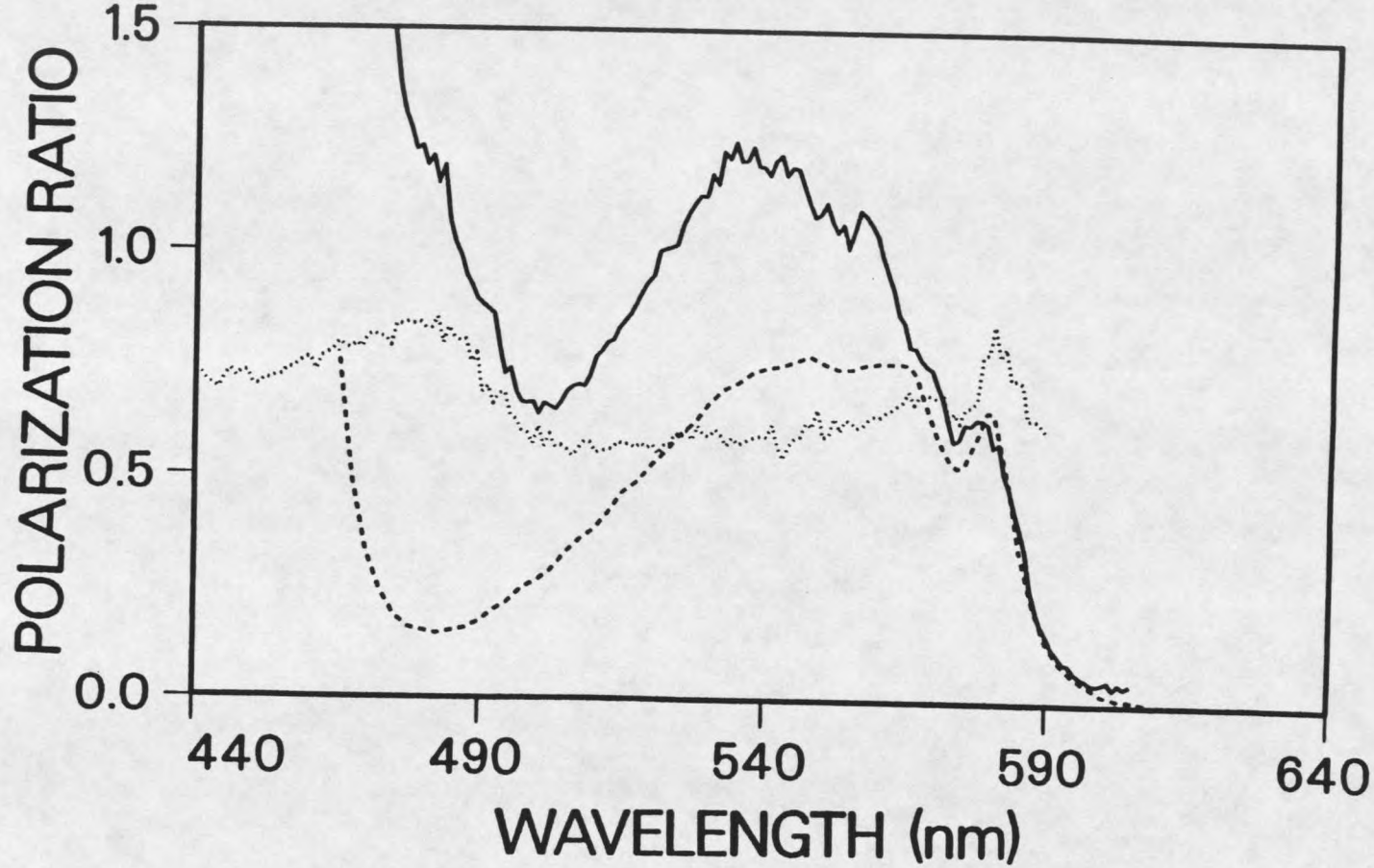

Figure 49: Two-photon fluorescence excitation (solid line), one-photon absorption (dashed line) and two-photon polarization (dotted line) spectra of Yohimbine dissolved in isopropanol at low pH (5x10-3M).

low pH in isopropanol (5 X 10-3M). Unprotonated yohimbine shows a red edge polarization ratio of ~0.5 indicating pure L_a absorption. The TPA and OPA also show extensive tailing to the red. The protonated form shows much more structure and higher ratios for the red edge. The polarization spectrum is much like that seen for indole in butanol. The tailing in the TPA and OPA has also disappeared. Low polarization is seen to move blue for L_a excitation.

The results for anionic 5-methoxytryptophan (0.01M pH 11 buffer) are shown in Figure 50. The polarization spectrum shows a very smooth profile like that seen for 5-methoxyindole. The polarization ratio is ~0.9 in the region of the origin. Lowering the pH to protonate the amino nitrogen (Figure 51) causes very little apparent change in the TPA but causes the polarization ratio to rise at the red edge to well above one, indicating that L_a has been blue shifted by the positive charge as in yohimbine. Results of polarized one-photon fluorescence excitation experiments with 5-methoxytryptophan in glycerol at pH 7 are also consistent with L_b being the predominantly lowest state, as is suggested by the two-photon polarization ratio. Lowering the pH further to protonate the carboxylic acid moiety (Figure 52) has little effect on the polarization spectrum and the TPA. The fluorescence does not shift to a significant degree in response to loss of the negative charge.

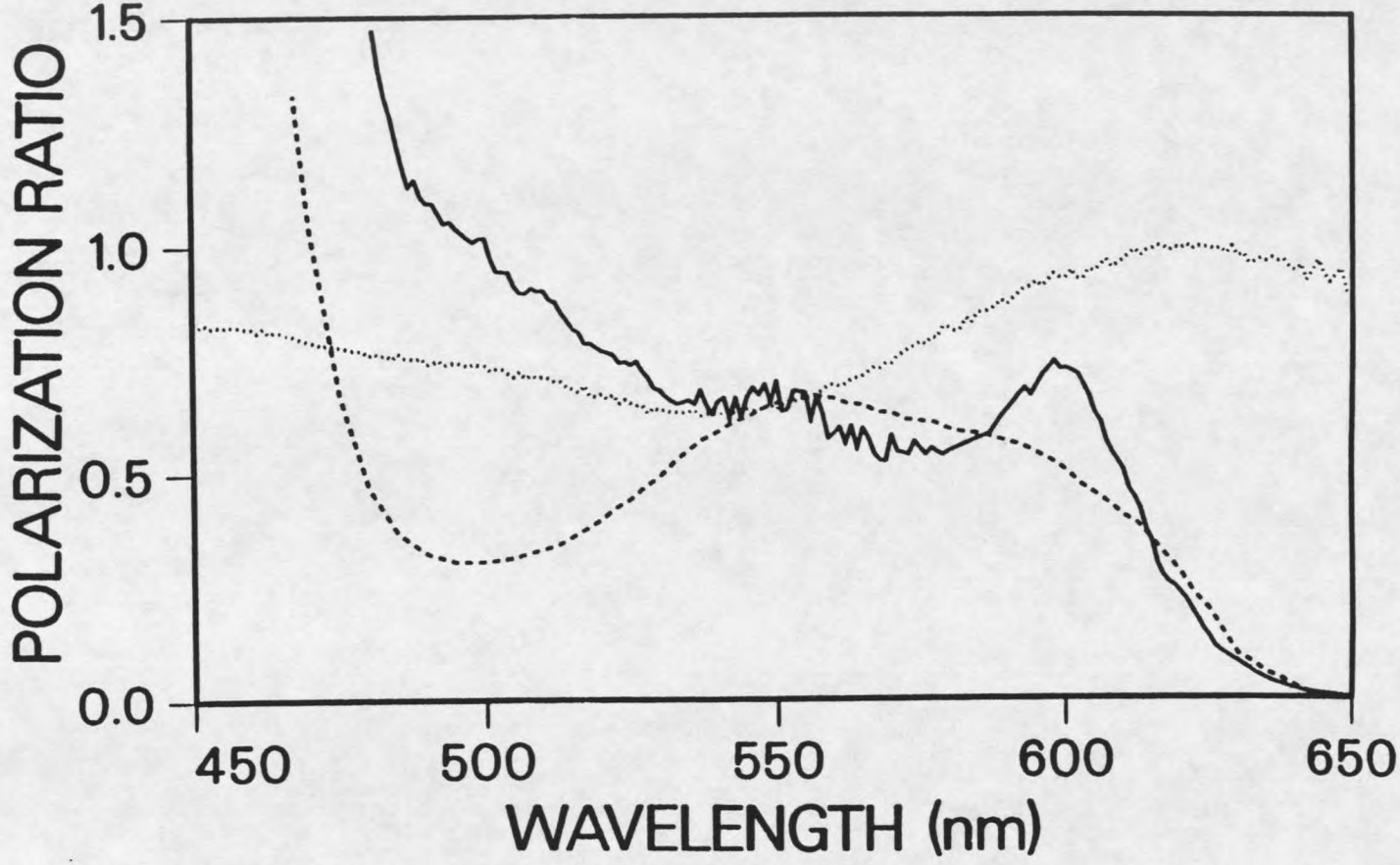

Figure 50: Two-photon fluorescence excitation (solid line), one-photon absorption (dashed line) and two-photon polarization (dotted line) spectra of 5-methoxytryptophan in pH 11 phosphate buffer (0.01M).

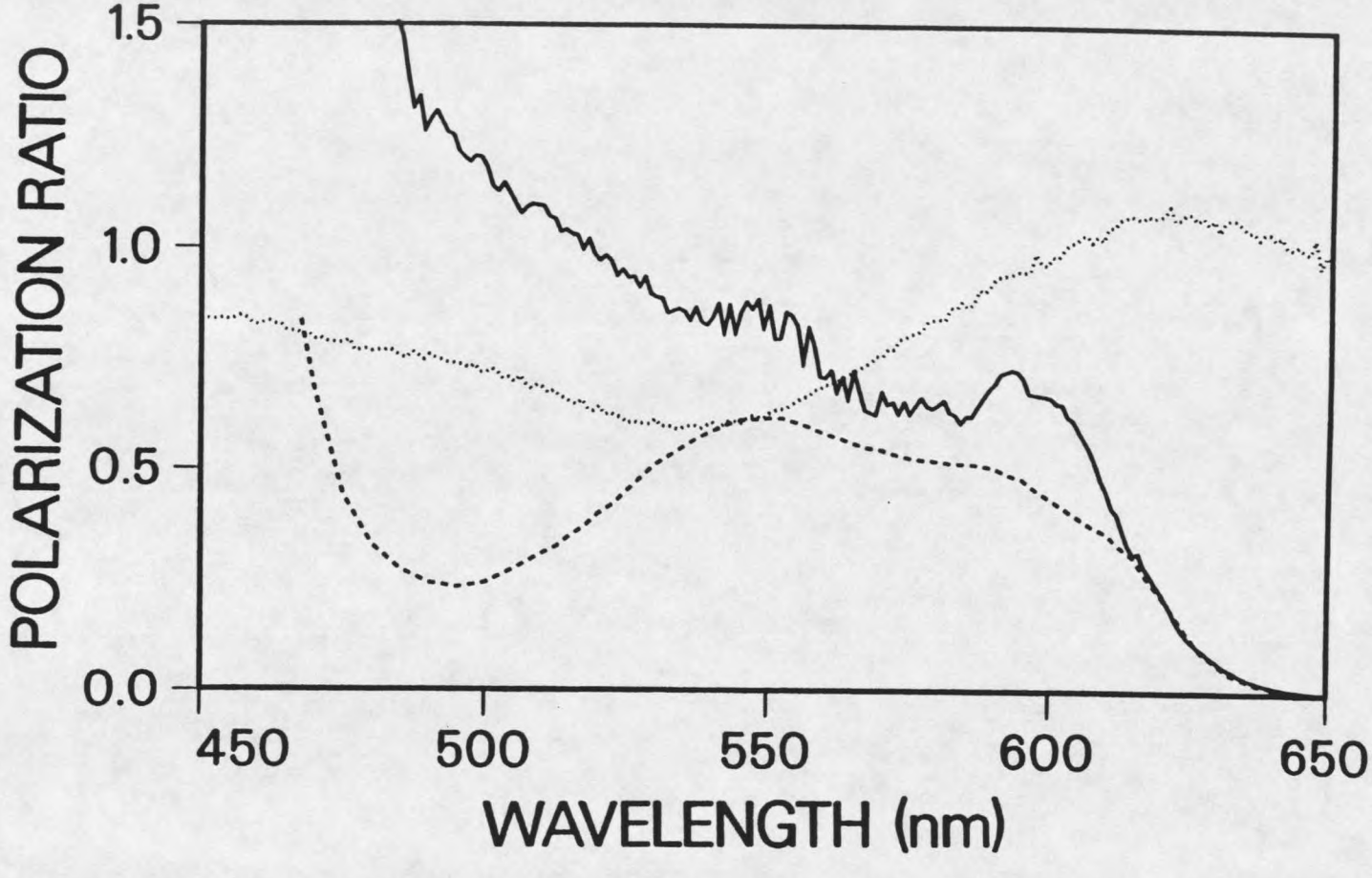

Figure 51: Two-photon fluorescence excitation (solid line), one-photon absorption (dashed line) and two-photon polarization (dotted line) spectra of 5-methoxytryptophan in pH 7 phosphate buffer (0.01M).

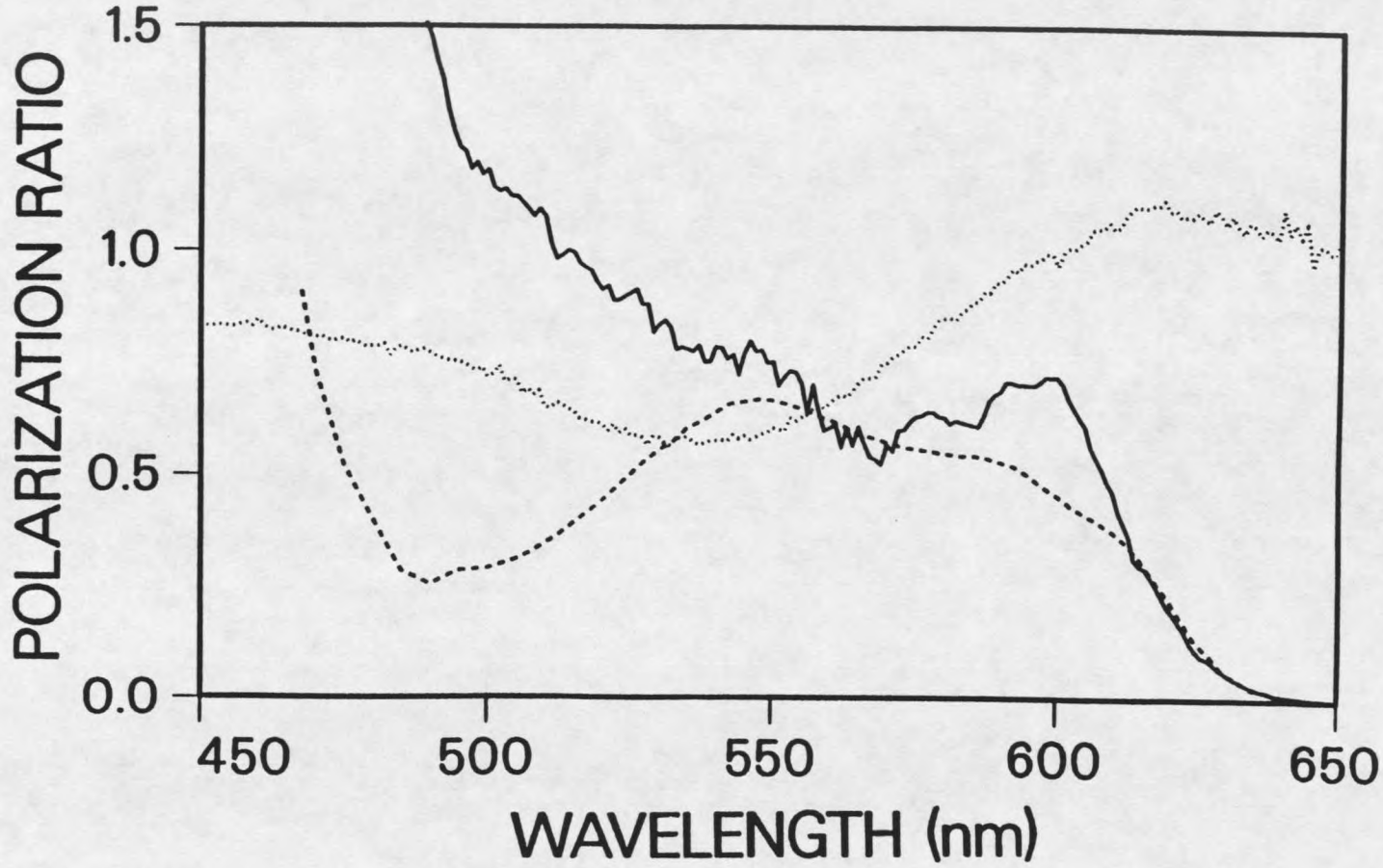

Figure 52: Two-photon fluorescence excitation (solid line), one-photon absorption (dashed line) and two-photon polarization (dotted line) spectra of 5-methoxytryptophan in pH 2 phosphate buffer (0.01M).

The results of tryptophan at pH11 are shown in Figure 53. The fluorescence associated with the anionic form of tryptophan has a maximum at 362nm. The polarization ratio is seen to level off at ~.6 and there is extensive tailing of the OPA and TPA. This result would seem to indicate a portion of the molecules might be emitting from L_b, however a somewhat surprising result was seen with a reduction of pH to 7 (Figure 54). The polarization ratio for red edge excitation actually dropped. Polarization changes for L_a excitation seem to indicate a blue shift of L_a and the fluorescence shifts blue to 356nm. The effect is again seen when the carboxl group is protonated at ph2 (Figure 55). The polarization spectra are compared in Figure 56.

Discussion

The results for all three molecules seem to indicate that L_a is blue shifted by a positive charge in the vicinity of the pyrrole ring of indole. This is consistent with experimental(11) and theoretical(72) results. The results for yohimbine suggest that the positive charge has enough of an effect to cause a significant number of molecules to emit from the L_b state due to the large blue shift of L_a. 5-methoxytryptophan appears to have L_b as the predominant emitting state for pH2 and pH7 and this manifests itself in a small stokes shift of fluorescence. Loss of the positive charge is accompanied by L_a-L_b level inversion leading to

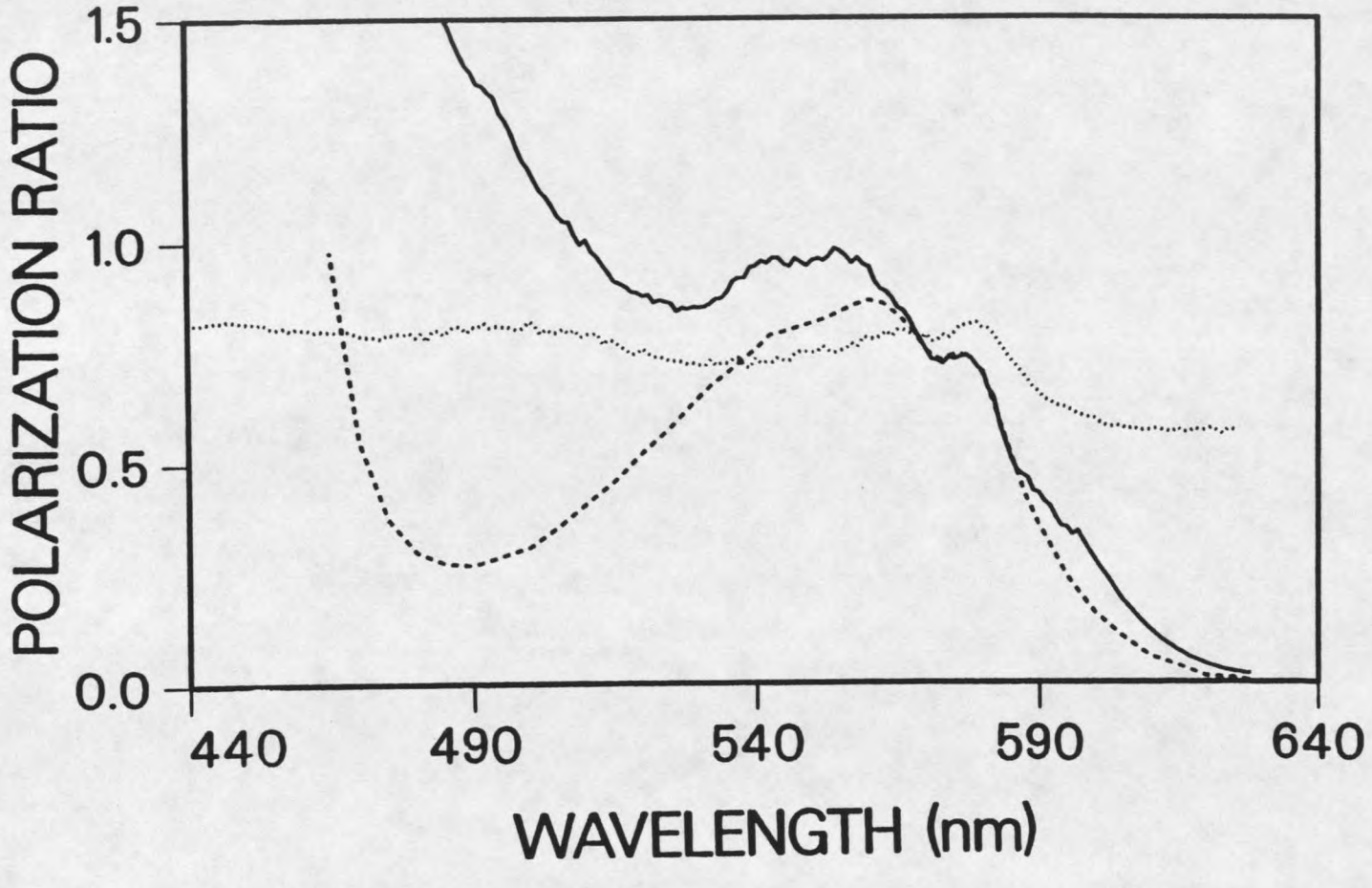

Figure 53: Two-photon fluorescence excitation (solid line), one-photon absorption (dashed line) and two-photon polarization (dotted line) spectra of tryptophan in pH 11 phosphate buffer (0.01M)

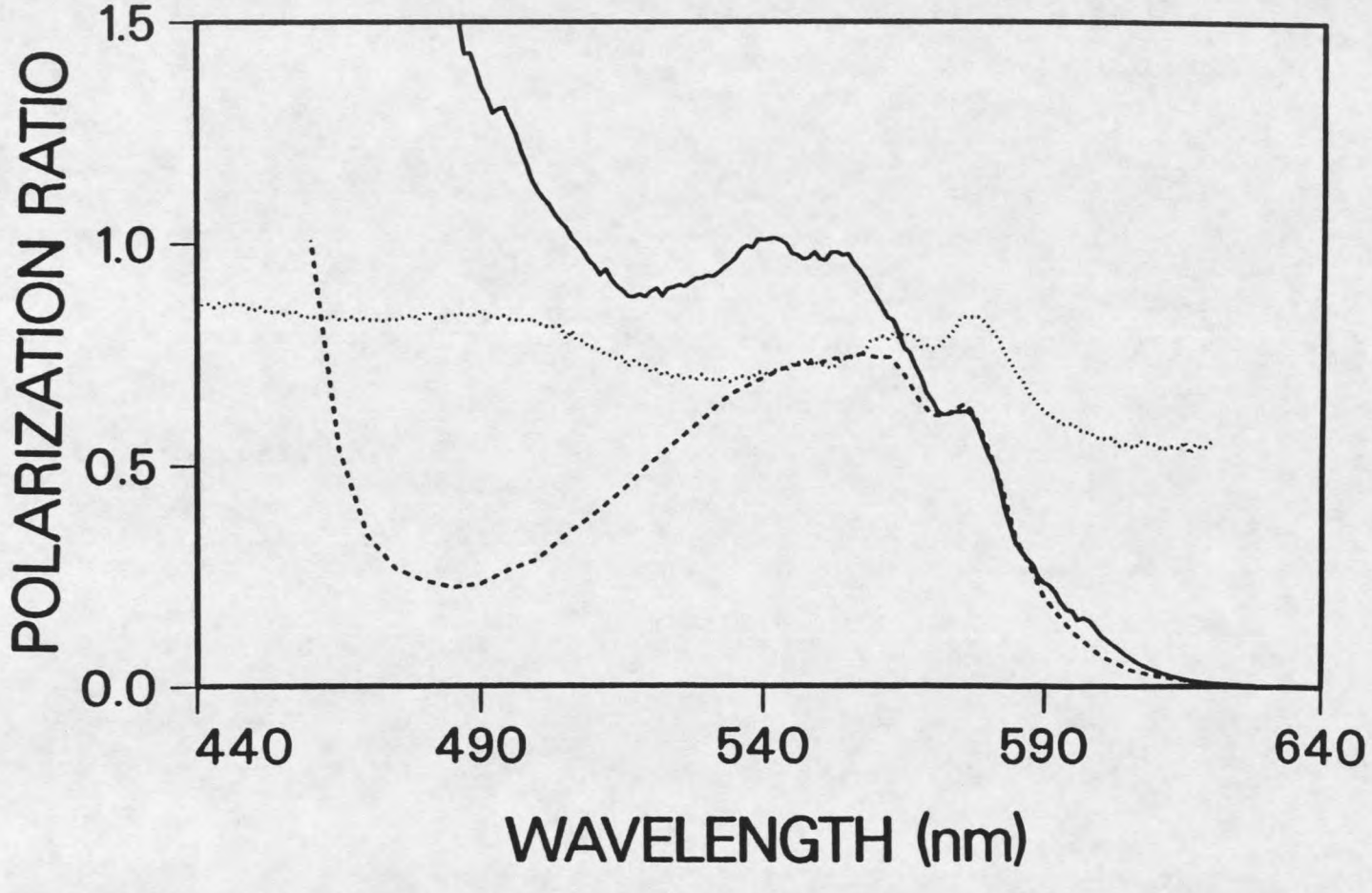

Figure 54: Two-photon fluorescence excitation (solid line), one-photon absorption (dashed line) and two-photon polarization (dotted line) spectra of tryptophan in pH 7 phosphate buffer (0.01M).

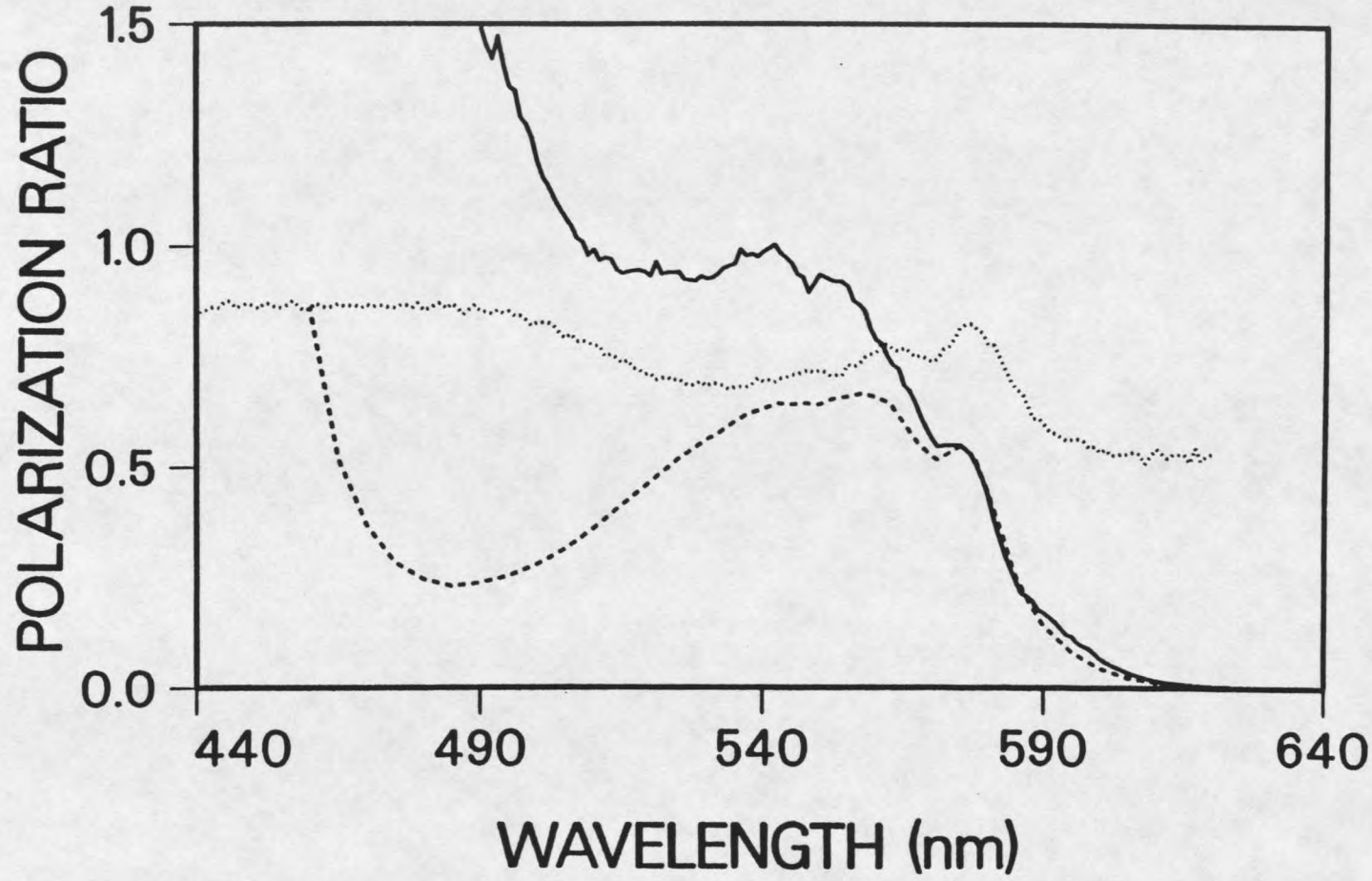

Figure 55: Two-photon fluorescence excitation (solid line), one-photon absorption (dashed line) and two-photon polarization (dotted line) spectra of tryptophan in pH 2 phosphate buffer (0.01M).

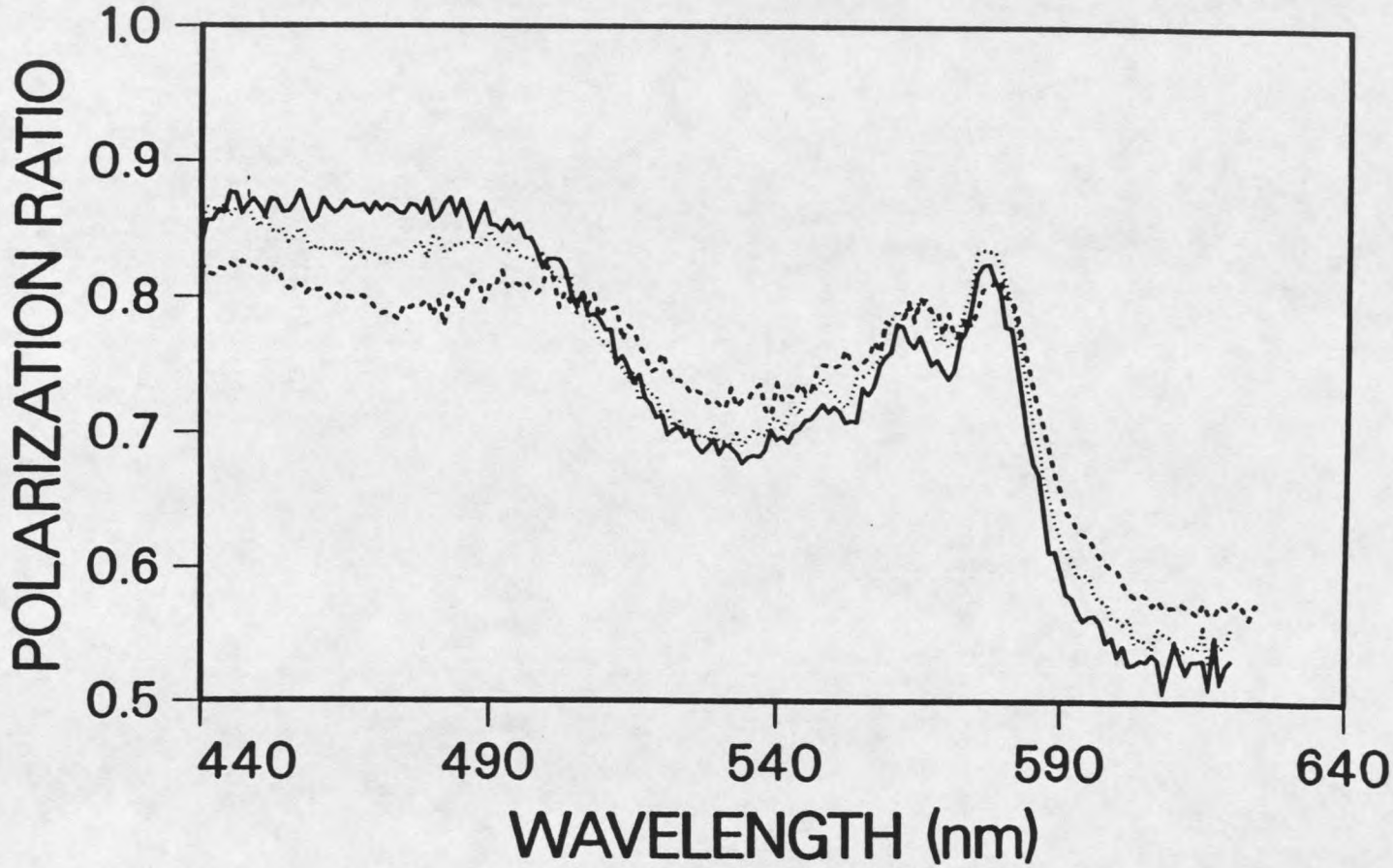

Figure 56: Comparison of the polarization spectra of tryptophan at pH 2 (solid line), pH 7 (dotted line) and pH 11 (dashed line).

broader and more red shifted fluorescence. The changes corresponding with loss of the positive charge are much more pronounced than the changes seen for loss of the negative charge and indicate that the positive charge is correlated with the indole ring to a larger degree. The ammonium ion is known to possess a hydrogen bonding geometry and strength very similar to water (74) and may become part of an "iceberg" formed around the indole ring.

The changes in the polarization spectra of tryptophan are much smaller due to the aqueous solvent and the 3-substitution which contribute to keep L_a as the predominant emitting state. The effect of the negative charge on the polarization ratio is very interesting. This may also take place for 5-methoxytryptophan but go unnoticed due to the large changes caused by L_a being largely above L_b. The effect can be understood by recalling that the low polarization ratio is due to a large change in dipole moment along the long axis of the indole ring. The negative charge attached to the positive end of the ground and excited state dipoles would reduce both. The reduced polarization ratio is predicted by INDO/S calculations where a small negative charge is placed near the pyrrole ring. After excitation, the negative charge seems to stabilize the charge transfer character of the L_a state and leads to the large stokes shift of fluorescence seen for the anionic tryptophans.

The polarization ratio of red edge excitation is never seen to reach the value of 0.5 seen for 2,3-dimethylindole and 3-methylindole in butanol. This opens the possibility of L_b contributing a small fraction of the emission for zwitterionic tryptophan. The Ω value of 0.53-0.54 would correspond to about 4 to 5% L_b for the red edge. The origin of the dual exponential decay in zwitterionic tryptophan has been the subject of many studies (75-80) yet remains a great mystery. The current consensus rests upon a model incorporating ground state rotamers which bring the charged groups close to the indole ring and quench the fluorescence with differing efficiencies. The existence of rotamers has been confirmed by jet spectroscopy (81) and NMR (82). The possibility of an L_b component to the fluorescence was initially postulated (78) but often seems out of favor. It is interesting that the contribution of the short lived component of tryptohan's fluorescence is about 5% (73). Such a contribution could arise due to a ground state conformer which brings the positive charge near the ring, resulting in a blue shift of L_a as seen for yohimbine. The two-photon results indicate that the contribution of L_b in tryptophan's emission should be re-examined. Small or large contributions of L_b to the emission of proteins could arise from charge interactions in proteins. The rise in the polarization ratio seen for the tryptophan anion could prove

useful in detecting charge effects in proteins with long wavelength emissions.

Summary

Two-photon spectroscopy has again proven itself immensely useful for directly observing the changes in relative L_a and L_b levels due to environmental perturbations. The blue shift of L_a under the influence of a positive charge in yohimbine has been confirmed. Charge effects due to the alanyl chain of tryptophan and 5-methoxytryptophan have been observed for the first time. A rise in the polarization ratio due to the negative charge of anionic tryptophan offers a new way to detect charge perturbations in proteins. INDO/S calculations (72) once again are shown to be reliable. The possibility of an L_b contribution to the mysterious dual exponential decay of zwitterionic tryptophan is also suggested.

AMINO ACIDS AND PROTEINS

Background

Two-photon spectroscopy of tryptophan residues in proteins offers great promise due to the sensitivity of the technique in observing changes in the L_a and L_b levels. The low transition probabilities for two-photon absorption and the low solubilities exhibited by proteins make it necessary for interfering signals to be small. For conventional one-photon spectroscopy the extinction coefficients for the amino acids make it necessary to perform spectroscopy of tryptophan residues above 290nm to avoid interference from tyrosine(83). Spectroscopy of phenylalanine residues is a futile endeavor at best due to their low absorptivity and energy transfer to tyrosine.

Two-photon spectroscopy seems to be blessed in regard to proteins. Tyrosine, due to its para-substitution of similarly electron-donating groups is predicted to have a very small two-photon cross-section (25). This is consistent with the reports of Jiang et al. (84) that two-photon excitation of proteins with 532nm light gives no detectable fluorescence from tyrosine. In order to investigate this further, the polarized two-photon excitation spectra of phenylalanine, tyrosine, and tryptophan were obtained.

Melittin, a small protein with interesting photophysical properties was also investigated to see if anything could be learned and to see if it was possible with a relatively weak laser to see a signal from a protein. High ionic strengths or high concentrations induce melittin to aggregate into a tetrameric form (85). This aggregation is accompanied by a shift in fluorescence wavelength from 353nm to 338nm. Both forms were investigated.

Two-photon Spectra

Figure 57 shows the two-photon excitation (solid line), one photon absorption (dashed line) and two-photon polarization (dotted line) for phenylalanine (0.01M pH7 buffer). Figures 58 and 59 show the same information for tyrosinamide and tryptophan (0.01M pH7 buffer) respectively. In Figure 60 is shown the relative signal observed for the amino acids with the same settings on the spectrometer except for the emission monochromator which was set at the emission maximum for each molecule. This signal was then corrected for fluorescence quantum yield differences. Figure 61 shows the two-photon excitation spectrum of melittin (5x10-3M) and the polarization spectra of both the monomeric and tetrameric forms.

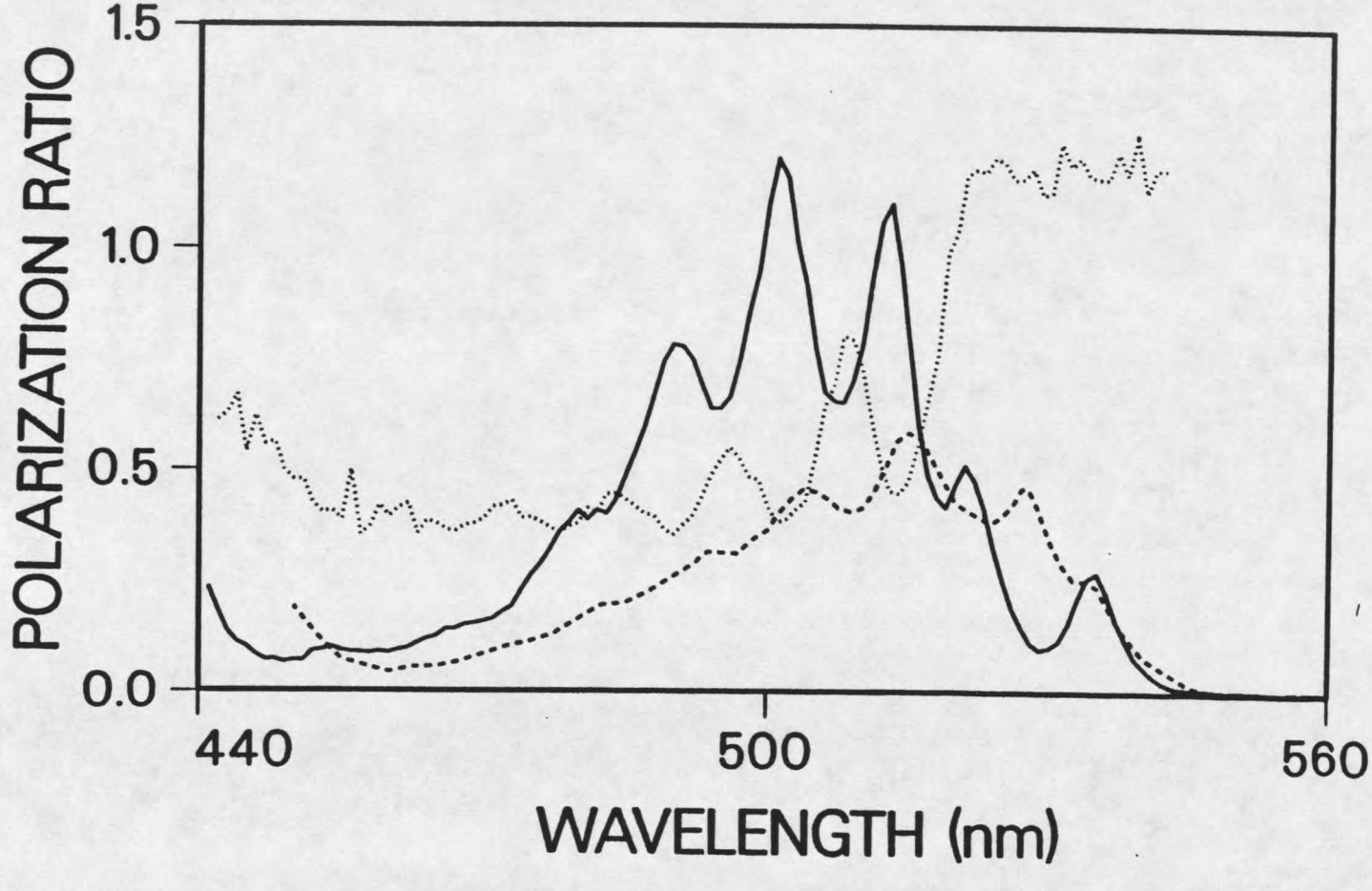

Figure 57: Two-photon fluorescence excitation (solid line), one-photon absorption (dashed line) and two-photon polarization (dotted line) spectra of phenylalanine in pH7 buffer (0.01M).

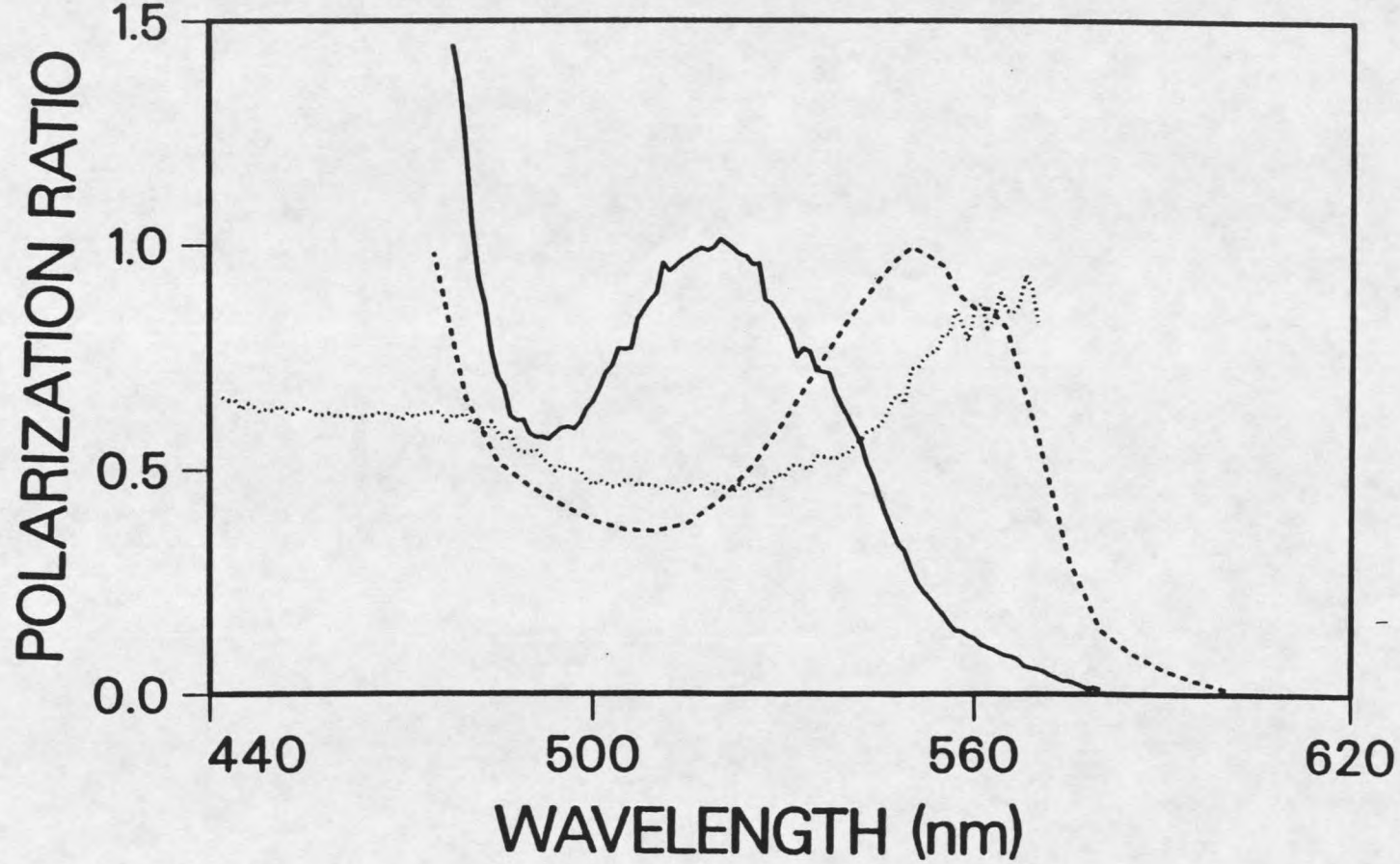

Figure 58: Two-photon fluorescence excitation (solid line), one-photon absorption (dashed line) and two-photon polarization (dotted line) spectra of tyrosinamide in pH 7 buffer.

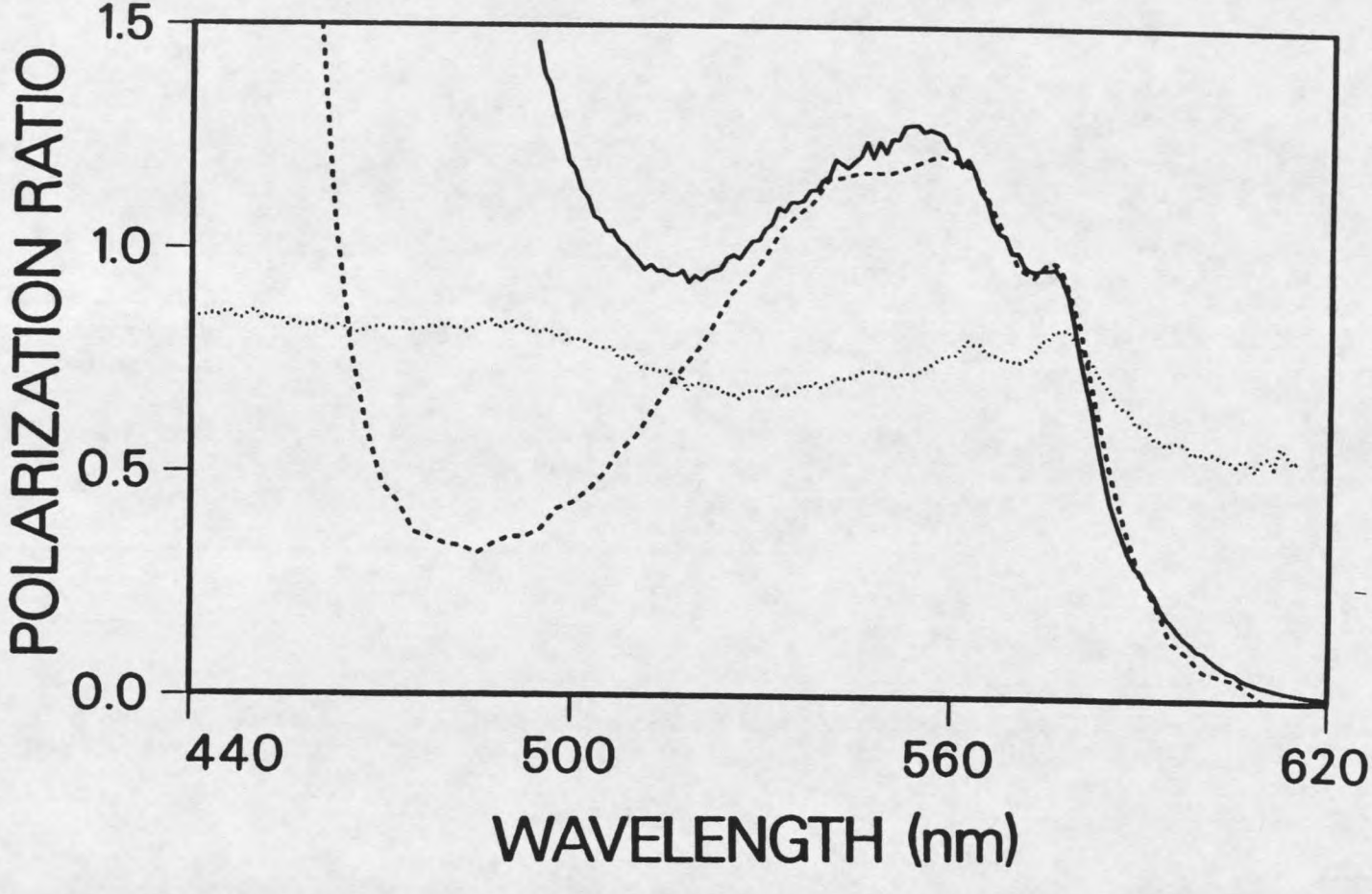

Figure 59: Two-photon fluorescence excitation (solid line), one-photon absorption (dashed line) and two-photon polarization (dotted line) spectra of tryptophan in pH 7 buffer.

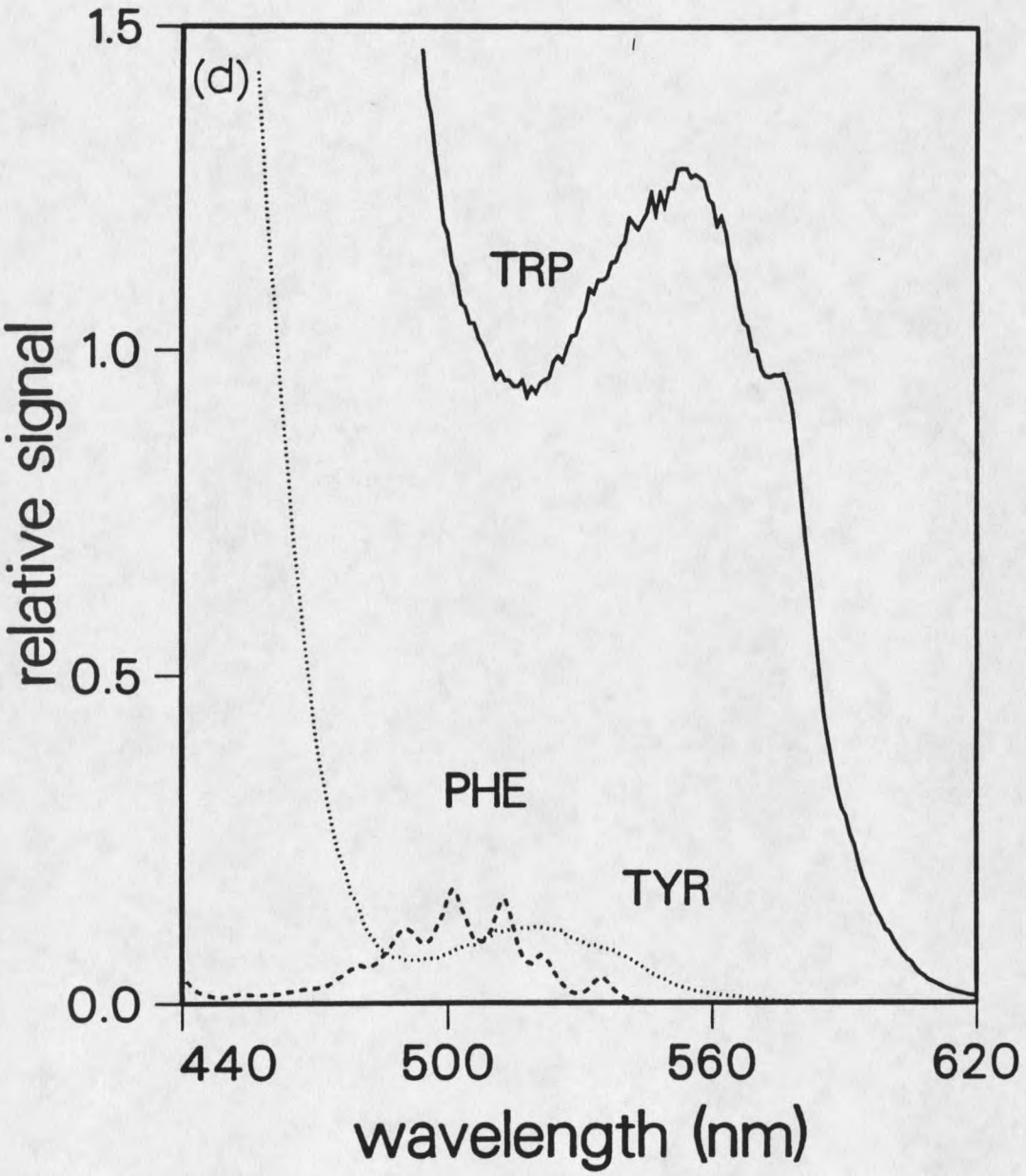

Figure 60: Relative signal from tryptophan (solid line), tyrosinamide (dashed line), and phenylalanine (dotted line) measured at their respective fluorescence maximum.

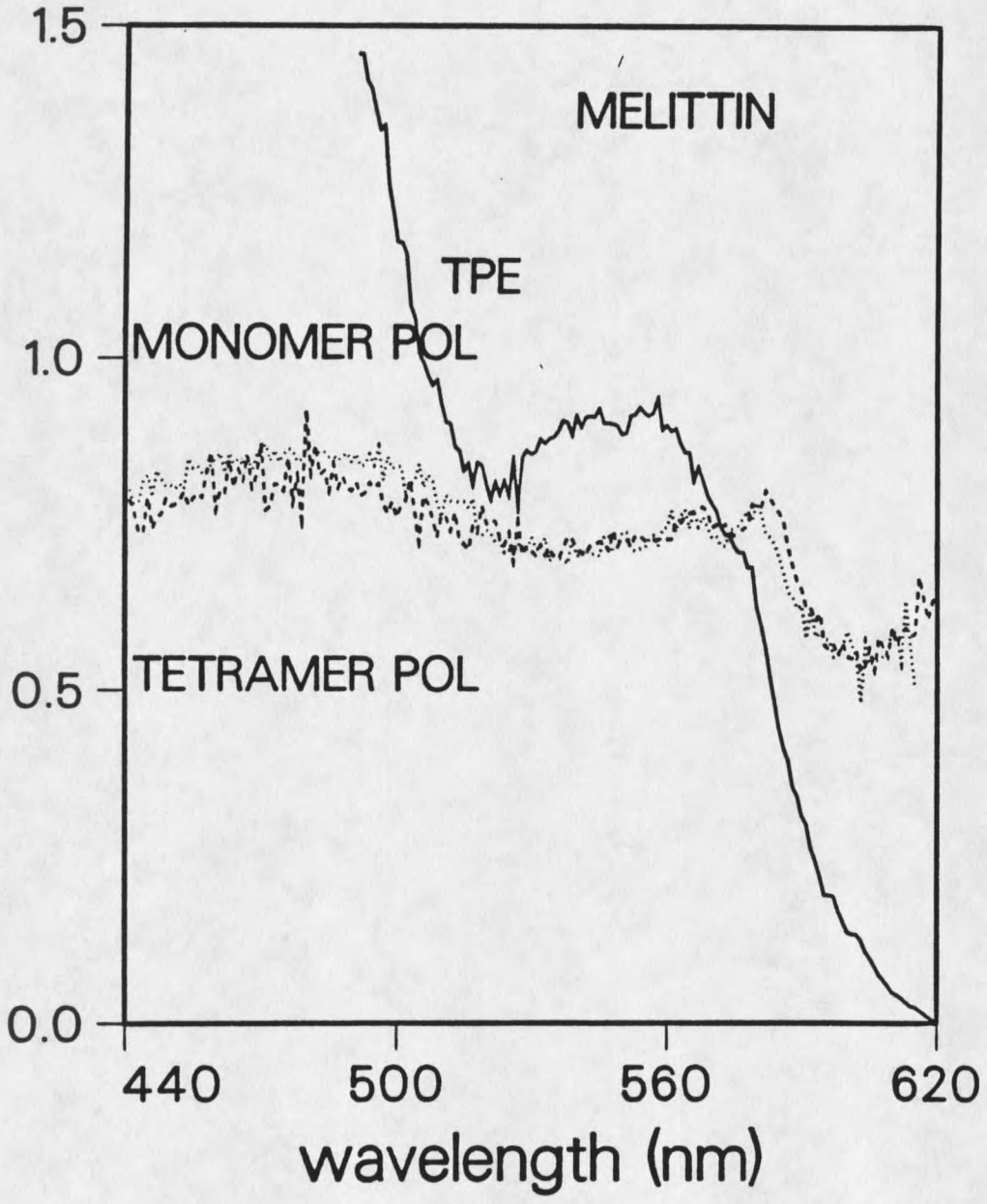

Figure 61. Two-photon fluorescence excitation (solid line) and two-photon polarization spectra for the monomeric (dotted line) and tetrameric (dashed line) forms.

Discussion

The lowest energy absorption of tyrosine and phenylalanine is due to a benzene like L_b transition which is not allowed for hexagonal geometry (in benzene) but gains intensity from vibronic coupling with the ground state. The L_b state in benzene is not allowed for both one and two-photon processes and relies on a skeletal bending vibration (606cm-1) for intensity in one photon and a skeletal stretching vibration (1563 cm-1) in two photon excitation. The addition of substituents to form phenylalanine and tyrosine breaks the high symmetry and makes the L_b state allowed. For tyrosine, in one-photon, this allowed part overwhelms the vibronic part and the maximum in absorption appears at 275nm. Phenylalanine remains weak in one photon like toluene. For two-photon processes, tyrosine's L_b is weakly allowed and the vibronic part overwhelms the allowed part. The result is that the maximum is shifted to higher energies. It would be expected that the maximum would shift an amount equal to the frequency of the promoting mode but the TPA is seen to have a maximum 2000cm-1 above that observed in the OPA. Phenylalanine is weak in two-photon also and the large peaks due to the ν 14 vibration are seen at their appropriate spacing. For both of these molecules the polarization ratio is seen to be high for the allowed parts and low for the vibronically induced peaks as was seen

for benzimidazole. As predicted, the intensity of tyrosine is reduced in two photon and is about equal to phenylalanine. The discussions of the preceding sections apply to tryptophan.

The spectrum of melittin looks like tryptophan, as would be expected, since this is the only aromatic residue it possesses. The small changes observed in the polarization spectra between the monomer and the tetramer are just above the noise level. If indeed these changes are small, the difference in fluorescence for the two forms must be due to a hinderance of SSR around the excited indole ring for the tetramer.

Summary

The two-photon spectra of the amino acids indicate that it should be possible to observe tryptophan residues at all wavelengths without significant interference from tyrosine. Phenylalanine residues may also be studied in proteins which do not contain tryptophan because of the similar strength of tyrosine. The first two-photon spectrum of a protein shows that it is possible to observe a signal from tryptophan residues and that some information may be extracted from it.

SUMMARY

The first ever two-photon spectra of benzimidazole, its cation, 9-substituted indoles dissolved in non-polar and polar solvent, yohimbine, 5-methoxytryptophan, tryptophan, tyrosine, phenylalanine, and a protein have yielded much information on the effects of solvation, substitution, and charge on the L_a and L_b states of indoles. The first experimental evidence for a contribution of dipole moment changes to the two-photon absorptivity has been obtained. The importance of the L_a state in leading to the broad red-shifted fluorescence seen in polar solvents has been demonstrated. The greater solvent sensitivity of the L_a state has been confirmed and the importance of ground state complexes in causing L_a-L_b level inversion was demonstrated. Also, the role of hydrogen bonding in these complexes has been reasserted. Intermediate values of Ω for red edge excitation were shown to correlate with dual fluorescence. The large effect a charge can have on L_a was shown to be important in the interesting photophysics of 5-methoxytryptophan. The large red-shift of L_a for protonated yohimbine was confirmed. Changes in the intrinsic polarization ratio for L_a demonstrated for tryptophan anion may offer a method of detecting charge effects in proteins. The possibility of L_b fluorescence as a component in the dual fluorescence decay of zwitterionic tryptophan has been disccused. Two-

photon spectroscopy apppears to be an effective tool for observing tryptophan residues in proteins without interference from tyrosine. Phenylalanine spectra in Class A proteins (without tryptophan) may be a possibility utlilizing the two-photon technique. These conclusions have served to clarify many longstanding questions about indole photophysics and will serve as a basis for the promising field of two-photon protein spectroscopy.

REFERENCES

1. W.J. Teale and G. Weber, Biochem., 65, 476 (1957).

2. J.W. Longworth, in "Excited States of Proteins and Nucleic Acids", edited by R.F. Steiner and I. Weinryb (Plenum Press, New York) 5, 319 (1971).

3. J.M. Beechem and L. Brand, Ann. Rev. Biochem., 54, 43 (1985).

4. D. Creed, Photochem. and Photobiol., 39, 537 (1984).

5. J.R. Platt, J. Chem Phys., 19, 101 (1951).

6. S.V. Konev, in "Fluorescence and Phosphorescence of Proteins and Nucleic Acids" (Plenum Press, New York, 1967).

7. E.H. Strickland, J. Horwitz, and C. Billups, Biochem., 9, 4914 (1970).

8. E.H. Strickland, C. Billups, and E. Kay, Biochem., 11, 3657 (1972).

9. E.H. Strickland and C. Billups, Biopolymers, 12, 1989 (1973).

10. M. Martinaud and A. Kadiri, Chem. Phys., 28, 473 (1978).

11. L.J. Andrews and L.S. Forster, Biochem., 11, 1875 (1972).

12. H. Lami and N. Glasser, J. Chem. Phys., 84, 597 (1986).

13. M.S. Walker, T.W. Bednar, and R. Lumry, J. Chem. Phys., 47, 1020 (1967).

14. B. Skalski, D.M. Rayner, and A.G. Szabo, Chem. Phys. Lett., 70, 587 (1980).

15. B.L Van Duuren, J. Org. Chem., 26, 2954 (1961).

16. N. Mataga, Y. Torihashi, and K. Ezumi, Theoret. Chim. Acta., 2, 158 (1964).

17. S. Suzuki, T. Fujll, A. Imal, and H. Akahorl, J. Phys. Chem., 81, 1592 (1977).

18. P. Song and W.E. Kurtin, J. Am. Chem. Soc., 91, 4892 (1969).

19. S.R. Meech and D. Phillips, Chem. Phys., 80, 317 (1983).

20. B. Valeur and G. Weber, Photochem. and Photobiol., 25, 441 (1977).

21. M.R. Eftink, L.A. Selvidge, P.R. Callis, and A.A. Rehms, to be submitted to: J. Phys. Chem.

22. A. Kadiri, M. Martinaud, and C. Cazeau-Dubroca, Chem. Phys. Lett., 65, 484 (1979).

23. A.Z. Britten and G. Lockwood, Spectrochimica Acta., 32, 1335 (1976).

24. R. Ragone, G. Colonna, L. Servillo, and G. Irace, Phytochem. and Phytobiol., 42, 505 (1985).

25. B.E. Anderson, R.D. Jones, A.A. Rehms, P. Ilich and P. Callis, Chem. Phys. Lett., 125, 106 (1986).

26. M. Goeppert-Mayer, Ann. Phys. 9, 273 (1931).

27. W. Kaiser and G.B. Garrett, Phys. Rev. Lett., 7, 229 (1961).

28. D.M. Friedrich and W.M. McClain, Ann. Rev. Phys. Chem. 31, 559 (1980).

29. L. Goodman and R.P. Rava, Acc. Chem. Res., 17, 250 (1984).

30. W.L. Peticolas, Annu. Rev. Phys. Chem., 18, 233 (1967).

31. W.M. McClain and R.A. Harris, in "Excited States", edited by E.C. Lim (Academic Press, New York) 3, 2 (1977).

32. B. Honig, J. Jortner, and A. Szoke, J. Chem. Phys., 46, 2714 (1967).

33. B. Honig and J. Jortner, J. Chem Phys., 47, 3698 (1967).

34. M. Inoue and Y. Toyozawa, J. Phys. Soc. Jap., 20, 363 (1965).

35. P.R. Callis, Chem. Phys. Lett., 107, 125 (1984).

36. G. Hohlneicher and B. Dick, J. Chem. Phys., 70, 5427 (1979).

37. B. Dick, H. Gonska, and G. Hohlneicher, Ber. Bunsenges. Phys. Chem., 85, 746 (1981).

38. F.T. Marchese, C.J. Seliskar, and H.H. Jaffe, J. Chem.

Phys., 72, 4194 (1980).

39. B. Dick and G. Hohlneicher, J. Chem. Phys., 76, 5755 (1982).

40. O.S. Mortensen and E.N. Svendsen, J. Chem. Phys., 74, 3185 (1981).

41. J.I. Steinfeld, in "Molecules and Radiation: An Introduction to Modern Molecular Spectroscopy", (Harper and Row, New York, 1974).

42. R.P. Feynmann, in "Quantum Electrodynamics", (W.A. Benjamin, Inc., New York) 1 (1961).

43. R. Guccione and J. Van Kranendonk, Phys. Rev. Lett., 14, 583 (1965).

44. A.A. Rehms and P.R. Callis, Chem. Phys. Lett., 140, 83 (1987).

45. R.D. Jones and P.R. Callis, J. Appl. Phys., 64, 4301 (1988).

46. J. Ridley and M. Zerner, Theoret. Chim. Acta., 32, 111 (1973).

47. P.R. Callis, Intern J. Quantum Chem., 518, 579 (1984).

48. P.R. Callis, Chem. Phys. Lett., 107, 125 (1984).

49. E.M. Evleth, Theoret. Chim. Acta., 16, 22 (1970).

50. J. Feitelson, J. Chem. Phys., 43, 2511 (1965).

51. N. Fuson, M.L. Josien, R.L. Powell, and E. Utterback, J. Chem. Phys., 20, 145 (1952).

52. R.R. Birge, in "Ultrasensitive Laser Spectroscopy", (Academic Press, New York) 2, 109 (1983).

53. R. Santus, M. Bazin, and M. Aubailly, in "Photophysics and Photochemistry of Indoles", (Verlag Chemie International, Inc., 1980).

54. P.S. Song and W.E. Kurtin, Photochem. and Photobiol., 9, 175 (1969).

55. M. Sun and P.S. Song, Photochem. and Photobiol., 25, 3 (1977).

56. N. Mikami and N. Ito, Chem. Phys., 23, 141 (1977).

57. M.J.S. Dewar, G.P. Ford, M.L. McKee, H.S. Rzepa, W. Thiel, and Y. Yamaguchi, J. Mol. Struct., 43, 135 (1978).

58. M.M. Cordes and J.L. Walter, Spectrochim. Acta., 24, 1421 (1968).

59. M. Kondo and H. Kuwano, Bull. Chem. Soc. Jap., 42, 1433 (1969).

60. P.C. Tway and L.J. Cline Love, J. Phys. Chem., 86, 5223 (1982).

61. M.V. Hershberger and R.W. Lumry, Photochem. and Photobiol., 23, 391 (1976).

62. N. Lasser, J. Feitelson, and R. Lumry, Israel J. Chem., 16, 330 (1977).

63. R. Lumry and M. Hershberger, Photochem. and Photobiol., 27, 819 (1978).

64. M.V. Hershberger, R. Lumry, and R. Verall, Photochem. and Photobiol., 33, 609 (1981).

65. N. Glasser and H. Lami, J. Chem. Phys., 74, 6526 (1981).

66. H. Zimmerman and N. Joop, Elektrochem., 65, 61 (1961).

67. L.J. Andrews and L.S. Forster, Photochem. and Photobiol., 9, 353 (1974).

68. T. Montoro, M. Chabbert, J. Tyrzyk, and H. Lami, J. Chem. Phys., 89, 2712 (1988).

69. H. Lami, J. Chem. Phys., 67, 3274 (1977).

70. J.W. Donovan, M. Laskowski, Jr., and H.A. Scheraga, J. Amer. Chem. Soc., 83, 2686 (1961).

71. S. Yanari and F.A. Bovey, J. Biol. Chem., 235, 2818 (1960).

72. P. Ilich, P.H. Azelsen, and F.G. Prendergast, Biophys. Chem., 29, 341 (1988).

73. E.F. Gudgin-Templeton and W.R. Ware, Chem. Phys. Lett., 101, 345 (1983).

74. J.L. Kavanau, in "Water and Solute-Water Interactions", (Holden-Day, Inc., San Francisco, California, 1964).

75. A.G. Szabo and D.M. Rayner, J. Am. Chem. Soc., 102, 554 (1980).

76. J.W. Petrich, M.C. Chang, D.B. McDonald, and G.R. Fleming, J. Am. Chem. Soc., 105, 3824 (1983).

77. M.C. Chang, J.W. Petrich, D.B. McDonald, and G.R. Fleming, J. Am. Chem. Soc., 105, 3819 (1983).

78. D.M. Rayner and A.G. Szabo, Can. J. Chem., 56, 743 (1978).

79. R.J. Robbins, G.R. Fleming, G.S. Beddard, G.W. Robinson, P.J. Thistlewaite, and G.J. Woolfe, J. Am. Chem. Soc., 102, 6271 (1980).

80. G.R. Fleming, J.M. Morris, R.J. Robbins, G.J. Woolfe, P.J. Thistlewaite, and G.W. Robinson, Proc. Natl. Acad. Sci., 75, 4652 (1978).

81. T.R. Rizzo, Y.D. Park, L.A. Peteanu, and D.H. Levy, J. Chem. Phys., 84, 2534 (1986).

82. J.R. Cavanaugh, J. Am. Chem. Soc., 92, 1488 (1970).

83. J.M. Longworth, in "Excited States of Proteins and Nucleic Acids", edited by R.F. Steiner and I. Weinryb, (Plenum Press New York) 5, 277 (1971).

84. Y.W. Xu, J.R. Zhang, Y.M. Deng and L.K. Hui, J. Photochem. and Photobiol., 1, 223 (1987).

85. J.C. Talbot, J. Dufourcq, J. Bony, J.F. Faucon, and C. Lussan, Febs. Lett., 102, 191 (1979).